"There is nothing more practical than a good theory."

– Vladimir Vapnik

University of Alberta

Design and Estimation for Multirate Systems

by

Yang Shi

A thesis submitted to the Faculty of Graduate Studies and Research in partial fulfillment of the requirements for the degree of **Doctor of Philosophy**.

Department of Electrical and Computer Engineering

Edmonton, Alberta
Spring 2006

Library and Archives Canada

Published Heritage Branch

395 Wellington Street
Ottawa ON K1A 0N4
Canada

Bibliothèque et Archives Canada

Direction du Patrimoine de l'édition

395, rue Wellington
Ottawa ON K1A 0N4
Canada

Your file Votre référence
ISBN: 0-494-14042-9
Our file Notre référence
ISBN: 0-494-14042-9

NOTICE:
The author has granted a non-exclusive license allowing Library and Archives Canada to reproduce, publish, archive, preserve, conserve, communicate to the public by telecommunication or on the Internet, loan, distribute and sell theses worldwide, for commercial or non-commercial purposes, in microform, paper, electronic and/or any other formats.

The author retains copyright ownership and moral rights in this thesis. Neither the thesis nor substantial extracts from it may be printed or otherwise reproduced without the author's permission.

AVIS:
L'auteur a accordé une licence non exclusive permettant à la Bibliothèque et Archives Canada de reproduire, publier, archiver, sauvegarder, conserver, transmettre au public par télécommunication ou par l'Internet, prêter, distribuer et vendre des thèses partout dans le monde, à des fins commerciales ou autres, sur support microforme, papier, électronique et/ou autres formats.

L'auteur conserve la propriété du droit d'auteur et des droits moraux qui protège cette thèse. Ni la thèse ni des extraits substantiels de celle-ci ne doivent être imprimés ou autrement reproduits sans son autorisation.

In compliance with the Canadian Privacy Act some supporting forms may have been removed from this thesis.

While these forms may be included in the document page count, their removal does not represent any loss of content from the thesis.

Conformément à la loi canadienne sur la protection de la vie privée, quelques formulaires secondaires ont été enlevés de cette thèse.

Bien que ces formulaires aient inclus dans la pagination, il n'y aura aucun contenu manquant.

Canada

To my mom and dad

Abstract

Multirate systems have been an active research area in recent years due to their wide range of applications in control, digital signal processing (DSP) and communication systems. This thesis aims to carry over control-theoretic methodologies to develop design and estimation methods for multirate DSP and communication systems.

A composite error criterion is proposed to capture all three traditional distortions for the multirate filterbank-based transceiver model that is a unifying framework able to encompass existing modulation and equalization schemes. Incorporating noise attenuation and filter bandlimiting properties into this error criterion, an optimal design procedure is developed and applied to the transceiver design, yielding a finite impulse response (FIR) transceiver that has good frequency-selectivity properties and is close to perfect reconstruction. A least squares solution is given in closed form in each iteration for which the algorithm is easy to implement. Next, the stopband energy and passband magnitude constraints are directly incoporated into transmultiplexers design, thus taking a step forward in addressing practical issues about frequency selectivity. Further, in order to design transmultiplexers with low implementation complexity, a novel method is developed and it can not only achieve close-to-perfect reconstruction but also obtain most appropriate filter length. The recursive feature of the algorithm greatly improves the computation efficiency.

For crosstalk estimation in digital subscriber line (DSL) services, a multi-channel multirate DSL model is proposed and a multirate recursive least squares identification algorithm is developed. Following this is the analysis of the convergence rate,

and an upper bound of the parameter estimation error is given. When the model order is unknown, a recursive algorithm is developed to identify the crosstalk model order and parameters simultaneously.

Finally, several open problems are listed as our future research directions.

Acknowledgements

It is a joyful moment for me to write these acknowledgements because finally there is an official place to say "thank you" to many people I am indebted to.

I am extremely grateful to my supervisor, Professor Tongwen Chen, because he gave me this opportunity to study in Canada and do research in his group. Tongwen is a fascinating teacher and a thoughtful mentor, always ready to share his expertise with the students. He is also a thorough, brilliant researcher and I benefited greatly from working under his guidance. His encouragement and friendship have been invaluable throughout my studies at the University of Alberta. Tongwen had a lot of confidence and faith in me. When I just joined the group, he asked me to participate in the project on multirate signal processing. This work has expedited my understanding of multirate systems and its future direction and lays the foundation of my thesis. During the course, Tongwen always gave enthusiastic encouragement on my small progress and offered insightful comments on the technical problems. I particularly look up to his spirit of diligence, creativity, humbleness, amiableness, and so on.

I would like to thank the members of my defense and candidacy examining committees, Professors Sirish L. Shah, Qing Zhao, Behrouz Nowrouzian, Samuel S. Shen, and Lihua Xie for their careful reading of this thesis and insightful technical guidance.

I am grateful for the support and help from everyone in the Advanced Control Systems Laboratory at the University of Alberta. My group members are like a new family to me in Canada. These talented people are so ready to offer help on both research and everyday life. In particular, I would like to thank Dr. Feng Ding. I discussed with him on my research intensively, and I benefited a lot from his brilliant ideas in modeling and identification. He read my thesis and provided me very constructive and rigorous comments. Many thanks are dedicated to Dr. Xi Sun, Dr. Donglin Li, Dr. Liqian Zhang, Dr. Jie Sheng, Dr. Aryan Saadat Mehr, Dr. Yajun Pan, Dr. Guofeng Zhang, Zhihan Xu, Jiandong Wang, Xiaorui Wang, Danlei Chu, and Jing Wu.

I would like to thank my family in China for their tremendous support. By talking to them, I've always been very optimistic about the future. This thesis is

also to commemorate my father, who unfortunately passed away several months ago and could only share the joyful moment in a different world. No words can express my deepest thanks to my mother. I thank my brother and all the relatives from my big warm family in China. Without their love and support, I would not be here today. Finally but most importantly, I would like to thank my wife – Jing Zhou – for her love, her understanding and her support at all times and whenever I needed. Without her, it would have been absolutely impossible for me to finish my thesis!

Contents

1 Introduction 1
- 1.1 Multirate Systems . . . 2
- 1.2 Multirate Signal Processing . . . 3
  - 1.2.1 Filterbanks and transmultiplexers . . . 4
  - 1.2.2 Overview on the design of filterbanks/transmultiplexers . . . 7
- 1.3 Digital Subscriber Line (DSL) Systems . . . 13
  - 1.3.1 DSL systems . . . 14
  - 1.3.2 DSL reference model . . . 15
  - 1.3.3 Types of DSL technology . . . 16
  - 1.3.4 DSL crosstalk . . . 16
  - 1.3.5 Overview on the DSL crosstalk identification . . . 17
- 1.4 Motivation and Objectives . . . 19
- 1.5 Organization of the Thesis . . . 21

2 Optimal Design for Filterbank-Based Transceivers 23
- 2.1 Introduction . . . 24
- 2.2 Blocked Models . . . 26
  - 2.2.1 Blocked signals . . . 27
  - 2.2.2 Blocked transmitter filterbank . . . 28
  - 2.2.3 Blocked channel . . . 29
  - 2.2.4 Blocked receiver filterbank . . . 29
- 2.3 Analysis . . . 30
  - 2.3.1 Perfect reconstruction analysis . . . 30
  - 2.3.2 Distortion analysis . . . 32
  - 2.3.3 Noise suppression . . . 35
  - 2.3.4 Frequency selectivity of filters . . . 37
- 2.4 Problem Formulation and Design . . . 38
- 2.5 Design Example . . . 41
- 2.6 Conclusion . . . 43

3 Design of Transmultiplexers with Practical Constraints 44
- 3.1 Introduction . . . 45
- 3.2 Problem Formulation . . . 46
- 3.3 Iterative Design Procedure and Examples . . . 49
- 3.4 Conclusion . . . 56

4 Design of Transmultiplexers with Designable Filter Length **59**
4.1 Introduction 60
4.2 2-Norm Based Analysis Filters Design 61
4.3 Description of the Algorithm 65
4.4 Numerical Examples 71
4.5 Conclusion 74

5 Multirate Crosstalk Identification in xDSL Systems **76**
5.1 Introduction 77
5.2 Problem Formulation 80
5.3 Multirate Crosstalk Model 82
5.3.1 State-space model for an FIR crosstalk function 82
5.3.2 The blocked state-space model 83
5.3.3 Mapping between available input and output data 85
5.4 Multirate Recursive Identification Algorithm and Analysis 86
5.4.1 Multirate recursive least squares algorithm 87
5.4.2 Convergence analysis 89
5.5 Illustrative Examples 92
5.6 Conclusion 97

6 Crosstalk Identification in xDSL Systems with Unknown Model Order **98**
6.1 Introduction 99
6.2 Problem Formulation 100
6.3 A Recursive Algorithm 102
6.4 Numerical Example 107
6.5 Conclusion 109

7 Conclusions and Future Work **110**
7.1 Conclusions 111
7.2 Future Work 112

Bibliography **115**

List of Figures

1.1 A general nonuniform filterbank. 4
1.2 An M-channel uniform-band transmultiplexer. 5
1.3 A nonuniform transmultiplexer using traditional building blocks. . . 6
1.4 Simplified DSL Structure. 14
1.5 Simplified DSL Structure. 15
1.6 NEXT and FEXT in a multipair cable. 17

2.1 Multirate discrete-time baseband equivalent transmitter/channel/receiver model. 24
2.2 A model of the noise effect at the receiver end. 36
2.3 The magnitude Bode plots for the initial transmitter filters F_0 (solid), F_1 (dash-dot) and F_2 (dotted): dB versus $\omega/2\pi$. 41
2.4 The magnitude Bode plots for the designed transmitter filters F_0 (solid), F_1 (dash-dot) and F_2 (dotted): dB versus $\omega/2\pi$. 42
2.5 The magnitude Bode plots for the designed receiver filters $H_0 - H_7$: dB versus $\omega/2\pi$. 42
2.6 Bit error rate (BER) versus signal-to-noise ratio (SNR) in dB. 43

3.1 Example 1: The optimal J (log scale) versus the stopband energy constraints (δ) 51
3.2 A three-channel nonuniform transmultiplexer using traditional building blocks. 52
3.3 Example 2: The magnitude Bode plots for the initial F_0 (solid), F_1 (dotted) and F_2 (dash-dot): dB versus $\omega/2\pi$ 53
3.4 Example 2: The magnitude plots for the designed F_0 (solid), F_1 (dotted) and F_2 (dash-dot): dB versus ω. 54
3.5 Example 2: The magnitude plots for the designed H_0 (solid), H_1 (dotted) and H_2 (dash-dot): magnitude versus ω. 54
3.6 A three-channel nonuniform transmultiplexer using general analysis building blocks. 55
3.7 Example 3: The magnitude plots for the designed F_0 (solid), F_1 (dotted) and F_2 (dash-dot): magnitude versus ω. 56
3.8 Example 3: The magnitude plots for the designed H_{00} (solid) and H_{01} (dotted): magnitude versus ω. 57
3.9 Example 3: The magnitude plots for the designed H_{10} (solid): magnitude versus ω. 57

3.10 Example 3: The magnitude plots for the designed H_{20} (solid), H_{21} (dotted), and H_{22} (dash-dot): magnitude versus ω. 58

4.1 The two-phase algorithm. 70
4.2 The magnitude Bode plots for pre-designed synthesis filters F_0 (solid) and F_1 (dotted): dB versus $\omega/2\pi$. 71
4.3 The magnitude Bode plots for the designed analysis filters (both of length 14) H_0 (solid) and H_1 (dotted): dB versus $\omega/2\pi$. 72
4.4 The composite distortion measure J_l versus l. 72
4.5 The magnitude Bode plots for the pre-designed synthesis filters F_0 (solid), F_1 (dotted), and F_2 (dash-dot): dB versus $\omega/2\pi$. 73
4.6 The magnitude Bode plots for the designed analysis filters (of length 18) H_0 (solid), H_1 (dotted), and H_2 (dash-dot): dB versus $\omega/2\pi$. . . 74
4.7 The magnitude Bode plots for the designed synthesis filters (of length 27) F_0 (solid), F_1 (dotted), and F_2 (dash-dot): dB versus $\omega/2\pi$. . . . 74

5.1 Network model of multirate xDSL systems for one receiver. 80
5.2 A simple network model of multirate xDSL system for one primary ADSL receiver with NEXTs. 93
5.3 A simple network model of multirate xDSL system for identifying NEXTs. 94
5.4 The absolute estimation error and its upper bound. 95

6.1 The network model of xDSL systems for one primary receiver. 101
6.2 An iterative algorithm with high computational burden. 104
6.3 The cost function $J(\hat{\theta}_n)$ vs. the number of involved parameters n. . 109

List of Tables

3.1 Example 1: Stopband energy of the designed synthesis filters. 50
3.2 Example 2: Preset stopband energy and passband magnitude constraints. 53
3.3 Example 3: Preset stopband energy and passband magnitude constraints. 55

4.1 Computational complexity. 69
4.2 Composite distortion measure J for recursively increasing l and m using the two-phase algorithm. 75

5.1 xDSL Characteristics 93
5.2 Prediction performance. 96

6.1 xDSL Characteristics. 108

Chapter 1

Introduction

1.1 Multirate Systems

Multirate systems, namely, digital systems with signals of different sampling rates, typically consist of downsamplers that decrease sampling rates, upsamplers that increase sampling rates, and linear systems for filtering of signals. Multirate systems have wide applications in the area of control [14], identification [27, 29], signal processing [89], communications, econometrics and numerical mathematics. There are several reasons for this [9]:

- In large scale multivariable digital systems, often it is unrealistic, or sometimes impossible, to sample all physical signals uniformly at one single rate. In such situations, one is forced to use multirate sampling.
- Multirate systems can often achieve objectives that cannot be achieved by single rate systems.
- Multirate systems can provide better tradeoffs between performance and implementation cost.

The study of multirate systems goes back to late 1950s [49]. The idea of blocking started with Kranc in 1957 for a multirate sampled-data control system. A renaissance of research in multirate systems has occurred since 1980 with increasing interest in multirate control, multirate signal processing and communications.

- In the control community, two directions of research stand out: first, using multirate control to achieve what single rate control cannot, as well as the limitations of doing this, and second, the optimal design of multirate controllers [14].

- The driving force for studying multirate systems in signal processing comes from the need of sampling rate conversion, subband coding, and their ability to generate wavelets [89].

- In the communications community, special multirate systems can be used as a unified model to characterize a wide range of communication systems [68].

1.2 Multirate Signal Processing

Multirate signal processing, providing an efficient way in processing signals via resampling (upsampling or downsampling) of the original signals by an appropriate factor, has recently received much attention and has been widely applied to subband coding for audio, image, and video, signal analysis and representation using wavelets, subband denoising, speech processing, and so forth. Different applications also require different filterbank designs and the topic of designing one-dimensional and multidimentional filterbanks for specific applications has been of great interest.

Recently, multirate signal processing has also found increasing application in digital communications [21, 96]. Multirate building blocks are crucial ingredients in many modern communication systems, for example, the discrete multitone (DMT), digital subscriber line (DSL) and the orthogonal frequency division multiplexing (OFDM) systems as well as general filterbank precoders, just to name a few.

In general, multirate signal processing systems have many different structures; multirate filterbanks and transmultiplexers seem to be the most important ones. Much research in the past decades has dealt with the signal reconstruction problem for these multirate systems, see [89, 16, 17, 18] and the references therein.

1.2.1 Filterbanks and transmultiplexers

One important issue in multirate signal processing is the design of multirate filterbanks. A filterbank is a system of parallel filters. It usually consists of an analysis bank and a synthesis bank and is designed to separate an input signal into subbands and then to recombine these subbands. Between separation and recombination the different subbands may be treated in different ways (e.g. for data compression). Compression of audio signals is a typical filterbank application. By using filterbanks it is possible to represent signals more efficiently, and without any perceivable loss in quality.

A nonuniform multirate filterbank is shown in Figure 1.1. If the ensemble average

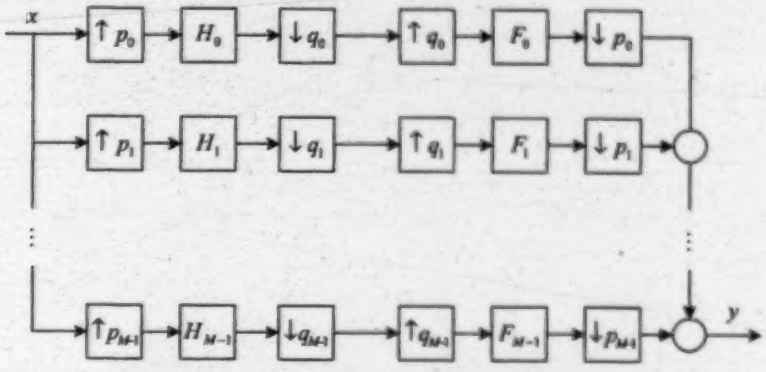

Figure 1.1: A general nonuniform filterbank.

of the energy of the signal varies greatly in different frequency bands, it will result in a high coding gain. In an M-channel maximally decimated uniform filterbank all channels have the same downsampling factor $q_i = M$ and upsampling factor $p_i = 1$. The design technique for these filterbanks are well developed, and it is generally possible to find filters so that the exact replica of the input is reconstructed in the output [89]. In a maximally decimated uniform filterbank, the bandwidth of

the filters should be equal to $\frac{\pi}{M}$ based on the Nyquist sampling theorem. In a nonuniform filterbank, the sampling rates are not the same in all channels, and thus filters in different channels may have different bandwidths.

Transmultiplexers are systems that convert time-division multiplexed (TDM) signals into frequency-division multiplexed (FDM) signals and vice versa [89]. The FDM format is often used for long distance transmission, whereas the TDM format is more convenient for digital switching. Generally, according to the sampling rates of the input signals, transmultiplexers can be divided into two types: uniform and nonuniform ones.

A schematic diagram of an M-channel uniform-band transmultiplexer is depicted in Figure 1.2: M signals $x_0, x_1, \cdots, x_{M-1}$, with the same sampling rate, are com-

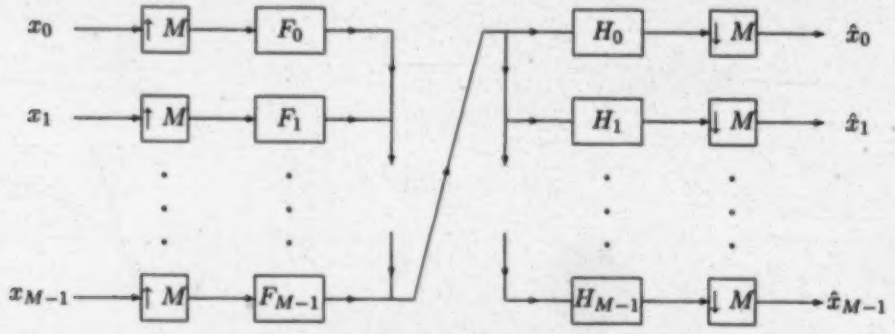

Figure 1.2: An M-channel uniform-band transmultiplexer.

bined together (TDM $\rightarrow$ FDM) through the upsamplers by a factor of M, $\uparrow M$, and the synthesis filters $F_0(z), F_1(z), \cdots, F_{M-1}(z)$; then the combined signal is coded and transmitted (not modeled), and processed (FDM $\rightarrow$ TDM) through the analysis filters $H_0(z), H_1(z), \cdots, H_{M-1}(z)$ and the downsamplers by a factor of M, $\downarrow M$, yielding reconstructed signals $\hat{x}_0, \hat{x}_1, \cdots, \hat{x}_{M-1}$.

A general nonuniform transmultiplexer built with traditional blocks is shown in Figure 1.3, where M signals x_i $(i = 0, 1, \cdots, M-1)$, with different sampling rates,

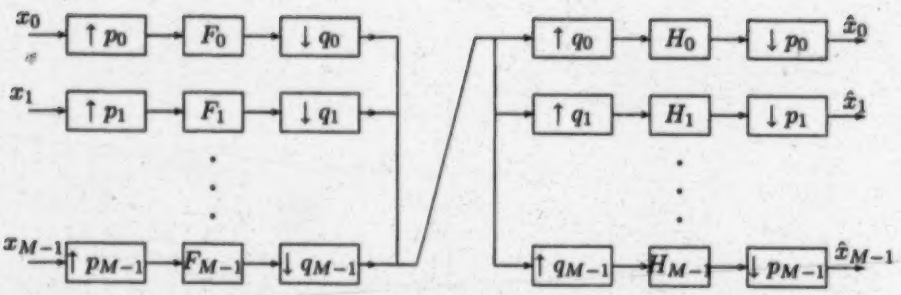

Figure 1.3: A nonuniform transmultiplexer using traditional building blocks.

are synthesized by m synthesis subsystems formed by the upsampler $\uparrow p_i$, LTI filter F_i, and downsampler $\downarrow q_i$ ($q_i < p_i$). Then, these signals are combined into a single channel and are transmitted (not modeled). In the receiver end, the combined signal is analyzed through M analysis subsystems consisting of the upsampler $\uparrow q_i$, LTI filter H_i, and downsampler $\downarrow p_i$, and hence generating the reconstructed signals $\hat{x}_i$ ($i = 0, 1, \cdots, M-1$).

In general, transmultiplexers and filterbanks are the dual of each other: A transmultiplexer can be obtained by interchanging the analysis and synthesis parts of a filterbank. A nonuniform transmultiplexer is obtained by interchanging the analysis and synthesis parts of a nonuniform filterbank. Contrary to a uniform transmultiplexer, a nonuniform transmultiplexer is not an LTI system, because the input of the different channels may have different sampling rates. A nonuniform transmultiplexers can be used for the interconversion of input signals that have different sampling rates between the TDM and FDM formats. It should be noted that the design of filterbanks can be extended to transmultiplexers, and vice versa. Therefore in the following literature review, we will not consider them separately.

1.2.2 Overview on the design of filterbanks/transmultiplexers

The first book in the area of multirate signal processing by Crochiere and Rabiner [25] in 1983 has triggered a tremendous growth of research activities in this field. The ability to process signals at multiple sampling rates has made it possible to reduce costs and improve performance in applications ranging from control engineering, signal compression to communication systems, in consumer entertainment products and sensor networks. After a decade of development (from 1983 to 1993), the theoretical work in multirate signal processing appeared to have reached a certain level of maturity, and then a detailed historical survey of the literature till 1992 was elaborated in [89] by Vaidyanathan in 1993. During the last decade (1993 to present), multirate signal processing has consistently been an active research area due to their wide range of applications in signal processing and communications.

In the following, we have generally classified current research on design of filterbanks or transmultiplexers into two categories based on their different perspectives: signal processing and control.

Perspective from Signal Processing

A major thrust of research in the design of filterbanks/transmultiplexers has focused on methods for achieving perfect reconstruction (PR), defined as the property wherein the reconstructed output signal is simply a delayed version of the input signal. There are several established types of PR filterbanks, the most popular of which are the paraunitary and the biorthogonal varieties, as well as a spates of others.

As the theory of filterbanks developed, more attention was given to systems employing aliasing cancellation, like two-band QMFs (Quadrature Mirror Filters), octave-band QMF tree-structures, and other efficient filterbanks. The PR filter-

banks began with the solution for the two-band system [24], and was later extended to multi-channel filterbanks [89]. As the traditional distortions (aliasing, magnitude, and phase) can be separately analyzed in the frequency domain, most of the early theoretical analysis and design methods were based on the frequency domain analysis. Filterbanks can also be formulated in the time domain, which was originally proposed in [60, 61]. Nussabumer's pioneering work [63] on pseudo QMF banks provides approximate alias cancellation, which is acceptable in some applications.

It is the invention of polyphase decomposition [8] that makes the multirate signal processing practically attractive. It enables the designer to carry out all computation at the "lowest rate permissable within the given context," and reduces the computational burden [89]. IIR (Infinite Impulse Response) filters can provide a computational advantages over FIR filters that are designed to meet the same specifications. However, in multirate signal processing, this advantages of IIR filters do not carry over to their use in sampling rate conversions because of the computational burden. By departing from conventional structures to the polyphase network [8], one can arrive at a unified framework that leads to a computationally efficient implementation of both IIR and FIR filters in sampling rate conversion. For IIR filterbanks design, see [87] and references therein.

In the past few years, the design of signal-dependent filterbanks has attracted the attention of the signal processing and data compression communities [86, 91, 101, 59]. These filterbanks are designed to match the statistical properties of input signals. Such filterbanks are designed to optimize a particular objective, e.g. coding gain or a multiresolution criterion, adapted for a specific class of input signals. For simplicity, the analysis and synthesis filters are often chosen to satisfy an orthonormality [91, 59] or biorthogonality [86] condition. In the orthonormal case, the optimal solution is an infinite order principal component filterbank (PCFB) [90, 6],

whereas in the biorthogonal case, the optimal filterbank is a PCFB with a parallel bank of half-whitening filters in the middle of the system [91, 59]. In the case of FIR filters, optimal signal-dependent FIR filterbanks were designed by using an iterative algorithm in [83], and general two-dimensional FIR principal component filterbanks were developed in [101].

More recently multirate systems have found application in digital communications [96, 4, 37, 21, 51, 93, 92, 52, 42]. It was shown [68] that redundant filterbank precoders offer a unifying discrete-time model that encompasses a wide range of digital modulation and coding schemes [96, 92], such as orthogonal frequency-division multiplexing (OFDM) and discrete multitone (DMT), fractional sampling, (de-)interleaving, as well as multiuser transmissions such as time division multiple access (TDMA), frequency division multiple access (FDMA), code division multiple access (CDMA), and the most recent discrete wavelet multiple access (DWMA) schemes. The research on multirate systems has been receiving new stimulus by envisioning the fact that redundant filterbank transceivers provide a common mathematical model in digital communications.

Perspective from Control

Sampled-data control systems are periodic (not time-invariant) continuous-time systems [14], while multirate filterbanks are periodic (not time-invariant) discrete-time systems [89]. Therefore, control-theoretic concept of model matching carries over very conveniently: It enables system theory to be applied to the multirate systems design for optimal reconstruction.

In the following, we briefly review the design of multirate systems starting off from the control perspective by different research groups.

- **Work by Shenoy, *et al.***

The idea of optimal model matching is central in modern control theory. The optimal model matching approach to multirate filter design was advocated by Shenoy in [70], as was the possibility of using H_∞ optimization. Shenoy, Burnside, and Parks [69] formulated the problem of l_2-induced norm and model matching for discrete-time periodic systems. They showed that the problem can be converted to a frequency-domain one of H_∞ norm optimization of the alias component matrix of the error system. They also observed that it is equivalent to convert this problem by blocking of signals to get an LTI error system. However, they did not treat the multirate filterbank systems.

As earlier methods for deriving multirate specifications may yield inappropriate structures, Shenoy [72] studied the alias-component (modulation) matrices that permit systematic specification of multirate structures, and are easily incorporated into model-matching design procedures.

- **Work by Chen, *et al.***

Since achieving perfect reconstruction alone will not necessarily result in good coding of the input, Chen and Francis [15] proposed a two-step design method to avoid designing analysis and synthesis filters simultaneously: One can design the analysis filters with regard to coding of the input signal, then design the synthesis filters for good reconstruction. In addition, a procedure was developed to design IIR synthesis filters in a multirate filterbank. The filters minimize the l_2-induced norm of the error system between the multirate filterbank and a desired pure time-delay system, and this criterion is reduced to one of H_∞ optimization, for which there is ready-made software. Further, Mirabbasi, Francis, and Chen established the connection between the traditional distortions (aliasing, magnitude, and phase

distortions) and the l_2-induced norm of the error system, which naturally bridges two research topics in different areas: signal reconstruction in signal processing and model matching in control [58].

In [79], Shu and Chen studied the synthesis filters design by minimizing the maximum energy gain of the error system for a hybrid multirate filterbank. The hybrid and multirate problem is reduced to one of H_∞ optimization involving only linear time-invariant, discrete-time systems. The filters designed are robust in the sense that uniformly good performance can be achieved for the class of all finite-energy signals.

The above work is for uniform filterbanks. A general multirate filterbank system with multiple channels and nonuniform bands was studied in [16]. The reconstruction performance was characterized by the worst-case energy gain (H_∞ norm) of the error system between the multirate systems and a pure time-delay system. Using blocking and polyphase decomposition, the multirate system was associated with an equivalent linear time-invariant (LTI) system whose transfer function can be computed by a simple procedure. Note that the proposed method cannot directly handle the so-called structural dependency involved in the nonuniform filterbank design.

Multirate filterbanks are linear periodically time-varying (LPTV) systems, for which Chen and Qiu proposed several ways to quantify aliasing effect, and also studied the optimal time-invariant approximations using operator norms [17].

In [18], Chen, Qiu and Bai proposed a general linear dual-rate structure for multirate signal processing, which encompasses the usual multirate building blocks - expanders, LTI filters, decimators, and their cascade combinations - as special cases. Using such general building blocks allows more design freedom and therefore can achieve what is otherwise impossible. This was illustrated in eliminating the structural dependency constraint in the nonuniform multirate filterbank design.

In [56], the general linear dual-rate structure was applied to the design of nonuniform filterbanks. Further in [57] the model matching problem was casted into the semidefinite programming (SDP) framework. The FIR filters involved can be achieved by efficiently solving a set of linear matrix inequalities (LMIs).

In [54], the design of uniform transmultiplexers was studied, and a measure based on the 2-norm of transfer matrices was proposed to quantify the degree of closeness to perfect reconstruction; connections of this error measure to the traditional crosstalk, magnitude, and phase distortions were established. Further in [55], using general building blocks [18], optimal design of nonuniform transmultiplexers was considered.

- **Work by Xie, *et al.***

Zhang, Wang, and Xie proposed a new multirate filterbank structure that uses a sequential sampling scheme and is different from other mutirate filterbanks where simultaneous sampling process is operating [106]. Such a structure can provide improvements in computation and implementation.

Traditional methods of converting an M-channel QMF filterbank into an LTI system via the lifting/blocking [14] usually result in a higher system dimension, which may pose some numerical difficulty [110]. In [108], following the sequential sampling scheme [106], Zhou, Xie, and Zhang studied the H_2 optimal deconvolution problem, and they showed that the H_2 norm of a periodic filter can be directly quantified in terms of periodic system matrices and LMIs without using the lifting/blocking technique.

A robust and optimal mixed H_2/H_∞ design for transmultiplexer systems was carried out in [110]. In contrast to existing work [13], where a sufficient condition is given, the result in [110] is necessary and sufficient for FIR filters.

- **Work by Gu, *et al.***

In order to design QMF banks using the least-squares type criterion, Gu and Huang [41] proposed two iterative algorithms and proved their convergence. In [44], a direct approach (without performing the polyphase decomposition) was adopted to the design of QMF banks using H_∞ optimization techniques.

Further in [42], Gu and Badran extended the filterbank design schemes to communications problems. Via the filterbank approach, channel equalization was studied [42], and state-space and transfer function methods were used in deriving the optimal channel equalizer.

- **Work by Chen, B. S., *et al.***

To deal with unavoidable channel noise, multirate Kalman synthesis filters [10] were developed to replace the conventional ones achieving optimal signal reconstruction in filterbank systems [10]. In [11], the authors studied the signal reconstruction problem for nonuniform filterbanks using the H_∞ filtering-based method without any a priori knowledge of the input signal and noise, and using the robust Kalman filtering-based method when the input signal is unknown but identifiable. Later, a mixed H_2/H_∞ design was proposed [13] for transmultiplexers with channel distortion and additive noise based on the multirate state-space model.

1.3 Digital Subscriber Line (DSL) Systems

Since the mid-1990's, we have experienced a rapid data-rate-hungry evolution of the Internet, especially with the emergence of the World Wide Web (WWW), its multimedia-intensive contents, and the booming growth of WWW hosts and users. In addition, the number of small offices/home offices (SOHO), which often require fast access to a corporate local area network (LAN), has been growing steadily in

recent years. Such high data-rate demands surpass the capability of now mature voiceband modems (< 56 kbit/s).

Digital subscriber line technology transforms an ordinary telephone line into a broadband communications link, much like adding express lanes to an existing highway. DSL increases data transmission rates by a factor of twenty or more by sending signals in previously unused high frequencies. DSL technology has added a new twist to the utility of twisted-pair telephone lines [81].

1.3.1 DSL systems

While there are many varieties of DSL technology, collectively referred to as xDSL, their overall systems are very similar. As illustrated in Figure 1.4, the DSL system

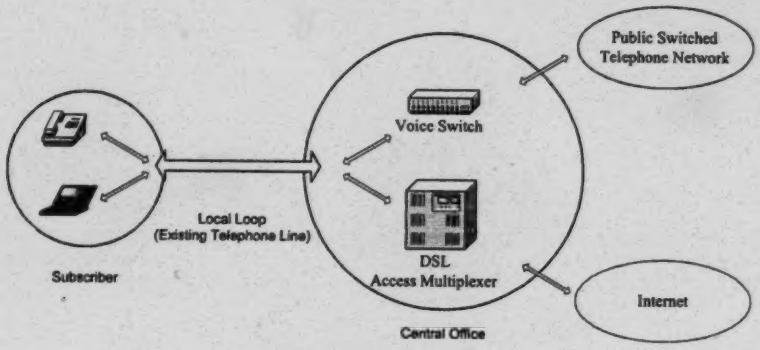

Figure 1.4: Simplified DSL Structure.

consists of the subscriber premise, central office (CO) premise, and the local loop, which connects two premises. Primary components of the CO are the DSL Access Multiplexer (DSLAM) and the CO-end modem (xTU-C). The DSLAM links the DSL traffic to a higher-speed backbone network, such as OC (Optical Carrier)-3 and OC-12, further connected to a Network Service Provider (NSP), and the xTU-C interfaces the local loop and the CO. The xTU-R is the subscriber-side counterpart

of the xTU-C. For those DSL technologies capable of coexisting with POTS – *e.g.*, Asynchronous DSL (ADSL) and Very High Speed DSL (VDSL) technologies – POTS splitters, which combine POTS and DSL service over a subscriber line, exist on the local loop side of both modems. The POTS connections are made to telephone devices on the subscriber side and to the public switched telephone network (PSTN) on the CO side [81, 82].

1.3.2 DSL reference model

As shown in the DSL reference model in Figure 1.5, a DSL consist of a local loop

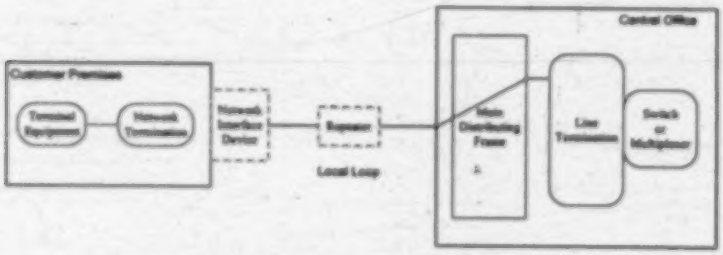

Figure 1.5: Simplified DSL Structure.

(telephone line) with a transceiver at each end of the wires. The transceiver is also known as a modem (modulator/demodulator). The transceiver at the network end of the line is called the line termination (LT) or the transmission unit at the central end (TU-C). The LT may reside within a digital subscriber line access multiplexer (DSLAM) or a DLC-RT for lines fed from a remote site. The transceiver at the customer end of line is known as the network termination (NT) or the transmission unit at the remote end (TU-R) [81, 82].

1.3.3 Types of DSL technology

Several species of DSL have resulted from the evolution of technology and the market service [104]. The DSL family includes ISDN (Integrated Services Digital Network), HDSL (High-bit-rate DSL), HDSL2 (second generation HDSL), SDSL (Single-pair, symmetric DSL), SHDSL (Single-pair, High-speed DSL), ADSL (Asymmetric DSL), and VDSL (Very-high-bit-rate DSL). Among these DSLs, ISDN, ADSL, and HDSL have been standardized by International Telecommunication Union (ITU). ITU-T Recommendation G.995.1 [45] provides a comprehensive overview of ADSL and HDSL recommendations. HDSL2, SHDSL, and VDSL are currently in the process of being standardized. SDSL is not standardized but has been deployed at various bit rate up to 2.32 Mbit/s. Characteristics of the above different DSL services can be found in [81, 104].

In summary, ADSL and VDSL offer asymmetrical data rates and coexist with the plain old telephone services by using the frequency division duplexing. VDSL also supports symmetric data transmission. In contrast, ISDN, HDSL, HDSL2, SDSL, and SHDSL offer symmetrical full-duplex data rates and uses separate pairs from the plain old telephone services [82].

1.3.4 DSL crosstalk

Crosstalk generally refers to the interference that enters a communication channel, such twisted pairs, through some coupling path. The diagram in Figure 1.6 shows two examples of crosstalk generated in a multi-pair cable [81, 82]. On the left-hand side of the figure, signal source $V_j(t)$ transmits a signal at full power on twisted wire pair j. This signal, when propagating through the loop, generated two types of crosstalk into the other wire pairs in the cable. The crosstalk that appears

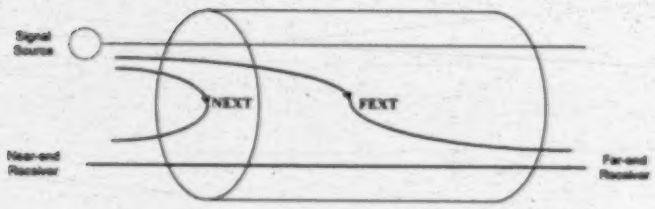

Figure 1.6: NEXT and FEXT in a multipair cable.

on the left-hand side, $x_n(t)$ in wire pair i, is called near-end crosstalk (NEXT) because it is at the same end of the cable as the crosstalk signal source. The crosstalk that appears on the right-hand side, $x_f(t)$ in wire pair i, is called far-end crosstalk (FEXT) because the crosstalk appears on the end of the loop opposite to the reference signal source.

In the loop plant, NEXT is generally far more damaging than FEXT because NEXT has a higher coupling coefficient - the near-end crosstalk coupling is approximately six orders of magnitude greater than that for far-end crosstalk. Unlike far-end crosstalk, near-end crosstalk directly disturbs the received signal transmitted from the far end after it has experienced the propagation loss from traversing the distance from the far end down the disturbed wire pair. On the other hand, the coupling for NEXT increases at 15 dB per decade with increasing frequency, whereas the coupling for FEXT increases at 20 dB per decade with increasing frequency.

1.3.5 Overview on the DSL crosstalk identification

One major impairment of the current xDSL systems is the severe crosstalk [81, 104] among the telephone lines in the same or neighboring bundles. The severe crosstalk not only limits the maximum data rate of any individual line but can also degrade the existing services if a new service is added to the bundle. Thus, in the currently deployed system, the worst crosstalk scenario is assumed to prevent the breakdown

of the system. However, this assumption is often too pessimistic in a real scenario and, hence, limits the overall performance of the system.

Recently, crosstalk identification in xDSL systems has attracted a lot of attention due to the significant benefits of having an accurate description of all cable services that generate crosstalk into a given pair [23, 36, 65, 105, 104].

- First, the crosstalk functions can be used by a multi-user detector in the modem to cancel the strong interference from other lines.
- Second, it can improve the service performance of DSL systems by a better spectrum assignment for different users.
- Third, the crosstalk profiles are invaluable for the telephone operators to maintain, diagnose, and expand the current systems.

Zeng, *et al.* [105] presented a method to identify the crosstalk transfer function between different services. A novel concept of an impartial central network maintenance center (NMC) is proposed to identify the crosstalk functions for all participated operators and feed back the identified crosstalk functions to them. The NMC captures the transmitted and received data from each DSL modem for a predefined time span. Essentially, the NMC has the knowledge of both the input and the output data from different modems. As the DSL modems are not synchronized, the time stamps associated with the data from different modems have timing offset up to several milliseconds. A cross-correlation technique was used in [105] to solve the timing offset problem.

Papandreou, *et al.* [65] proposed a crosstalk identification method for ADSL systems operating in the same binder. The method estimates the crosstalk coupling functions in real time, by exploiting the initialization procedure of a new activated modem.

1.4 Motivation and Objectives

The main objective of this thesis is to carry over control-theoretic methodologies to solve DSP and communications problems, and to develop design methods to address practical issues for multirate systems and DSL systems. Our motivations and objectives are given below:

1. The multirate filterbank-based transceiver model was proposed [37, 68] as a unifying framework able to encompass existing modulations and equalization schemes. Motivated by the generality and importance of filterbank-based transceivers, we aim to design transceivers in the frequency-domain based on the composite criterion that captures traditional distortions. Different from the work in [37, 68] in time-domain, the frequency-domain scheme can easily incorporate frequency selectivity constraints and noise suppression into the design.

2. The performance of a transmultiplexer system is affected significantly by the overall structure and the reconstruction quality as well as by the characteristics of the individual analysis and synthesis filters. On one hand, structural properties include the number of frequency bands, the bandwidths of the filters, and the overall frequency coverage. The reconstruction quality is mainly a function of its ability to reconstruct the input signal at the output. On the other hand, the characteristics of involved filters include the passband ripples, the transition bandwidths and behavior, the stopband ripples, the phase characteristics, the filter type (i.e., FIR or IIR), the order of the filters, and the computational efficiency of the implementation. Sometimes, a small loss in reconstruction accuracy can be traded for gains elsewhere, such as in computational complexity. Therefore, in order to address all of these separate issues

simultaneously in a single design context, we aim to incorporate some practical constraints on the individual filters into the overall reconstruction design by using the model matching methodology.

3. In most existing work on the design of filterbanks/transmultiplexers, the analysis and synthesis filters always have pre-determined filter length, which, of course, do not consider how to design the most appropriate filter length and reduce the overall complexity. Especially, in applications where it is important to minimize the complexity of either analysis or synthesis filters, the traditional design methods are not suitable. It seems that little attention has been paid to this design problem in the literature. In this study, we aim to develop a computationally efficient transmultiplexer design scheme that can not only achieve close-to-perfect reconstruction performance but also obtain designable filter length.

4. The crosstalk among the twisted pairs in the same or neighboring bundles in a cable is a major impairment in the current xDSL systems. It is invaluable for a service operator to obtain the crosstalk profile because this information can be used to facilitate the provisioning, maintenance, and diagnosis of the xDSL systems, and to significantly improve the xDSL systems performance. However, xDSL crosstalk identification, an emerging topic that is extremely useful for service operators, has not been fully investigated. In this study, we target at two practical and important problems that have not been studied in this area in the literature: Multirate xDSL crosstalk identification, and crosstalk identification in xDSL systems with unknown model order.

1.5 Organization of the Thesis

In Chapter 2, we consider the design of filterbank-based transceivers. A composite error criterion is proposed to capture all three traditional distortions. Incorporating noise attenuation and filter bandlimiting properties into this error criterion, an optimal design procedure is developed and applied to a transceiver design example, yielding an FIR transceiver that has good frequency-selective properties and is close to perfect reconstruction. As a least squares solution is given in closed form in each iteration, the algorithm is easy to implement.

In Chapter 3, we study uniform and nonuniform transmultiplexer design problems. The main contribution is the incorporation of stopband energy and passband magnitude constraints directly in the design optimization, thus making an important step forward in addressing practical issues about frequency selectivity. The design procedure proposed considers both signal reconstruction and filter characteristics.

In Chapter 4, motivated by the facts that shorter length filters offer considerable improvements in computation and hardware implementation and that designable filter length brings more design flexibility, we propose a novel transmultiplexer design method that can not only achieve close-to-perfect reconstruction but also obtain designable filter length. The proposed method is based on a composite distortion measure – 2-norm of the error transfer matrix of the transmultiplexer. Central to the development is to provide an efficient way to recursively design the filters in the transmultiplexer and evaluate the composite distortion measure, which greatly improves the computation efficiency.

Chapter 5 and 6 are about the crosstalk identification for xDSL systems. Crosstalk between multiple services transmitting through the same telephone cable is the primary limitation to digital subscriber line services. From a spectrum management

point of view, it is important to have an accurate map of all the services that generate crosstalk into a given pair.

Inspired by practical considerations that the transmitted signals are operating in different symbol rates in xDSL systems, Chapter 5 focuses on multirate xDSL crosstalk identification. In particular, by using the blocking technique, we derive blocked state-space models for multirate xDSL networks, and set up the mapping relationship between available input and output data. Further, we use the least squares principle to identify the crosstalk functions, and study the convergence rate and upper bound of the parameter estimation error.

In practice, the model order of the crosstalk function is generally unknown. Chapter 6 focuses on the xDSL crosstalk identification with unknown model order. A recursive algorithm for multi-channel FIR xDSL systems is proposed to identify the crosstalk model order and parameters simultaneously. The most appropriate model order is then determined by examination of the cost functions. The recursive formulae for the cost function and the parameter estimate are derived, which greatly improve the computational efficiency.

The last chapter summarizes the work in this thesis, and outlines some possible future research directions.

Chapter 2

Optimal Design for Filterbank-Based Transceivers

2.1 Introduction

Inter-symbol interference (ISI) is a common problem in telecommunication systems, such as terrestrial television broadcasting, digital data communication systems, and cellular mobile communication systems. Usually the channel distortion results in ISI, which, if left uncompensated, causes high error rates. The solution to the ISI problem is to design a receiver that employs a means for compensating or reducing the ISI in the received signal. The compensator for the ISI is the so called equalizer. For these problems, the filterbank approach [21, 52, 37, 42, 68] has gained practical interest recently.

The multirate filterbank-based transceiver model was proposed in [37] as a unifying framework able to encompass existing modulations and equalization schemes. Further in [68], the multirate filterbank-based transceiver model, as shown in Figure 2.1, was studied in detail. The filterbank-based transceiver introduces trans-

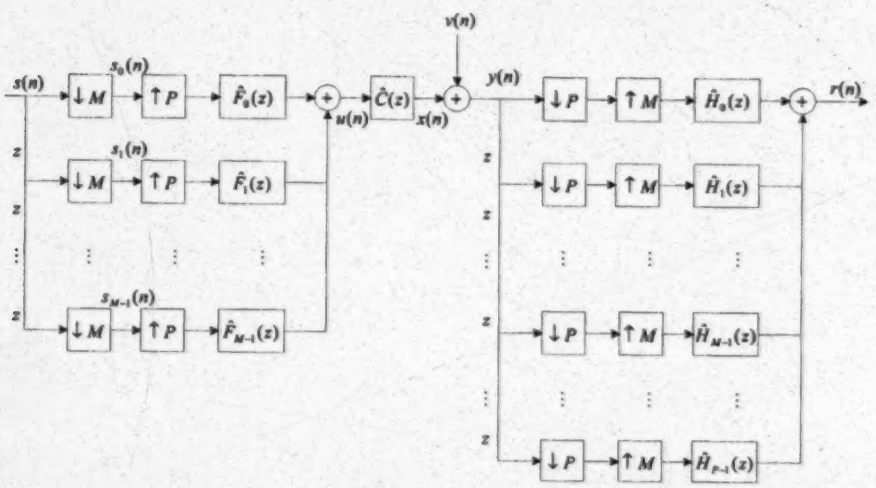

Figure 2.1: Multirate discrete-time baseband equivalent transmitter/channel/receiver model.

mitter redundancy using filterbank precoders, and generalizes existing modulations

including OFDM, DMT, TDMA and CDMA schemes encountered with single- and multiuser communications [68]. Recently in [42], based on the filterbank approach, the optimal channel equalization is studied: An optimal receiver filterbank, which is a modified Kalman filter, is obtained.

Motivated by the generality and importance of filterbank-based transceivers, this chapter focuses on frequency-domain analysis and optimal design issues for filterbank-based transceivers. The contributions of this work is as follows:

- Contrary to a time-domain study [68], our work is developed along the line of frequency-domain analysis. Frequency-domain models are obtained using the blocking technique. Based on such models, a composite error criterion is proposed to quantify the degree to perfect reconstruction. This frequency-domain criterion captures the traditional distortions.

- In the transceiver design, we apply and incorporate the model matching methodology [16]: Instead of designing for perfect reconstruction, we design for close-to-perfect reconstruction with effective band separation. This idea was explored in filterbanks [16] and transmultiplexers [74]. Under some mild condition, one can always get arbitrarily close to perfect reconstruction by trading off filter complexity and time delay in reconstruction.

- Control of filter stopband energy is incorporated in our design. This is important, since narrowband noise could induce serious impairment due to poor stopbands of filters involved [96]: If the receiving filters have poor stopband attenuation, all the neighboring bands would be affected when there is a strong narrowband noise. The resulting ISI can seriously degrade the system performance [64].

The rest of the chapter is organized as follows. In Section 2.2 the blocked model of

the filterbank-based transceiver and the perfect reconstruction are briefly reviewed. In Section 2.3 the transceiver system is analyzed in several aspects based on the blocked model. Section 2.4 formulates the optimal design problem as a least squares one and develops an iterative design procedure for the filterbank-based transceiver. The proposed design method is illustrated in detail with an example in Section 2.5. Finally, Section 2.6 offers some concluding remarks.

We conclude this section by introducing some notation. The signals are denoted by small letters, e.g., r. $\underline{r}$ (underlining denotes blocking) is the blocked signal. $\hat{\underline{r}}(z)$ denotes the z-transform of $\underline{r}$. The systems are represented as time-domain operators, denoted by capital letters, e.g., T. If a system T is linear time invariant (LTI), its transfer function (matrix) is written as $\hat{T}(z)$. The notation $\|\cdot\|_2$ stands for the 2-norm for transceiver matrices.

2.2 Blocked Models

Figure 2.1 shows the discrete-time multirate filterbank model for the baseband communication system [68]. It consists of the transmitter filterbank $\hat{F}_m(z)$ ($m = 0, \cdots, M-1$), the receiver filterbank $\hat{H}_p(z)$ ($p = 0, \cdots, P-1$), and the communication channel modeled by the transfer function $C(z)$, which is assumed to be causal and stable. The input serial data stream $s(n)$ and its successively time-advanced versions are downsampled by a factor M to get M parallel substreams $s_0(n), s_1(n), \cdots s_{M-1}(n)$ as shown in Figure 2.1. These substreams are then upsampled by a factor P and processed by filters $\hat{F}_m(z)$; the combined output $u(n)$ is then transmitted over the channel $\hat{C}(z)$, which is corrupted at the output by an additive noise $v(n)$, assumed to be stationary and white. At the receiver end, the received signal $y(n)$ and its successively shifted versions are then downsampled by a factor P, upsampled by a factor M, and processed by filters $\hat{H}_p(z)$; the combined output

forms the reconstructed signal $r(n)$.

The overall system $T(s \mapsto r)$ in Figure 2.1 is

$$T = (A)\,C\,(S) = \left(\sum_{j=0}^{P-1} A_j\right) C \left(\sum_{i=0}^{M-1} S_i\right).$$

Here S_i and A_j are the i-th transmitter subsystem and the j-th receiver subsystem:

$$S_i = F_i E_P D_M U^{-i}, \quad A_j = H_j E_M D_P U^{-j},$$

U being the unit time delay with transfer function z^{-1}.

In the following, we develop the blocked model for the multirate system in Figure 2.1 [42]. As we will see later, the polyphase representation will facilitate a systematic study of filterbank-based transceivers.

2.2.1 Blocked signals

Let ℓ be the space of discrete-time signals defined on the set of time set $\{0, 1, 2, \cdots\}$. A signal a in ℓ can be written

$$\{a(0), a(1), a(2), \cdots\}.$$

For an integer $p > 0$, define the p-fold *blocking operator*, L_p, via $\underline{a} = L_p a$ (underlining denotes blocking):

$$\{a(0), a(1), \cdots\} \mapsto \left\{ \begin{bmatrix} a(0) \\ a(1) \\ \vdots \\ a(p-1) \end{bmatrix}, \begin{bmatrix} a(p) \\ a(p+1) \\ \vdots \\ a(2p-1) \end{bmatrix}, \cdots \right\}. \tag{2.1}$$

L_p maps ℓ to ℓ^p, the external direct sum of p copies of ℓ. If the underlying period for a is h, the underlying period for the blocked signal $\underline{a}$ is ph. The inverse L_p^{-1}, mapping ℓ^p to ℓ, amounts to reversing the operation in (2.1).

In the frequency domain, bring in the p-fold *polyphase decomposition* [89] for the z-transform of a:

$$\hat{a}(z) = \sum_{j=0}^{p-1} z^{-j} \hat{a}_j(z^p). \tag{2.2}$$

This representation is unique for a given integer p. Now define the p-fold *polyphase vector* of $\hat{a}$ as

$$\begin{bmatrix} \hat{a}_0(z) \\ \hat{a}_1(z) \\ \vdots \\ \hat{a}_{p-1}(z) \end{bmatrix}.$$

This is the z-transform of $\underline{a}$.

2.2.2 Blocked transmitter filterbank

In Figure 2.1, the M substreams $s_m(n) := s(nM+m)$ $(m = 0, 1, \cdots, M)$ form the components of the blocked input stream

$$\underline{s} = L_M s,$$

the z-transform of the blocked input $\underline{s}$ being

$$\hat{\underline{s}}(z) = \sum_{n=0}^{\infty} \underline{s}(n) z^{-n} = \left[\begin{array}{cccc} \hat{s}_0(z), & \hat{s}_1(z), & \cdots, & \hat{s}_{M-1}(z) \end{array} \right]^T,$$

where

$$\hat{s}_m(z) = \sum_{n=0}^{\infty} s(nM+m) z^{-n}.$$

We wish to do P-fold blocking to the input signal of the channel, u

$$\underline{u} = L_P u.$$

The P-fold polyphase decomposition of $\hat{F}_m(z)$ is

$$\hat{F}_m(z) = \sum_{p=0}^{P-1} z^{-p} \hat{F}_{pm}(z^P), \quad m = 0, 1, \cdots, M-1.$$

Here, $\hat{F}_{pm}(z)$ $(p = 0, \cdots, P-1)$ represent the polyphase components of the m-th transmitter filter.

Then, we have

$$\hat{\underline{u}}(z) = \hat{\underline{F}}(z) \hat{\underline{s}}(z),$$

where the transfer matrix of the blocked transmitter filterbank is

$$\underline{\hat{F}}(z) = \begin{bmatrix} \hat{F}_{00}(z) & \hat{F}_{01}(z) & \cdots & \hat{F}_{0,M-1}(z) \\ \hat{F}_{10}(z) & \hat{F}_{11}(z) & \cdots & \hat{F}_{1,M-1}(z) \\ \vdots & \vdots & \cdots & \vdots \\ \hat{F}_{P-1,0}(z) & \hat{F}_{P-1,1}(z) & \cdots & \hat{F}_{P-1,M-1}(z) \end{bmatrix}. \tag{2.3}$$

2.2.3 Blocked channel

Block the channel's output signal x and the noise signal v both with L_P, we can get

$$\underline{x} = L_P x, \quad \underline{v} = L_P v.$$

In light of **Lemma 3** in [16], the P-fold polyphase matrix of the channel transfer function $\hat{C}(z)$ is

$$\underline{\hat{C}}(z) = \begin{bmatrix} \hat{C}_0(z) & z^{-1}\hat{C}_{P-1}(z) & \cdots & z^{-1}\hat{C}_1(z) \\ \hat{C}_1(z) & \hat{C}_0(z) & \cdots & z^{-1}\hat{C}_2(z) \\ \vdots & \vdots & \cdots & \vdots \\ \hat{C}_{P-1}(z) & \hat{C}_{P-2}(z) & \cdots & \hat{C}_0(z) \end{bmatrix}, \tag{2.4}$$

where $\hat{C}_p(z)$ $(p = 0, \cdots, P-1)$ are the polyphase components of the $\hat{C}(z)$, which are defined in

$$\hat{C}(z) = \sum_{p=0}^{P-1} z^{-p}\hat{C}_p(z^P).$$

Then, the z-transform of the blocked received signal (considering the noise) can be written as

$$\underline{\hat{y}}(z) = \underline{\hat{x}}(z) + \underline{\hat{v}}(z) = \underline{\hat{C}}(z)\underline{\hat{E}}(z)\underline{\hat{s}}(z) + \underline{\hat{v}}(z).$$

2.2.4 Blocked receiver filterbank

Similarly as in Section 2.2.2, block the reconstructed signal r

$$\underline{r} = L_M r,$$

and define the M-fold polyphase decomposition of $\hat{H}_p(z)$ as

$$\hat{H}_p(z) = \sum_{m=0}^{M-1} z^{-m}\hat{H}_{mp}(z^M), \quad p = 0, 1, \cdots, P-1,$$

where $\hat{H}_{mp}(z)$ $(m = 0, \cdots, M-1)$ represent the polyphase components of the p-th receiver filter; then we have

$$\hat{\underline{r}}(z) = \hat{\underline{H}}(z)\hat{\underline{y}}(z),$$

where the transfer matrix of the blocked receiver filterbank is

$$\hat{\underline{H}}(z) = \begin{bmatrix} \hat{H}_{00}(z) & \hat{H}_{01}(z) & \cdots & \hat{H}_{0,P-1}(z) \\ \hat{H}_{10}(z) & \hat{H}_{11}(z) & \cdots & \hat{H}_{1,P-1}(z) \\ \vdots & \vdots & \cdots & \vdots \\ \hat{H}_{M-1,1}(z) & \hat{H}_{M-1,1}(z) & \cdots & \hat{H}_{M-1,P-1}(z) \end{bmatrix}. \tag{2.5}$$

Therefore

$$\hat{\underline{r}}(z) = \hat{\underline{H}}(z)\hat{\underline{C}}(z)\hat{\underline{E}}(z)\hat{\underline{s}}(z) + \hat{\underline{H}}(z)\hat{\underline{v}}(z).$$

Thus $\hat{\underline{T}}(z) = \hat{\underline{H}}(z)\hat{\underline{C}}(z)\hat{\underline{E}}(z)$ serves as a frequency-domain model for the general multirate system (in the absence of noise) in Figure 2.1.

2.3 Analysis

In this section, we study analysis issues such as perfect reconstruction, distortion analysis, and the effect of noise.

2.3.1 Perfect reconstruction analysis

The blocked general multirate system (in the absence of noise) is LTI with $\hat{\underline{T}}(z) = \hat{\underline{H}}(z)\hat{\underline{C}}(z)\hat{\underline{E}}(z)$. We can write $\hat{\underline{T}}(z)$ as an $M \times M$ matrix:

$$\hat{\underline{T}}(z) = \begin{bmatrix} \hat{T}_{00}(z) & \hat{T}_{01}(z) & \cdots & \hat{T}_{0,M-1}(z) \\ \hat{T}_{10}(z) & \hat{T}_{11}(z) & \cdots & \hat{T}_{1,M-1}(z) \\ \vdots & \vdots & & \vdots \\ \hat{T}_{M-1,0}(z) & \hat{T}_{M-1,1}(z) & \cdots & \hat{T}_{M-1,M-1}(z) \end{bmatrix}. \tag{2.6}$$

The transceiver achieves perfect reconstruction if in Figure 2.1 r is a delayed version of s, i.e., if there exists nonnegative integer d such that $T = T_d$, where T_d is the time-delay system with transfer function $\hat{T}_d(z) = z^{-d}$. Blocking T_d the same way as we blocked T, we can state a condition for perfect reconstruction in terms of the blocked transfer matrices.

Theorem 1 *The general multirate system (free of noise) in Figure 2.1 achieves perfect reconstruction iff there exist some integers k and l, $k \geq 0$, $0 \leq l \leq M-1$, such that*

$$\underline{\hat{H}}(z)\underline{\hat{C}}(z)\underline{\hat{F}}(z) = z^{-k}\begin{bmatrix} 0 & z^{-1}I_l \\ I_{M-l} & 0 \end{bmatrix}, \tag{2.7}$$

where I_l and I_{M-l} are the $l \times l$ and $(M-l) \times (M-l)$ identity matrices, respectively. Moreover, if this condition is satisfied, $\hat{T}(z) = z^{-(kM+l)}$.

Proof: From the previous discussion, perfect reconstruction is obtained iff for some integers d, $\underline{\hat{T}}(z) = \underline{\hat{T}_d}(z)$. To get $\underline{\hat{T}_d}(z)$, the M-fold polyphase matrix for $\hat{T}_d(z)$, write $d = kM + l$ for some unique integers k and l with $k \geq 0$ and $0 \leq l \leq M-1$; then the polyphase components of $\hat{T}_d(z)$ are given by

$$\hat{T}_d^j(z) = \begin{cases} z^{-k}, & j = l, \\ 0, & j \neq l. \end{cases}$$

Hence $\underline{\hat{T}_d}$ equals to the right-hand side of (2.7) by **Lemma 3** in [16]. The theorem is thus proven. □

Theorem 2 *Given the channel transfer function $C(z)$, assume that the transmitter and receiver subsystems are stable and designable. Then perfect reconstruction is possible to achieve if the following two conditions are satisfied:*

1. *$P \geq M$;*
2. *$C(z)$ is minimum-phase.*

Furthermore, if perfect reconstruction is possible, then $P \geq M$.

Proof:

- **Part 1.** If $P \geq M$ and $C(z)$ is minimum phase, then we can always choose $\underline{\hat{F}}(z)$ to satisfy

$$\operatorname{rank}\left\{\underline{\hat{C}}(z)\underline{\hat{F}}(z)\left\{z^{-k}\begin{bmatrix} 0 & z^{-1}I_l \\ I_{M-l} & 0 \end{bmatrix}\right\}^{-1}\right\} = M. \tag{2.8}$$

Therefore, taking $\underline{\hat{H}}(z)$ as a causal and stable left inverse of the transfer matrix in (2.8), we have perfect reconstruction.

- **Part 2.** If the perfect reconstruction is possible, then the rank of the left-hand side of (2.7) should be equal to that of the right-hand side, which is M. Observing the size of the matrices on the left-hand side, the rank is less than or equal to $\min(P, M)$. Therefore $P \geq M$.

□

Remark: Here, for perfect reconstruction, the channel is not necessary to be minimum-phase, which is one of the benefits of the introduced transmitter redundancy [68] (as shown in Figure 2.1). This property is attractive because channels are usually non-minimum phase in many applications. The following counterexample serves to illustrate this advantage.

A counterexample: Set $P = 2$ and $M = 1$. Choose $l = 0$ and $k = 0$. The non-minimum phase channel is $\hat{C}(z) = \frac{1}{3} + \frac{1}{2}z^{-3}$, and thus by (2.4) we have

$$\underline{\hat{C}}(z) = \begin{bmatrix} \hat{C}_0(z) & z^{-1}\hat{C}_1(z) \\ \hat{C}_1(z) & \hat{C}_0(z) \end{bmatrix} = \begin{bmatrix} \frac{1}{3} & z^{-1}\hat{C}_1(z) \\ \frac{1}{2}z^{-1} & \hat{C}_0(z) \end{bmatrix}.$$

Then we can design $\hat{F}_0(z) = 1$, $\hat{H}_0(z) = -\frac{3}{2}z^{-1} + 3$, and $\hat{H}_1(z) = 1$. By (2.3) and (2.5) we have

$$\underline{\hat{F}}(z) = \begin{bmatrix} 1 \\ 0 \end{bmatrix}, \quad \underline{\hat{H}}(z) = \begin{bmatrix} -\frac{3}{2}z^{-1} + 3, & 1 \end{bmatrix}.$$

Therefore $\underline{\hat{H}}(z)\underline{\hat{C}}(z)\underline{\hat{F}}(z) = 1$, which means perfect reconstruction (although the channel is non-minimum phase.

2.3.2 Distortion analysis

Perfect reconstruction synthesis filterbanks at the transmitter and analysis filterbanks at the receiver allow perfect recovery of communication symbols, but the challenges arise with ISI-inducing channels and noise, either of which destroy the

perfect reconstruction property. Many practical transceivers do not achieve perfect reconstruction but get close to perfect reconstruction. In order to measure the degree of closeness to perfect reconstruction, we shall introduce three traditional quantities to measure sources of distortions: aliasing distortion, magnitude and phase distortions [89]. These distortion measures are based on the blocked model $\underline{\hat{T}}(z)$.

Lemma 1 *[17] An LPTV system G with period t can be uniquely decomposed into*

$$G = G^{ti} + G^{tv}$$

satisfying the two properties

(i) G^{ti} is the optimal LTI approximation of G in the sense that it minimizes $\|\underline{G}(z) - \underline{Q}(z)\|_2$ over the class of LTI Q's [$\underline{G}$ denotes the blocked system $L_t G L_t^{-1}$; similarly for $\underline{Q}$].

(ii) $\|\underline{G}(z)\|_2^2 = t\|G^{ti}(z)\|_2^2 + \|\underline{G^{tv}}(z)\|_2^2$.

Back to our transceiver problem, the system from s to r is LPTV with period M; decompose this into $G^{ti} + G^{tv}$, where G^{ti} is the LTI component and G^{tv} the time-varying component. Thus we have

$$\underline{\hat{T}}(z) = \underline{G^{ti}}(z) + \underline{G^{tv}}(z). \tag{2.9}$$

Aliasing distortion in the system is defined by

$$\text{AD} = \|\underline{G^{tv}}(z)\|_2. \tag{2.10}$$

Even if AD is zero, and then the LPTV system reduces to an LTI system G^{ti}, it may still have errors in magnitude and phase compared with the ideal time delay

z^{-d}; define the following quantities

$$\text{MD} = \left[\frac{1}{2\pi}\int_0^{2\pi} \left(|G^{ti}(e^{j\omega})| - 1\right)^2 \, d\omega\right]^{1/2}, \tag{2.11}$$

$$\text{PD} = \left\{\frac{1}{2\pi}\int_0^{2\pi} \sin^2\left[\angle G^{ti}(e^{j\omega}) + d\omega\right] \, d\omega\right\}^{1/2}. \tag{2.12}$$

Note that MD and PD are defined across all frequencies: $(\text{MD})^2$ is the energy of the magnitude distortion, and PD the energy of sine of the phase distortion $\phi(\omega) = \angle G^{ti}(e^{j\omega}) + d\omega$.

Next, we propose a composite distortion measure which captures all the three types of distortions and is relatively easy to use in design. The new distortion measure is the 2-norm of the blocked error transfer matrix:

$$J = \|\underline{\hat{T}}(z) - \underline{\hat{T}}_d(z)\|_2.$$

Such a measure is appropriate because in the next theorem we establish connections between J and the three types of distortions discussed earlier.

Lemma 2 *[55] Let G be a stable LTI system. Comparing $G(z)$ with the time delay z^{-d}, we have the following inequalities:*

$$|G(e^{j\omega}) - e^{-jd\omega}| \geq \left||G(e^{j\omega})| - 1\right|, \tag{2.13}$$

$$|G(e^{j\omega}) - e^{-jd\omega}|^2 \geq \sin^2\left[\angle G(e^{j\omega}) + d\omega\right]. \tag{2.14}$$

Theorem 3 AD *and* MD *relate to J via*

$$\text{AD}^2 + M(\text{MD})^2 \leq J^2; \tag{2.15}$$

whereas AD *and* PD *relate to J via*

$$\text{AD}^2 + M(\text{PD})^2 \leq J^2. \tag{2.16}$$

Proof: From (2.9) and Lemma 1 we get

$$J^2 = \|\hat{\underline{T}}(z) - \hat{\underline{T}}_d(z)\|_2^2 = \|\underline{G^{ti}}(z) + \underline{G^{tv}}(z) - \hat{\underline{T}}_d(z)\|_2^2 \quad (2.17)$$

$$= M\|G^{ti}(z) - z^{-d}\|_2^2 + \|\underline{G^{tv}}(z)\|_2^2. \quad (2.18)$$

Note (2.10) to get

$$J^2 = \mathrm{AD}^2 + M\|G^{ti}(z) - z^{-d}\|_2^2. \quad (2.19)$$

Now by definition,

$$\|G^{ti}(z) - z^{-d}\|_2^2 = \frac{1}{2\pi}\int_0^{2\pi} |G^{ti}(e^{j\omega}) - e^{-jd\omega}|^2\, d\omega. \quad (2.20)$$

Invoke Lemma 2 to get

$$|G^{ti}(e^{j\omega}) - e^{-jd\omega}| \geq \left||G^{ti}(e^{j\omega})| - 1\right|,$$

$$|G^{ti}(e^{j\omega}) - e^{-jd\omega}|^2 \geq \sin^2\left[\angle G^{ti}(e^{j\omega}) + d\omega\right].$$

Combining these two equalities with (2.20) and noting the definitions of MD and PD in (2.11) and (2.12), we have

$$\|G^{ti}(z) - z^{-d}\|_2 \geq \mathrm{MD},$$

$$\|G^{ti}(z) - z^{-d}\|_2 \geq \mathrm{PD}.$$

The proof is complete by noting (2.19) and the above two inequalities. □

Then it is clear from Theorem 3 that all distortions (AD, MD, and PD) are bounded above by J. Therefore it makes sense to minimize J in transceiver design because this suboptimizes the three distortions simultaneously.

2.3.3 Noise suppression

In Figure 2.2, $q(n)$ represents the noise effect at the receiver end. If we want to minimize the root-mean-square value of q, it is equivalent to minimize the 2-norm

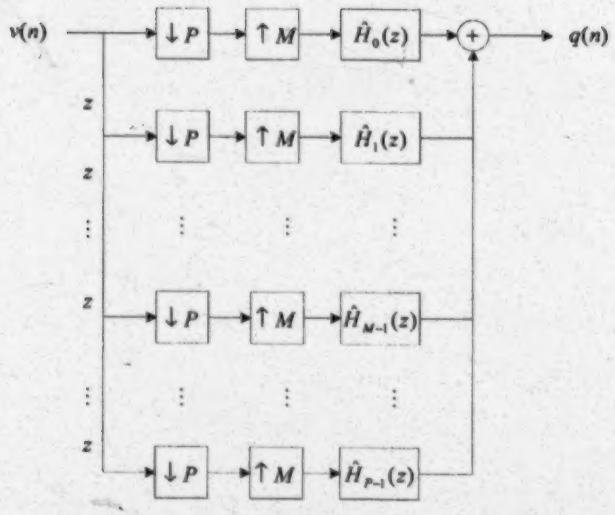

Figure 2.2: A model of the noise effect at the receiver end.

of the blocked transfer matrix from $\underline{v}(n)$ (standard white noise) to $\underline{q}(n)$. Therefore, the objective function for attenuating the output noise effect can be

$$J_N = \|\underline{\hat{H}}(z)\|_2. \tag{2.21}$$

Fortunately, minimizing the objective function J_N is consistent with not only minimizing transmitter power but also maximizing bit rate. We will show this in the following. For simplicity we assume that $s(n)$'s are Pulse Amplitude Modulated (PAM) symbols. Assuming that $s(n)$ is a random variable with 2^b equiprobable levels, its variance represents the average power P_w in the symbol $s(n)$. For the purpose of variance calculation, the model of the noise effect $q(n)$ at the receiver end can therefore be taken as in Figure 2.2. Let σ_q^2 be the variance of $q(n)$. Then the probability of error in detecting the symbol $s(n)$ is [64]

$$\mathcal{P}_e = 2(1-2^{-b})\mathcal{Q}\left(\sqrt{\frac{2P_w}{(2^{2b}-1)\sigma_q^2}}\right), \tag{2.22}$$

where $\mathcal{Q}(v) = \int_v^\infty e^{-u^2/2}du/\sqrt{2\pi}$.

1. **Minimizing transmitted power:** Since the Q-function can be inverted for any nonnegative argument, we can invert (2.22) to obtain [93]

$$P_w = \beta(\mathcal{P}_e, b) \times \sigma_q^2,$$

where the function $\beta(\cdot,\cdot)$ is certain function related with the inverting operation. The above expression means that if the probability of error has to be $\mathcal{P}_e$ or less at the bit rate b, then the power in $s(n)$ has to be at least as large as P_w. Let us assume that the bit rate b and the probability of error $\mathcal{P}_e$ are fixed, the power required depends on the distribution of noise variance σ_q^2.

2. **Maximizing bit rate:** Revisiting the error probability expression (2.22), let us now invert it to obtain a formula for the bit rate b [93]

$$b = 0.5 \log_2 \left(1 + \frac{3}{[Q^{-1}(\mathcal{P}_e)/2]^2} \frac{P_w}{\sigma_q^2}\right).$$

If we assume that the probability of error $\mathcal{P}_e$ and the average power P_w are fixed, then the bit rate b increases with the decrease of the distribution of noise variance σ_q^2.

2.3.4 Frequency selectivity of filters

Filters with frequency selectivity are of particular importance in communications systems. In order to obtain better bandlimiting property, we minimize the stopband energy of filters involved. To see this, take the objective function(s) for H_i in the receiver filterbank as an example; we have

$$J_{H_i} = \int_{\Omega_{H_i}} |H_i(w)|^2 \, dw, \quad i = 0, 1, \cdots, P-1, \tag{2.23}$$

where Ω_{H_i} defines the stopband frequency interval(s) for H_i. Similarly, J_{F_i} can be computed.

In this chapter, we will consider only FIR filters. The frequency response of a real N-tap FIR filter H_i is given by

$$H_i(\omega) = \sum_{n=0}^{N-1} h_i(n) e^{-jn\omega} = h_i^T \phi_i(\omega),$$

where

$$\begin{aligned} h_i^T &= [\ h_i(0),\ \ h_i(1),\ \ h_i(2),\ \ \cdots,\ \ h_i(N-1)\ ], \\ \phi_i^H(\omega) &= [\ 1,\ \ e^{j\omega},\ \ e^{j2\omega},\ \ \cdots,\ \ e^{j(N-1)\omega}\ ]. \end{aligned}$$

(The superscript H indicates the complex conjugate transpose.) The objective function in (2.23) can then be written as

$$J_{H_i} = h_i^T Q_i h_i, \tag{2.24}$$

where the fixed $N \times N$ matrix Q_i is defined by

$$Q_i = \int_{\Omega_{H_i}} \phi_i(w) \phi_i^H(w)\, dw.$$

The elements q_{mn} for Q_i can be calculated easily if Ω_{H_i} is given; for example, assume the filters H_i have the passband $[\omega_{pi1}, \omega_{pi2}]$ over $[0, \pi]$, then

$$Q_i = \int_0^{\omega_{pi1}} \phi_i(w) \phi_i^H(w)\, dw + \int_{\omega_{pi2}}^{\pi} \phi_i(w) \phi_i^H(w)\, dw,$$

and thus the elements q_{mn} for Q_i are

$$q_{mn} = \begin{cases} \frac{\sin(w_{pi1}(m-n)) - \sin(w_{pi2}(m-n))}{(m-n)}, & m \neq n, \\ \pi + w_{pi1} - w_{pi2}, & m = n. \end{cases}$$

2.4 Problem Formulation and Design

In view of the new distortion measure J discussed in the preceding section, we wish to design transmitter and receiver subsystems to minimize J. Thus our optimal filterbank-based transceiver design problem using FIR subsystems can be stated as follows:

Given the FIR channel and desired reconstruction time delay d, design FIR transmitter and receiver subsystems of some given lengths to minimize J subject to some constraint on J_N in (2.21) and the stopband energy constraints on J_{H_i} in (2.24).

In order to incorporate both the noise attenuation and filter bandlimiting constraints, such an optimal design problem can be recast by including penalties on J_N and J_{H_i}: Given $\underline{\hat{T}}_d(z)$, design $\underline{\hat{F}}(z)$ and $\underline{\hat{H}}(z)$ of some given lengths to minimize

$$J' = J^2 + \alpha_N J_N^2 + \sum_{i=1}^{P-1} \alpha_{H_i} J_{H_i}. \tag{2.25}$$

Because both $\underline{\hat{F}}(z)$ and $\underline{\hat{H}}(z)$ are designable, this optimization problem is in general nonlinear and difficult to solve. Thus we take the following iterative design procedure which turns out to be very effective in the design example to follow.

Step 1 Design transmitter subsystems to satisfy desired frequency limiting properties (without considering reconstruction performance); these are used to initiate the iteration.

Step 2 Fixing the transmitter subsystems, design FIR receiver subsystems by minimizing J'; using the blocked models, this is equivalent to

$$\min_{\underline{\hat{H}}(z)} \left(\|\underline{\hat{H}}(z)\underline{\hat{C}}(z)\underline{\hat{F}}(z) - \underline{\hat{T}}_d(z)\|_2^2 + \alpha_N \|\underline{\hat{H}}(z)\|_2^2 + \sum_{i=1}^{P} \alpha_{H_i} J_{H_i} \right).$$

Step 3 Fixing the receiver subsystems just designed, now redesign FIR transmitter subsystems by minimizing J'; using the blocked models, this is equivalent to

$$\min_{\underline{\hat{F}}(z)} \left(\|\underline{\hat{H}}(z)\underline{\hat{C}}(z)\underline{\hat{F}}(z) - \underline{\hat{T}}_d(z)\|_2^2 + \sum_{j=1}^{M} \alpha_{F_j} J_{F_j} \right).$$

Step 4 Repeat Steps 2 and 3 until J' is sufficiently small.

We note that the idea of iteratively designing transmitter and receiver filters was used effectively in transmultiplexers design in [74]. The advantage of this procedure is evident: By fixing either $\underline{\hat{F}}(z)$ or $\underline{\hat{H}}(z)$ in Steps 2 and 3, the optimization problems become mathematically tractable; in fact, they are finite-dimensional, convex optimization with a quadratic cost function, whose global optimal solution can be always computed. Even analytical solutions can be obtained.

For example, looking at the optimal design problem in Step 2, we define

$$P(z) = \underline{\hat{H}}(z)\underline{\hat{C}}(z)\underline{\hat{F}}(z) - \underline{\hat{T}_d}(z).$$

This system is FIR and hence can be represented by its finitely many coefficient matrices P_i. By Parseval's equality,

$$J^2 = \|P(z)\|_2^2 = \left[\sum_i \text{trace}\left(P_i P_i'\right)\right]. \tag{2.26}$$

Since $\underline{\hat{F}}(z)$ and $\underline{\hat{T}_d}(z)$ are given and thus $P(z)$ depends on $\underline{\hat{H}}(z)$ in an affine manner, it follows that P_i relates to the coefficients of $\underline{\hat{H}}(z)$ (to be designed) too in an affine manner. It is obvious that both J_N and J_{H_i} are of quadratic forms, therefore we can rewrite the quantity in (2.25) in the following way:

$$J'^2 = (M_F x - b)'(M_F x - b) + x' M_N x + x' M_H x.$$

Here, x is a column vector containing all the parameters in $\underline{\hat{H}}(z)$ to be designed, b is a column vector depending on only $\underline{\hat{T}_d}(z)$, M_F is a matrix depending on $\underline{\hat{F}}(z)$ and the way x is formed, M_N depends on α_N and $\underline{\hat{H}}(z)$, and finally M_H depends on α_{H_i} and $H_i(z)$. The matrices M, M_N, M_H and b can be computed and are independent of the design parameters (x). Now the optimal design problem in Step 2 becomes a least squares problem:

$$\min_x \left[(M_F x - b)'(M_F x - b) + x' \left(M_N + M_H\right) x\right].$$

If $M_F'M_F + M_N + M_H$ is invertible, the optimal solution can be obtained to be

$$x_{opt} = (M_F'M_F + M_N + M_H)^{-1}M_F'b.$$

From here we can recover the optimal receiver subsystems. The optimal design problem in Step 3 can be solved similarly.

2.5 Design Example

The filterbank-based transceiver with $M = 3$ and $P = 8$ is designed. The channel to be used in this example is

$$C(z) = 1 - 0.3z^{-1} + 0.5z^{-2} - 0.4z^{-3} + 0.1z^{-4} - 0.02z^{-5} + 0.3z^{-6} - 0.1z^{-7}.$$

The transmitter and receiver filters involved in design are all FIR and causal with a fixed order of 12. The magnitude Bode plots of the initial transmitter filters are given in Figure 2.3, and the reconstruction time delay is taken as $d = 8$. The

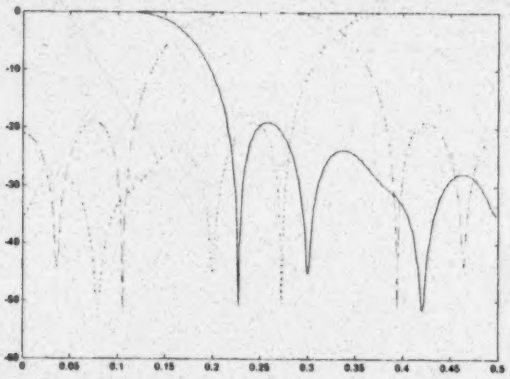

Figure 2.3: The magnitude Bode plots for the initial transmitter filters F_0 (solid), F_1 (dash-dot) and F_2 (dotted): dB versus $\omega/2\pi$.

constants α_N, α_{H_i}, and α_{F_j}, reflecting relative weightings among multiple objectives, are tuned in the design process. In our design, these are taken to be

$$\alpha_N = 0.02, \quad \alpha_{H_i} = 0.03 \ (i = 0, 1, \cdots, 7), \quad \alpha_{F_j} = 0.01 \ (j = 0, 1, 2).$$

Next we apply the iterative design procedure to the example. After a good number of iterations, J' converges to the value $J' = 0.156$ and finally $J = 0.048$. The designed transmitter and receiver filters are shown in Figures 2.4 and 2.5,

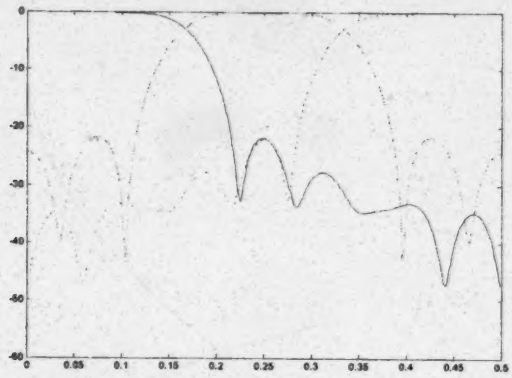

Figure 2.4: The magnitude Bode plots for the designed transmitter filters F_0 (solid), F_1 (dash-dot) and F_2 (dotted): dB versus $\omega/2\pi$.

respectively.

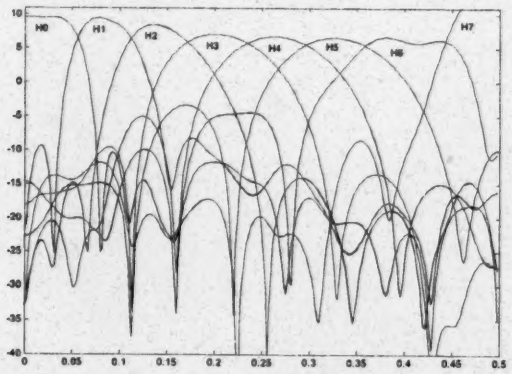

Figure 2.5: The magnitude Bode plots for the designed receiver filters $H_0 - H_7$: dB versus $\omega/2\pi$.

Consider the LTI channel in the design example. In this example, we apply the

transceiver designed earlier to evaluate the performance. Channel noise to be used is the white noise with variance = 0.0125. The simulation result is shown in Figure 2.6

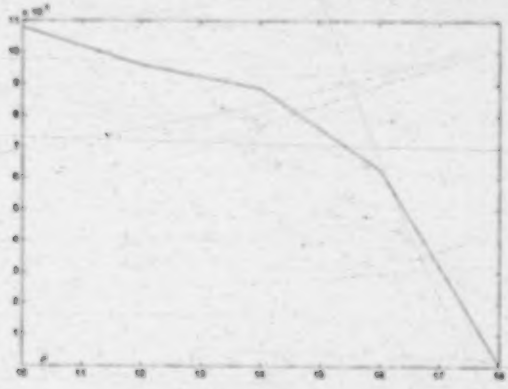

Figure 2.6: Bit error rate (BER) versus signal-to-noise ratio (SNR) in dB.

, in which the bit error rate (BER) is plotted as a function of the signal-to-noise ratio (SNR). Clearly, the BER decreases as the SNR increases.

2.6 Conclusion

In this chapter we investigated the problem of optimal design of filterbank-based transceivers. We proposed quantities to measure various distortions. We also introduced a composite distortion (J) that captures all distortions. Finally, by incorporating two important practical issues, the noise suppression and filter bandlimiting property, we developed an iterative design procedure based on minimizing J' and successfully applied this procedure to design of a filterbank-based transceiver. At each iteration, the least squares solution should be found, thus the final transmitter and receiver filters can be obtained with relative ease.

Chapter 3

Design of Transmultiplexers with Practical Constraints

3.1 Introduction

Multirate signal processing has recently received much attention and has been widely applied to communication systems [96], speech processing, and image processing [89]. It provides a more efficient way of processing signals via resampling (upsampling or downsampling) of the original signals by an appropriate factor. In general, multirate systems have many different structures; multirate filterbanks and transmultiplexers seem to be the most important ones. Much research in the past decades has dealt with the signal reconstruction problem for these multirate systems, see [89, 18, 103, 85] and the references therein.

Transmultiplexers are systems that convert time-division multiplexed (TDM) signals into frequency-division multiplexed (FDM) signals and vice versa [89]. The FDM format is often used for long distance transmission, whereas the TDM format is more convenient for digital switching. Generally, according to the sampling rates of the input signals, transmultiplexers can be divided into two types: uniform and nonuniform ones. In order to achieve perfect reconstruction for nonuniform filterbanks, general building blocks – some linear dual-rate systems [18] – were proposed to allow more design freedom. Similarly, we can use such building blocks to construct nonuniform transmultiplexers.

In [54], a measure J based on the 2-norm of transfer matrices was proposed to quantify the degree of closeness to perfect reconstruction for uniform transmultiplexers; connections of this error measure to the traditional crosstalk, magnitude, and phase distortions were established. Further in [55], optimal design of nonuniform transmultiplexers was considered.

In typical applications, transmultiplexers are required with two properties: First, the reconstruction performance should be good, i.e., J should be as small as possible; second, the filters involved should have certain frequency selectivity. In [54], optimal

design based on minimizing J was formulated as a least squares problem. This captures the first requirement well; but there is no direct control of filter frequency characteristics. In [55], penalties on the stopband energy in the synthesis filters were added to the cost function; however, combining the penalties with the cost function casts only a type of "soft" constraints on the stopband energy, while it is more desirable to have direct control over stopband energy and passband magnitude of the filter(s) involved.

The goal in this chapter is to consider both requirements in design by imposing "hard" constraints on stopband energy and passband magnitude. The improvement over the results in [55] lies in two aspects: (1) the "soft" constraints only take the frequency characteristics into account to some restrictive extent, and the final results will depend on the tradeoff parameters that can be chosen only by trial and error; in contrast, the "hard" constraints give a more realistic mathematical description of the frequency requirements; (2) the optimal design problem is formulated as a quadratic programming problem with quadratic constraints and semi-infinite constraints, which can be solved numerically.

Briefly, this chapter is organized as follows. Section 3.2 formulates the optimal design problem and constraints. Section 3.3 presents an iterative design procedure and applies it to some examples. Section 3.4 gives some concluding remarks.

3.2 Problem Formulation

Stopband energy constraints: The frequency selectivity of filters can be taken into account by considering the stopband energy constraints. To see this, take the constraint(s) for H_i in the M-channel analysis filterbank as an example; we have

$$\int_{\Omega_{H_i}} |H_i(\omega)|^2 \, d\omega \leq \delta_i, \quad i = 0, 1, \cdots, M-1, \tag{3.1}$$

where Ω_{H_i} defines the stopband frequency interval(s) for H_i, and δ_i is a pre-specified level (positive).

In this chapter, we will consider only FIR filters. The frequency response of a real N-tap FIR filter H_i is given by

$$H_i(\omega) = \sum_{n=0}^{N-1} h_i(n) e^{-jn\omega} = h_i^T \phi_i(\omega),$$

where

$$h_i^T = \left[\ h_i(0),\ \ h_i(1),\ \ \cdots,\ \ h_i(N-1)\ \right],\quad \phi_i^H(\omega) = \left[\ 1,\ \ e^{j\omega},\ \ \cdots,\ \ e^{j(N-1)\omega}\ \right].$$

(The superscript H indicates the complex conjugate transpose.) The constraint in (3.1) can then be written as $h_i^T Q_i h_i \le \delta_i$, where the fixed $N \times N$ matrix Q_i is defined by

$$Q_i = \int_{\Omega_{H_i}} \phi_i(\omega) \phi_i^H(\omega)\, d\omega.$$

The elements q_{mn} for Q_i can be calculated easily if Ω_{H_i} is given.

Passband magnitude constraints: Considering the following passband magnitude constraints:

$$\left||H_i(\omega)| - A_{H_i}\right| \le \varepsilon_i, \quad \omega \in \Theta_{H_i}, \quad i = 0, 1, \cdots, M-1. \tag{3.2}$$

Here Θ_{H_i} defines the passband frequency interval(s) for H_i, A_{H_i} is the expected passband magnitude of H_i and ε_i is pre-specified. The above semi-infinite inequality constraints can be approximated in a straightforward way by sampling or discretizing the frequency. If $\Theta_{H_i} = \left[\omega_{p1}^i, \omega_{p2}^i\right]$, we choose a set of uniformly spaced frequency points $\omega_{p1}^i = \omega_1^i \le \omega_2^i \le \cdots \le \omega_N^i = \omega_{p2}^i$, and replace the semi-infinite inequality constraints with the set of N ordinary constraints

$$\left||H_i(\omega_k^i)| - A_{H_i}\right| \le \varepsilon_i, \quad k = 1, 2, \cdots, N, \quad i = 0, 1, \cdots, M-1. \tag{3.3}$$

Note that sampling preserves convexity. When N is sufficiently large, discretization yields a good approximation to the semi-infinite problem [19].

Uniform and nonuniform transmultiplexers: In the frequency domain, an M-channel uniform transmultiplexer is modeled by the $M \times M$ transfer matrix $T(z)$, which can be computed based on the polyphase matrices for the synthesis and analysis filters [89]. For perfect reconstruction, there exist positive integers $d_0, d_1, \cdots, d_{M-1}$ such that $T(z)$ equals the ideal system:

$$T(z) = T_d(z) := \text{diag}\{z^{-d_0}, z^{-d_1}, \cdots, z^{-d_{M-1}}\}.$$

If $T(z) \neq T_d(z)$, $J = \|T(z) - T_d(z)\|_2$ (2-norm of the error system), which captures crosstalk, magnitude, and phase distortions, can be used as a composite distortion measure to quantify the degree of closeness to perfect reconstruction [54].

For nonuniform transmultiplexers, since the channels have different downsampling ratios, we need to block them differently to get an LTI model. The transfer matrices of the blocked transmultiplexer and the blocked ideal system are represented by $\underline{T}$ and $\underline{T_d}$, respectively [55]. How do we compute the frequency-domain model $\underline{T}(z)$? We adopt the structure studied in [18] using linear switching time-varying (LSTV) systems for implementation of the general blocks. Similarly, a composite distortion measure, $J = \|\underline{T}(z) - \underline{T_d}(z)\|_2$, can be used to capture all four distortions (cross-talk, aliasing, magnitude and phase distortions) [55].

The dual-rate building blocks H_i (analysis) and F_i (synthesis) in nonuniform transmultiplexers can be represented by the LSTV structure proposed in [18]: For example, H_i can be modeled by the structure with l_i LTI systems, denoted by $H_{i,j}$, $j = 0, 1, \cdots, l_i - 1$. These LTI systems are designed directly. The stopband energy and passband magnitude constraints on H_i are expressed in terms of $H_{i,j}$ according to (3.1) and (3.3) by replacing H_i with H_{ij}.

To this end, the optimal uniform (nonuniform) transmultiplexer design problems incorporating frequency-domain constraints can be formulated as follows:

> Given the desired reconstruction time delays $d_0, d_1, ..., d_{M-1}$ and the FIR synthesis filters $F_0, F_1, ..., F_{M-1}$, design FIR analysis filters $H_0, H_1, ..., H_{M-1}$ of a given length to minimize J subject to the stopband energy constraints in (3.1) and passband magnitude constraints in (3.3).

The optimization problem is a quadratic programming problem with quadratic constraints and semi-infinite constraints.

3.3 Iterative Design Procedure and Examples

Finding the optimal analysis and synthesis filters of given orders is a nonlinear optimization problem. However by fixing either the analysis or synthesis filters and finding the other set, we can design a transmultiplexer iteratively, leading to joint (local) optimization of both sets. Thus we propose the following iterative design procedure for uniform transmultiplexer design, which turns out to be very effective in the design examples to follow. For the nonuniform transmultiplexer design, the design procedure will be similar except the calculations of the objective functions involved.

> **Step 0** Assume the desired reconstruction time delays $d_0, d_1, ..., d_{M-1}$ are given. Choose some initial FIR synthesis filters $F_0, F_1, \cdots, F_{M-1}$ satisfying the stopband energy constraints and passband magnitude constraints.
>
> **Step 1** Design FIR analysis filters $H_0, H_1, \cdots, H_{M-1}$ of a given length to minimize J with stopband energy and passband magnitudes constraints.
>
> **Step 2** Fixing the analysis filters $H_0, H_1, \cdots, H_{M-1}$ designed in the previous step, design FIR synthesis filters $F_0, F_1, \cdots, F_{M-1}$ of a given length to

minimize J with stopband energy and passband magnitudes constraints.

Step 3 Repeat if necessary: Fix the synthesis filters just designed and go back to Steps 1 and 2 to improve J.

Example 1. *A three-channel uniform transmultiplexer with only stopband energy constraints*: Analogy of transmultiplexer and filterbanks was given in [95] and the design of transmultiplexers was related to that of filterbanks. It is shown that the filters for a crosstalk free transmultiplexer are the same as those for a 1-skewed alias-free QMF bank [48]. This three-channel example is based on a filterbank system designed in [88], where the FIR analysis and synthesis filters are all of order of 14. For the transmultiplexer application, we modify the synthesis filters by multiplying by the factor z^{-3} to handle the skewness condition [48]. We redesign the transmultiplexer using the method introduced in this chapter.

First, without adding the stopband energy constraints to the FIR filters involved, the iterative optimal approach is to design the filters of the same length by optimizing J, taking the reconstruction time delays to be the same: $d_0 = d_1 = d_2 = 8$. After a few thousands of iterations, J converges to the value $J = 2.9297 \times 10^{-10}$, indicating almost perfect reconstruction is achieved. In this case, the stopband energy of F_0, F_1 and F_2 are listed in the second column in Table 3.1.

Table 3.1: Example 1: Stopband energy of the designed synthesis filters.

synthesis filters	stopband energy (without adding constraints)	stopband energy (with constraints $\delta_i = 0.001$)
F_0	0.0088	0.001
F_1	0.0074	0.001
F_2	0.0088	0.001

Second, using one iteration design procedure, changing the stopband energy constraints of the three synthesis filters [assuming they have the same constraint

(δ), and the three analysis filters have no constraints], we can observe that with the constraints increasing, the J is decreasing, as shown in Figure 3.1. We comment

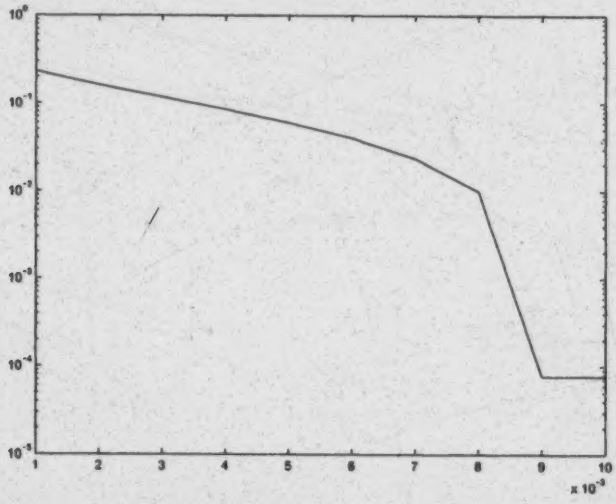

Figure 3.1: Example 1: The optimal J (log scale) versus the stopband energy constraints (δ)

that there exists a tradeoff between the reconstruction performance and the involved filters' stopband energy. When choosing $\delta_0 = \delta_1 = \delta_2 = 0.001$, the stopband energy of the designed synthesis filters are listed in the third column in Table 3.1, from which we can observe a great improvement in reducing the stopband energy of the synthesis filters.

Third, set the stopband energy constraints of the three synthesis filters to be 0.005, and those of the three analysis filters to be 0.060, using the iterative optimal design, J finally converges to 0.0019. The merit of the optimal method incorporating the stopband energy constraints is evident: Not only the designed transmultiplexer has good reconstruction performance, but also the filters involved have frequency selectivity.

Example 2: **A three-channel nonuniform transmultiplexer design based on traditional building blocks, with both stopband energy and passband magnitude constraints.** Consider the three-channel nonuniform transmultiplexer depicted in Figure 3.2, built with traditional blocks – the filters involved are all

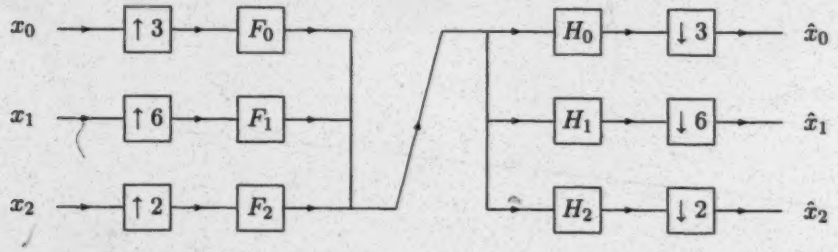

Figure 3.2: A three-channel nonuniform transmultiplexer using traditional building blocks.

causal and LTI.

To initiate the iterative procedure, we choose the initial synthesis filters from the ideal, brick-wall ones. If we choose $H_i = F_i$ and F_0, F_1, and F_2 to be ideal filters with passband, $[0, \pi/3)$, $[\pi/3, \pi/2)$, and $[\pi/2, \pi)$, respectively, it is readily verified that perfect reconstruction is achieved with $\hat{x}_i = x_i$; but these ideal filters do not satisfy the stability and causality properties. Suppose that FIR and causal synthesis filters of order 35 are to be designed; we initially use truncated and shifted ideal filters to start the iterative procedure. The magnitude Bode plots of these initial synthesis filters (FIR and causal with order 35) are given in Figure 3.3. Next we apply the iterative design procedure to the example in Figure 3.2. Shifting the truncated ideal filters for causality introduces time delays in the reconstruction; it is easy to calculate that these are $d_0 = 12$, $d_1 = 6$, and $d_2 = 18$. The analysis and synthesis filters involved in design are all FIR and causal with a fixed order of 35. The stopband energy constraints and passband magnitude constraints are preset as shown in the second and third rows of Table 3.2. The expected passband

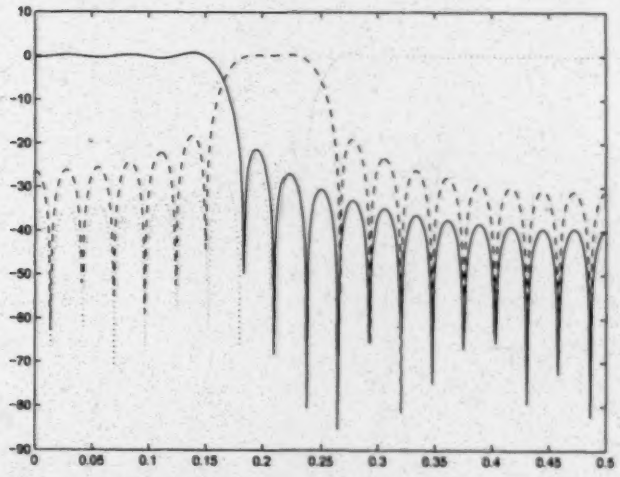

Figure 3.3: Example 2: The magnitude Bode plots for the initial F_0 (solid), F_1 (dotted) and F_2 (dash-dot): dB versus $\omega/2\pi$

Table 3.2: Example 2: Preset stopband energy and passband magnitude constraints.

filters	passband magnitude constraints (preset)	stopband energy constraints (preset)	stopband energy (designed)
F_0	0.03	0.2	0.0155
F_1	0.08	0.9	0.0859
F_2	0.03	0.2	0.0145
H_0	0.03	0.2	0.1462
H_1	0.08	0.9	0.8809
H_2	0.03	0.2	0.1009

magnitudes are $A_{F_0} = A_{F_1} = A_{F_2} = 1$, $A_{H_0} = 3$, $A_{H_1} = 6$, $A_{H_2} = 2$. After 180 iterations, J converges to the value $J = 0.0653$. The designed synthesis and analysis filters are shown in Figures 3.4 and Figures 3.5, respectively, from which we can observe that the passband magnitudes are all bounded by the preset constraints; and the stopband energy of the design filters are listed in the fourth column of Table 3.2. We remark that by using the numerical optimization approach, we can deal with the structural constraints that often appear in the design of nonuniform

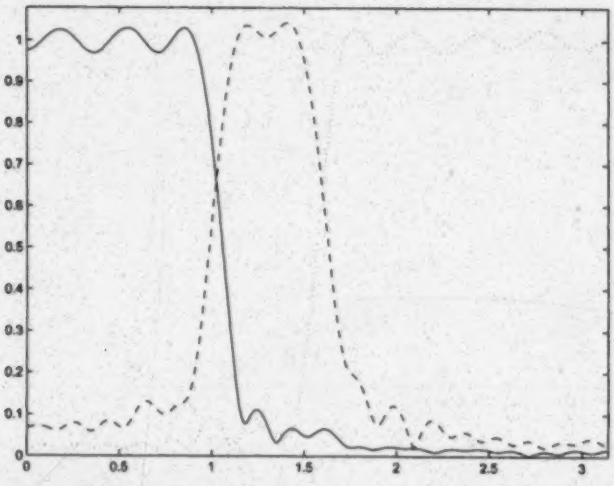

Figure 3.4: Example 2: The magnitude plots for the designed F_0 (solid), F_1 (dotted) and F_2 (dash-dot): dB versus ω.

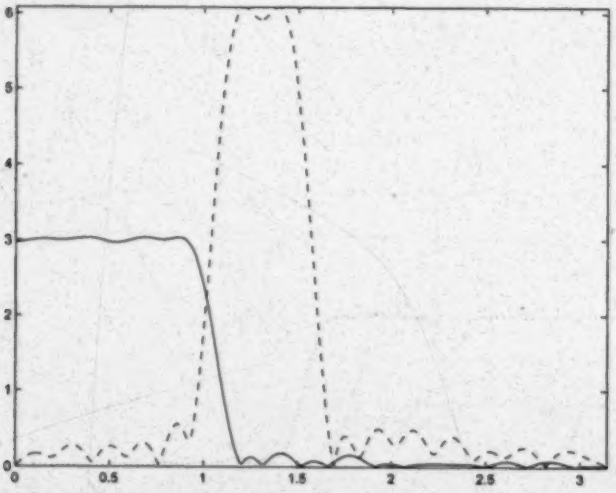

Figure 3.5: Example 2: The magnitude plots for the designed H_0 (solid), H_1 (dotted) and H_2 (dash-dot): magnitude versus ω.

transmultiplexer based on traditional building blocks.

Example 3: *A three-channel nonuniform transmultiplexer with mixed building blocks*: We adopt general building blocks [18] for analysis subsystems as shown in

Figure 3.6. This structure is mixed in that the synthesis part is built with traditional

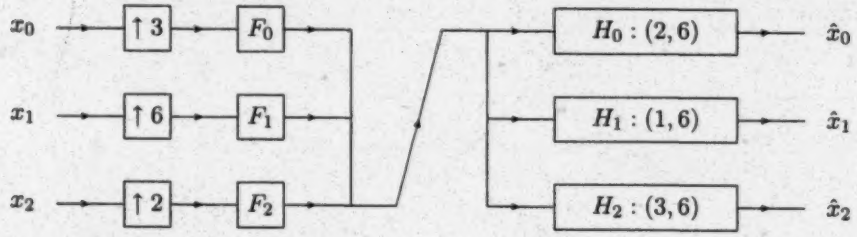

Figure 3.6: A three-channel nonuniform transmultiplexer using general analysis building blocks.

blocks, whereas the analysis part with general blocks.

We use the same initial synthesis filters and time delays as in Example 2. The general blocks for analysis are represented by the LSTV structure [18]: $H_0 : (2,6)$ is implemented by an LSTV system with two LTI systems denoted by $H_{0,0}$ and $H_{0,1}$ followed by $\downarrow 3$; $H_1 : (1,6)$ is implemented by a single LTI system ($H_{1,0}$) followed by $\downarrow 6$; and $H_2 : (3,6)$ is implemented by an LSTV system with three LTI systems denoted by $H_{2,0}$, $H_{2,1}$, and $H_{2,2}$ followed by $\downarrow 2$. Thus for the analysis part, there are six LTI filters to be designed: $H_{0,0}, H_{0,1}, H_{1,0}, H_{2,0}, H_{2,1}$, and $H_{2,2}$. All the six LTI filters are causal and FIR with order 35 in the design exercise. The stopband energy constraints and passband magnitude constraints are preset as shown in the second and third columns of Table 3.3. The expected passband magnitudes are

Table 3.3: Example 3: Preset stopband energy and passband magnitude constraints.

filters	passband magnitude constraints (preset)	stopband energy constraints (preset)
F_0	0.03	0.2
F_1	0.08	0.9
F_2	0.03	0.2
$H_{0,0}, H_{0,1}$	0.03	0.2
$H_{1,0}$	0.08	0.9
$H_{2,0}, H_{2,1}, H_{2,2}$	0.03	0.2

$A_{F_0} = A_{F_1} = A_{F_2} = 1$, $A_{H_{0,0}} = A_{H_{0,1}} = 3$, $A_{H_{1,0}} = 6$, $A_{H_{2,0}} = A_{H_{2,1}} = A_{H_{2,2}} = 2$. After about one thousand of iterations, J converges to the value $J = 0.0012$, which is several orders of magnitude better than the design using traditional building blocks (omitted here). All frequency specifications of the designed filters are satisfied. The magnitude plots for the three synthesis and six analysis filters designed are given in Figure 3.7-3.10.

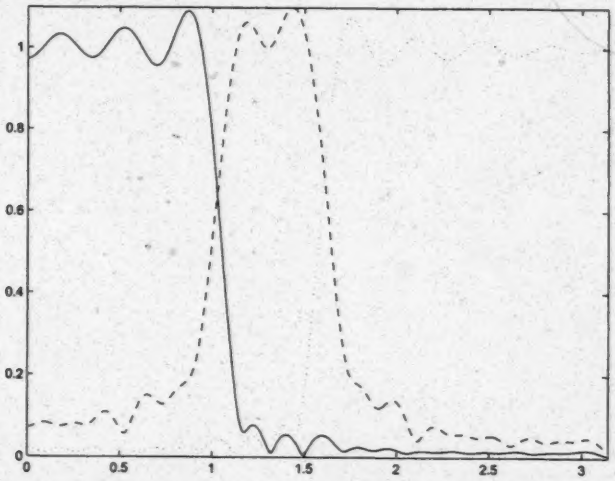

Figure 3.7: Example 3: The magnitude plots for the designed F_0 (solid), F_1 (dotted) and F_2 (dash-dot): magnitude versus ω.

3.4 Conclusion

In this chapter, we studied uniform and nonuniform transmultiplexer design problems. The main contribution is the incorporation of stopband energy and passband magnitude constraints directly in the design optimization, thus making an important step forward in addressing practical issues about frequency selectivity. The design procedure proposed considers both signal reconstruction (by minimizing J) and filter characteristics (by adding constraints). The practical usefulness of the

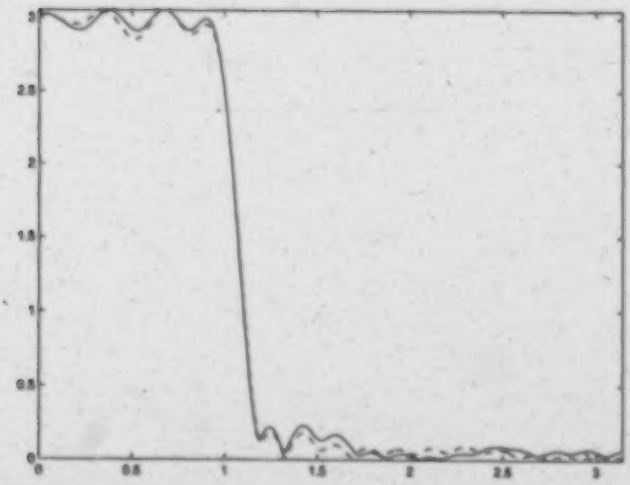

Figure 3.8: Example 3: The magnitude plots for the designed H_{00} (solid) and H_{01} (dotted): magnitude versus ω.

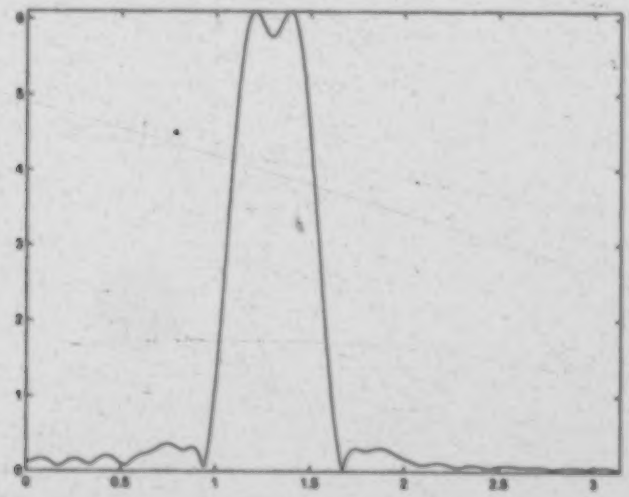

Figure 3.9: Example 3: The magnitude plots for the designed H_{10} (solid): magnitude versus ω.

method is illustrated well with two examples.

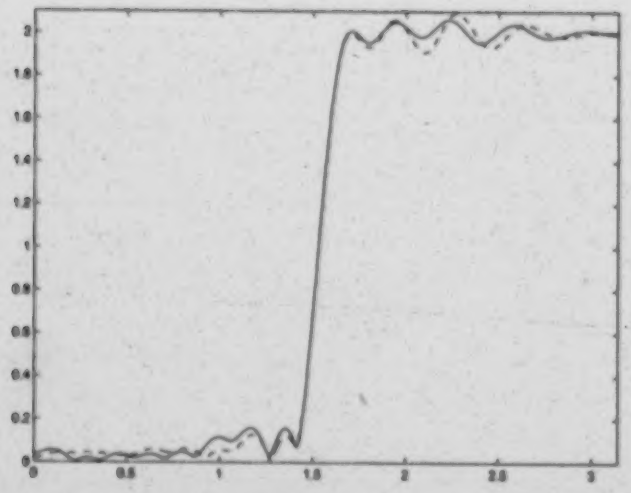

Figure 3.10: Example 3: The magnitude plots for the designed H_{20} (solid), H_{21} (dotted), and H_{22} (dash-dot): magnitude versus ω.

Chapter 4

Design of Transmultiplexers with Designable Filter Length

4.1 Introduction

Recent studies towards the development of transmultiplexer design can be found in [54, 12, 13, 74, 98], just to name a few. In [54], a composite distortion measure based on the 2-norm of transfer matrices was proposed to quantify the degree of closeness to perfect reconstruction; connections of this error measure to the traditional crosstalk, magnitude, and phase distortions were established; by pre-choosing the appropriate synthesis filters and fixing the lengths of the analysis filters involved, the near optimal transmultiplexer was then designed by minimizing the measure. In [74], stopband energy and passband magnitude constraints were directly incorporated in the design optimization to make an important step forward in addressing practical issues about frequency selectivity. However, both of them did not take the filter length into the design optimization. In consideration of noises, analysis filters of the transmultiplexer were designed by a Wiener filtering technique [12] using spectral factorization in the frequency domain, and under the mixed H_2/H_∞ optimization performance [13], respectively, both assuming the lengths of filters involved are fixed.

In fact, to our best knowledge, most existing methods for transmultiplexer design require a previous determination of the lengths of filters in the transmultiplexer to be designed, and they are inherently quite sensitive to inappropriate length choice: If the lengths are chosen too long, the computation complexity will increase; if short, the reconstruction performance will deteriorate although shorter filters (filters with shorter filter length) require fewer circuit elements in a hardware implementation and less computational cost in a software implementation. Therefore, the best way is to make a tradeoff between the reconstruction performance and the lengths of filters involved in a transmultiplexer. To this end, a problem in the transmultiplexer design is still open: How to design both the appropriate filter length and the parameters

of filters involved, in addition to guarantee certain reconstruction performance requirement? In this chapter, by means of the recursive principle, we introduce a new approach for designing transmultiplexers with *designable* filter length in addition to satisfying 2-norm based reconstruction performance requirements. Our objective is two-fold:

- First, simultaneously design the most appropriate filter length and the parameters of filters involved in the transmultiplexer by recursively increasing the length of filters. It gives rise to more design flexibility and also reduces the implementation cost.

- Second, reduce the computation complexity of the algorithm, which motivates us to develop a recursive algorithm.

The rest of the chapter is organized as follows. Section 4.2 describes the 2-norm based analysis filters design for a uniform-band transmultiplexer. In Section 4.3, we propose the recursive algorithms for simultaneously designing the filter length and parameters. Section 4.4 presents illustrative examples to demonstrate the effectiveness of the proposed method. Finally, Section 4.5 offers some concluding remarks and points out possible extensions.

4.2 2-Norm Based Analysis Filters Design

The transmultiplexer system in Figure 1.2 represents a linear, time-invariant (LTI) system. Suppose the FIR synthesis filters $F_i(z)$ are designed based on certain frequency band combining requirement [74], and the FIR analysis filters $H_i(z)$ (of equal length) are to be designed. In this section, we will derive the 2-norm based analysis filters design for different filter length, following the method for fixed filter length design [54, 74].

Define the (vector) input and output as follows:

$$x(n) = \begin{bmatrix} x_0(n) \\ x_1(n) \\ \vdots \\ x_{M-1}(n) \end{bmatrix}, \quad \hat{x}(n) = \begin{bmatrix} \hat{x}_0(n) \\ \hat{x}_1(n) \\ \vdots \\ \hat{x}_{M-1}(n) \end{bmatrix}.$$

In the frequency domain, the transmultiplexer is modeled by the $M \times M$ transfer matrix $T(z)$ relating $X(z)$ to $\hat{X}(z)$ ($X(z)$ and $\hat{X}(z)$ are the z-transforms of $x(n)$ and $\hat{x}(n)$, respectively):

$$\hat{X}(z) = T(z)X(z).$$

This transfer matrix can be determined based on the polyphase matrices for the synthesis and analysis filters [54, 89]:

$$T(z) = E(z)\Gamma(z)R(z), \tag{4.1}$$

where $R(z) \in \mathbb{R}^{M\times M}$, the polyphase matrix for the synthesis bank, and $E(z) \in \mathbb{R}^{M\times M}$, the polyphase matrix for the analysis bank. The matrix $R(z)$ is uniquely related to filters $F_0(z), F_1(z), \cdots, F_{M-1}(z)$; so is $E(z)$ to $H_0(z), H_1(z), \cdots, H_{M-1}(z)$. $\Gamma(z)$ is a fixed matrix given by [89]

$$\Gamma(z) = \begin{bmatrix} 0 & 1 \\ z^{-1}I_{M-1} & 0 \end{bmatrix},$$

I_{M-1} being an $(M-1) \times (M-1)$ identity matrix.

For perfect reconstruction, there exist positive integers $d_0, d_1, \cdots, d_{M-1}$ such that $T(z)$ equals the ideal system $T_d(z)$ defined by

$$T_d(z) = \begin{bmatrix} z^{-d_0} & 0 & \cdots & 0 \\ 0 & z^{-d_1} & \cdots & 0 \\ \vdots & \vdots & & \vdots \\ 0 & 0 & \cdots & z^{-d_{M-1}} \end{bmatrix}.$$

If $T(z) \neq T_d(z)$, the following quantity based on the 2-norm of transfer matrices, which captures crosstalk, magnitude, and phase distortions, can be used as a composite distortion measure to quantify the degree of closeness to perfect reconstruction

[54]:

$$\begin{aligned} J &= \|T(z) - T_d(z)\|_2 \\ &= \|E(z)\Gamma(z)R(z) - T_d(z)\|_2. \end{aligned} \tag{4.2}$$

Here, the optimization problem – minimizing J to design $E(z)$ and $R(z)$ simultaneously – is nonlinear and difficult to solve. In practice, we can pre-design the synthesis filters based on band-splitting and coding requirements. Therefore, it is assumed that $\Gamma(z)$, $R(z)$, and $T_d(z)$ are all FIR and given and only $E(z)$, the FIR polyphase matrix of the analysis filters [89], is designable. Define $Q(z) = \Gamma(z)R(z)$ to get that $Q(z)$ is again FIR and given; and the equivalent design problem is:

$$J_{opt} = \min_{E(z)} \|E(z)Q(z) - T_d(z)\|_2,$$

where the minimization is over the class of FIR $E(z)$.

To reduce the latter minimization problem to a solvable matrix problem, we look at the impulse response matrix of the MIMO system $P := EQ - T_d$. Let the orders of $Q(z)$ and $E(z)$ be m and l, respectively, and define

$$Q(z) = \sum_{i=0}^{m} z^{-i}Q_i, \quad E(z) = \sum_{i=0}^{l} z^{-i}E_i, \quad T_d(z) = \sum_{i=0}^{m+l} z^{-i}D_i.$$

The matrices $Q_0, Q_1, \cdots, Q_m$ can be computed from the given data, and $D_0, D_1, \cdots, D_{m+l}$ can be determined from the pre-set delays; but $E_0, E_1, \cdots, E_l$ are designable. If $0 \leqslant d_i \leqslant m + l, i = 0, 1, \cdots, M - 1$, then the impulse response matrix of P is FIR with order $m + l$:

$$P(z) = \sum_{i=0}^{m+l} z^{-i}P_i.$$

By Parseval's equality [89],

$$J = \|P(z)\|_2 = \left[\sum_{0}^{m+l} \mathrm{tr}(P_i P_i')\right]^{1/2} = \left[\mathrm{tr}(\underline{P}\,\underline{P}')\right]^{1/2},$$

where we have defined the block row matrix

$$\underline{P}_l = [P_0,\ P_1,\ \cdots,\ P_{m+l}].$$

Since $P(z) = E(z)Q(z) - T_d(z)$, it can be verified that

$$\underline{P}_l = \underline{E}_l \underline{Q}_l - \underline{D}_l,$$

where $\underline{E}_l = [E_0\ E_1\ \cdots\ E_l] \in \mathbb{R}^{M\times(l+1)M}$, $\underline{D}_l = [D_0\ \ D_1\ \ \cdots\ \ D_{m+l}] \in \mathbb{R}^{M\times(m+l+1)M}$, and $\underline{Q}_l \in \mathbb{R}^{(l+1)M\times(m+l+1)M}$ depends on only known matrices $Q_0, Q_1, \cdots, Q_m$:

$$\underline{Q}_l = \begin{bmatrix} Q_0 & Q_1 & \cdots & Q_m & 0 & 0 & 0 & \cdots & 0 \\ 0 & Q_0 & Q_1 & \cdots & Q_m & 0 & 0 & \cdots & 0 \\ & \cdots & & \cdots & & \cdots & & \cdots & \\ 0 & \cdots & 0 & Q_0 & Q_1 & \cdots & \cdots & Q_m & 0 \\ 0 & \cdots & \cdots & 0 & Q_0 & Q_1 & \cdots & \cdots & Q_m \end{bmatrix}, \tag{4.3}$$

where $0 \in \mathbb{R}^{M\times M}$ with all elements being 0. To this end, the problem in (4.2) reduces to the following matrix problem:

$$J_l^2 = \text{trace}\left[(\underline{E}_l\underline{Q}_l - \underline{D}_l)(\underline{E}_l\underline{Q}_l - \underline{D}_l)^{\mathrm{T}}\right]. \tag{4.4}$$

If the matrix $\underline{Q}_l$ has full row rank, or equivalently $\underline{Q}_l\underline{Q}_l^{\mathrm{T}}$ is invertible, the optimal solution can be obtained as

$$\underline{E}_l = \underline{D}_l\underline{Q}_l^{\mathrm{T}}(\underline{Q}_l\underline{Q}_l^{\mathrm{T}})^{-1}. \tag{4.5}$$

Observing (4.4) and (4.5), one straightforward way to study the tradeoff between the filter length and the reconstruction performance is to calculate $\underline{E}_l$ and J_l for each different l. However, obviously the calculation of the inversion of a matrix with dimension $(l+1)M \times (l+1)M$ is needed for each l, which greatly increases the computational burden. Therefore, we are aiming at developing a recursive algorithm that can not only design the filter length and filter parameters simultaneously, but also has less computational complexity.

4.3 Description of the Algorithm

In this section, we develop an algorithm to design the appropriate filter length and filter coefficients for the analysis filters simultaneously, as l recursively increases. In order to derive the recursive algorithm, we introduce the matrix inversion Lemma [111] first.

Lemma 3 *[111] Let A be a square matrix partitioned as followed*

$$A := \begin{bmatrix} A_{11} & A_{12} \\ A_{21} & A_{22} \end{bmatrix},$$

where A_{11} and A_{22} are also square matrices. If A and A_{11} are nonsingular, then

$$\begin{bmatrix} A_{11} & A_{12} \\ A_{21} & A_{22} \end{bmatrix}^{-1} = \begin{bmatrix} A_{11}^{-1} + A_{11}^{-1}A_{12}\Delta^{-1}A_{21}A_{11}^{-1} & -A_{11}^{-1}A_{12}\Delta^{-1} \\ -\Delta^{-1}A_{21}A_{11}^{-1} & \Delta^{-1} \end{bmatrix},$$

where

$$\Delta := A_{22} - A_{21}A_{11}^{-1}A_{12}.$$

Proof: The proof can be done along the similar way as in [111] and is omitted here. □

We note that the order (l) of $E(z)$ is determined by the length of analysis filters (to be designed) for fixed number (M) of channels in the transmultiplxer. When the order of $E(z)$ becomes $(l+1)$, $\underline{D}_{l+1}$ and $\underline{Q}_{l+1}$ can be expressed as:

$$\underline{D}_{l+1} = [\ \underline{D}_l \mid \mathbf{0}\ ], \tag{4.6}$$

and

$$\underline{Q}_{l+1} = \left[\begin{array}{cccccccccc|c} Q_0 & Q_1 & \cdots & Q_m & 0 & 0 & 0 & \cdots & 0 & 0 \\ 0 & Q_0 & Q_1 & \cdots & Q_m & 0 & 0 & \cdots & 0 & 0 \\ & \cdots & & \cdots & & \cdots & & \cdots & & \\ 0 & \cdots & 0 & Q_0 & Q_1 & \cdots & \cdots & Q_m & 0 & 0 \\ 0 & \cdots & \cdots & 0 & Q_0 & Q_1 & \cdots & \cdots & Q_m & 0 \\ \hline 0 & 0 & \cdots & \cdots & 0 & Q_0 & Q_1 & \cdots & Q_{m-1} & Q_m \end{array}\right] =: \left[\begin{array}{c|c} Q_l & B_0 \\ \hline B & Q_m \end{array}\right], \tag{4.7}$$

where $B_0 := [\mathbf{0},\ \mathbf{0},\ \cdots,\ \mathbf{0}]^{\mathrm{T}} \in \mathbb{R}^{(l+1)M\times M}$, and $B := [\mathbf{0},\ \mathbf{0},\ \cdots,\ \mathbf{0},\ Q_0,\ Q_1,\ \cdots,\ Q_{m-1}] \in \mathbb{R}^{M\times(l+m+1)M}$. Defining

$$S_{l+1} := \left[\underline{Q}_{l+1}\underline{Q}_{l+1}^{\mathrm{T}}\right]^{-1}, \tag{4.8}$$

and substituting (4.7) into (4.8) give

$$\begin{aligned} S_{l+1} &= \left(\left[\begin{array}{c|c} Q_l & B_0 \\ \hline B & Q_m \end{array}\right]\left[\begin{array}{c|c} Q_l^{\mathrm{T}} & B^{\mathrm{T}} \\ \hline B_0^{\mathrm{T}} & Q_m^{\mathrm{T}} \end{array}\right]\right)^{-1} \\ &= \left[\begin{array}{c|c} Q_lQ_l^{\mathrm{T}} & Q_lB^{\mathrm{T}} \\ \hline B\underline{Q}_l^{\mathrm{T}} & \sum_{i=0}^{m} Q_iQ_i^{T} \end{array}\right]^{-1} \\ &= \left[\begin{array}{c|c} S_l^{-1} & \Omega_l^{\mathrm{T}} \\ \hline \Omega_l & Q \end{array}\right]^{-1}, \end{aligned} \tag{4.9}$$

where $\Omega_l := B\underline{Q}_l^{\mathrm{T}}$, $Q := \sum_{i=0}^{m} Q_iQ_i^{T}$.

Directly applying Lemma 1 to (4.9), it is easy to obtain

$$S_{l+1} = \left[\begin{array}{c|c} S_l + S_l\Omega_l^{\mathrm{T}}A_l\Omega_lS_l & -S_l\Omega_l^{\mathrm{T}}A_l \\ \hline -A_l\Omega_lS_l & A_l \end{array}\right], \tag{4.10}$$

where $A_l := \left(Q - \Omega_lS_l\Omega_l^{\mathrm{T}}\right)^{-1} \in \mathbb{R}^{M\times M}$.

From (4.5), we have:

$$\underline{E}_{l+1} = \underline{D}_{l+1}\underline{Q}_{l+1}^{\mathrm{T}}(\underline{Q}_{l+1}\underline{Q}_{l+1}^{\mathrm{T}})^{-1}. \tag{4.11}$$

Substituting (4.6) and (4.10) into (4.11) gives the recursive formula for calculating $\underline{E}_{l+1}$:

$$\begin{aligned} \underline{E}_{l+1} &= \underline{D}_{l+1}\underline{Q}_{l+1}^{\mathrm{T}}(\underline{Q}_{l+1}\underline{Q}_{l+1}^{\mathrm{T}})^{-1} \\ &= \underline{D}_{l+1}\underline{Q}_{l+1}^{\mathrm{T}}S_{l+1} \\ &= [\underline{D}_l \,|\, \mathbf{0}]\left[\begin{array}{c|c} Q_l^{\mathrm{T}} & B^{\mathrm{T}} \\ \hline B_0^{\mathrm{T}} & Q^{\mathrm{T}} \end{array}\right]\left[\begin{array}{c|c} S_l + S_l\Omega_l^{\mathrm{T}}A_l\Omega_lS_l & -S_l\Omega_l^{\mathrm{T}}A_l \\ \hline -A_l\Omega_lS_l & A_l \end{array}\right] \\ &= \left[\underline{D}_lQ_l^{\mathrm{T}} \,\middle|\, \underline{D}_lB^{\mathrm{T}}\right]\left[\begin{array}{c|c} S_l + S_l\Omega_l^{\mathrm{T}}A_l\Omega_lS_l & -S_l\Omega_l^{\mathrm{T}}A_l \\ \hline -A_l\Omega_lS_l & A_l \end{array}\right] \\ &= \left[\ \underline{D}_lQ_l^{\mathrm{T}}S_l + \underline{D}_lQ_l^{\mathrm{T}}S_l\Omega_l^{\mathrm{T}}A_l\Omega_lS_l - \underline{D}_lB^{\mathrm{T}}A_l\Omega_lS_l \,\middle|\, -\underline{D}_lQ_l^{\mathrm{T}}S_l\Omega_l^{\mathrm{T}}A_l + \underline{D}_lB^{\mathrm{T}}A_l\ \right] \\ &= \left[\ \underline{E}_l + \underline{E}_l\Omega_l^{\mathrm{T}}A_l\Omega_lS_l - \underline{D}_lB^{\mathrm{T}}A_l\Omega_lS_l \,\middle|\, -\underline{E}_l\Omega_l^{\mathrm{T}}A_l + \underline{D}_lB^{\mathrm{T}}A_l\ \right] \\ &= \left[\ \underline{E}_l \,|\, \mathbf{0}\ \right] + \underline{E}_l\Omega_l^{\mathrm{T}}A_l\left[\ \Omega_lS_l \,\middle|\, -I\ \right] + \underline{D}_lB^{T}\left[\ -A_l\Omega_lS_l \,\middle|\, A_l\ \right] \end{aligned} \tag{4.12}$$

With this recursive formula for $\underline{E}_{l+1}$, the computational complexity is greatly reduced. In order to determine the appropriate length of the filters involved, we still need another recursive formula for evaluating the 2-norm based composite distortion measure as shown in (4.2). Recalling the equivalent measure in (4.4), when the order of $E(z)$ becomes $(l+1)$, the measure is

$$J_{l+1}^2 = \text{trace}\left[(\underline{E}_{l+1}\underline{Q}_{l+1} - \underline{D}_{l+1})(\underline{E}_{l+1}\underline{Q}_{l+1} - \underline{D}_{l+1})^{\mathrm{T}}\right]. \tag{4.13}$$

A practical and efficient way to determine the filter length is: We compare J_{l+1} with J_l, and if they are sufficiently close, or for some pre-set small ε, if

$$|J_{l+1} - J_l| \leqslant \varepsilon,$$

terminate the procedure and obtain the appropriate filter length.

Using (4.12), (4.6) and (4.7), we have

$$\begin{aligned}
&\underline{E}_{l+1}\underline{Q}_{l+1} - \underline{D}_{l+1} \\
&\quad = \underline{E}_{l+1}\left[\begin{array}{c|c} \underline{Q}_l & B_0 \\ \hline B & Q_m \end{array}\right] - \left[\begin{array}{c|c} \underline{D}_l & \mathbf{0} \end{array}\right] \\
&\quad = \left[\begin{array}{c} \underline{E}_l\underline{Q}_l + \underline{E}_l\Omega_l^{\mathrm{T}}A_l\Omega_l S_l\underline{Q}_l - \underline{D}_l B^{\mathrm{T}}A_l\Omega_l S_l\underline{Q}_l - \underline{E}_l\Omega_l^{\mathrm{T}}A_l B + \underline{D}_l B^{\mathrm{T}}A_l B - \underline{D}_l \\ -\underline{E}_l\Omega_l^{\mathrm{T}}A_l Q_m + \underline{D}_l B^{\mathrm{T}}A_l Q_m \end{array}\right]^{\mathrm{T}}.
\end{aligned}$$

If we define $P_{l1} := \underline{E}_l\Omega_l^{\mathrm{T}}A_l\Omega_l S_l\underline{Q}_l - \underline{D}_l B^{\mathrm{T}}A_l\Omega_l S_l\underline{Q}_l - \underline{E}_l\Omega_l^{\mathrm{T}}A_l B + \underline{D}_l B^{\mathrm{T}}A_l B$, and $P_{l2} := -\underline{E}_l\Omega_l^{\mathrm{T}}A_l Q_m + \underline{D}_l B^{\mathrm{T}}A_l Q_m$, then

$$\underline{E}_{l+1}\underline{Q}_{l+1} - \underline{D}_{l+1} = \left[\begin{array}{c|c} \underline{E}_l\underline{Q}_l - \underline{D}_l + P_{l1} & P_{l2} \end{array}\right]. \tag{4.14}$$

Substituting (4.14) into (4.13) leads to another recursive formula for evaluating the 2-norm based composite distortion measure J_{l+1}:

$$\begin{aligned}
J_{l+1}^2 &= \text{trace}\left[(\underline{E}_{l+1}\underline{Q}_{l+1} - \underline{D}_{l+1})(\underline{E}_{l+1}\underline{Q}_{l+1} - \underline{D}_{l+1})^{\mathrm{T}}\right] \\
&= \text{trace}\left[\begin{array}{c|c} \underline{E}_l\underline{Q}_l - \underline{D}_l + P_{l1} & P_{l2} \end{array}\right]\left[\begin{array}{c} (\underline{E}_l\underline{Q}_l - \underline{D}_l + P_{l1})^{\mathrm{T}} \\ \hline P_{l2}^{\mathrm{T}} \end{array}\right] \\
&= \text{trace}\left[(\underline{E}_l\underline{Q}_l - \underline{D}_l)(\underline{E}_l\underline{Q}_l - \underline{D}_l)^{\mathrm{T}}\right] + \text{trace}\left[(\underline{E}_l\underline{Q}_l - \underline{D}_l)P_{l1}^{\mathrm{T}}\right]
\end{aligned}$$

$$
\begin{aligned}
& + \text{trace}\left[P_{l1}(\underline{E}_l\underline{Q}_l - \underline{D}_l)^{\mathrm{T}}\right] + \text{trace}(P_{l2}P_{l2}^{\mathrm{T}}) \\
= \; & J_l^2 + \text{trace}\left[(\underline{E}_l\underline{Q}_l - \underline{D}_l)P_{l1}^{\mathrm{T}}\right] + \text{trace}\left[P_{l1}(\underline{E}_l\underline{Q}_l - \underline{D}_l)^{\mathrm{T}}\right] \qquad (4.15) \\
& + \text{trace}(P_{l2}P_{l2}^{\mathrm{T}}).
\end{aligned}
$$

With the recursive formula in (4.15), we can evaluate J_l recursively as l increases, and thus, results in less computation complexity compared with directly using (4.13).

To this end, we can recursively calculate $\underline{E}_l$ (from (4.12)) and J_l (from (4.15)) to achieve the goal of designing the filter length and the parameters of filters of the transmultiplexer simultaneously. To summarize, for the recursive algorithm for designing analysis filters of the transmultiplexer – RAD-ANA for short, we list the steps involved in recursively computing $\underline{E}_l$ and J_l as l increases:

Step 0 Assume the desired reconstruction time delays $d_0, d_1, \cdots, d_{M-1}$ are given. Choose some initial FIR synthesis filters $F_0, F_1, \cdots, F_{M-1}$.

Step 1 To initialize, let the order of $E(z)$ be $l = 1$, then $S_1 = \left[\underline{Q}_1\underline{Q}_1^{\mathrm{T}}\right]^{-1}$, $\underline{E}_1 = \underline{D}_1\underline{Q}_1^{\mathrm{T}}(\underline{Q}_1\underline{Q}_1^{\mathrm{T}})^{-1}$ and $J_1^2 = \text{trace}\left[(\underline{E}_1\underline{Q}_1 - \underline{D}_1)(\underline{E}_1\underline{Q}_1 - \underline{D}_1)^{\mathrm{T}}\right]$.

Step 2 By using the recursive formulae in (4.6), (4.7), (4.10), (4.12) and (4.15), compute $\underline{E}_{l+1}$ and J_{l+1}.

Step 3 Compare J_{l+1} with J_l: if they are sufficiently close, or for some pre-set small ε, if

$$|J_{l+1} - J_l| \leqslant \varepsilon,$$

terminate the procedure and obtain the appropriate l (order of $E(z)$), from which we can determine the corresponding filter length, and $\underline{E}_l$; then we can obtain the parameters of designed filters; otherwise, increment l by 1 and go to step 2.

Remarks:

1. The facility of designable filter length is one of the prime advantages of this new design method. In practice, shorter filters will offer considerable improvements in computation and hardware implementation (such as reduced number of multipliers and silicon area), and thus, result in an economical usage of filter taps.

2. The RAD-ANA algorithm, mainly consisting of two recursive formulae in (4.12) and (4.15), provides a simple means of designing analysis FIR filters with $E(z)$'s order $(l+1)$ given those with order l. Starting from $l=1$, we can recursively compute $\underline{E}_l$ – the matrix containing the parameters of analysis FIR filters, and J_l – the 2-norm based composite distortion measure, by increasing l until the appropriate order is determined. This recursive feature can reduce the computational burden.

3. From (4.5) and (4.8), we can see that the calculation of matrix inverse (S_{l+1}) is a computationally intensive task for each iteration of different l. The proposed recursive algorithm greatly reduces the computational burden. We compare the computational complexities of directly calculating S_{l+1} in [38] and recursively obtaining S_{l+1} using (4.10) in Table 4.1. It is shown that the recursive calculation is $O\left((l+2)M\right)$ faster than directly computing S_{l+1}. Here $O(n)$ means that the algorithm has order of n time complexity [112].

Table 4.1: Computational complexity.

Directly calculating S_{l+1}	Recursively calculating S_{l+1} using (4.10)
$O\left(((l+2)M)^3\right)$	$O\left(((l+2)M)^2\right)$

4. It is well known that the co-design of synthesis and analysis FIR filters is, in general, a nonlinear optimization problem and difficult to solve. Thus in

the RAD-ANA algorithm, we fix the synthesis filters and design the analysis ones. Similarly, by fixing the analysis filters, we can also develop two recursive formulae for calculating $\underline{R}_m$ and J_m using the techniques discussed above, and get a recursive algorithm for designing FIR synthesis filters (RAD-SYN). Based on these two recursive design procedures – RAD-ANA and RAD-SYN, we propose a two-phase algorithm for designing synthesis and analysis filters in the transmultiplexer: By fixing either the analysis or synthesis filters and finding the other set, we can design a transmultiplexer with appropriate filters' length, leading to joint optimization of both sets. The two-phase algorithm with two recursive design procedures - RAD-ANA and RAD-SYN - internally embedded is illustrated in Figure 4.1. Please note that the derivation of the design

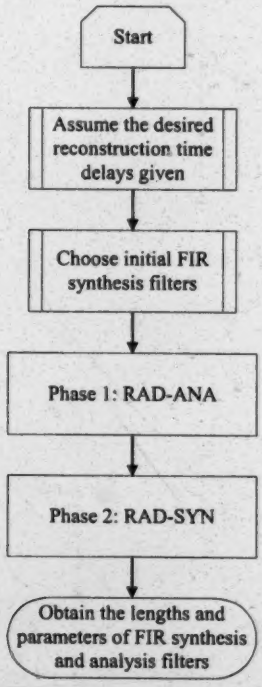
Start
Assume the desired reconstruction time delays given
Choose initial FIR synthesis filters
Phase 1: RAD-ANA
Phase 2: RAD-SYN
Obtain the lengths and parameters of FIR synthesis and analysis filters

Figure 4.1: The two-phase algorithm.

procedure RAD-SYN is similar as that of RAD-ANA as shown in Section 4.3, and is omitted here. Although we cannot provide the convergence proof for the two-phase algorithm to this end, it turns out to be very effective in the design example to follow.

4.4 Numerical Examples

Two examples are given to demonstrate the effectiveness of the proposed algorithms in this section.

Example 1: A two-channel uniform-band transmultiplexer. In this two-channel example, firstly, we preset $\epsilon = 0.002$ and time delays $d_0 = d_1 = 7$. Then, we choose synthesis filters F_0 and F_1 both with length 13, as shown in Figure 4.2, and design analysis filters H_0 and H_1 by applying the RAD-ANA algorithm. The

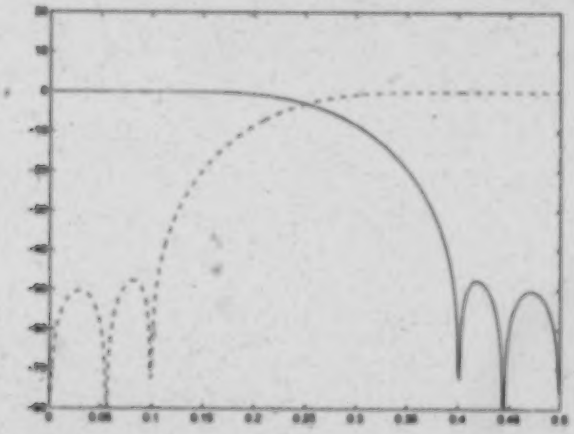

Figure 4.2: The magnitude Bode plots for pre-designed synthesis filters F_0 (solid) and F_1 (dotted): dB versus $\omega/2\pi$.

recursive procedure terminates at $l = 6$ and the length of analysis filters is finally designed to be 14; the designed analysis filters H_0 and H_1 are shown in Figure 4.3. The composite distortion measure J_l as a function of the l is given in Figure 4.4. Figure 4.4 shows that: 1) extra larger l (or equivalently extra longer filter length),

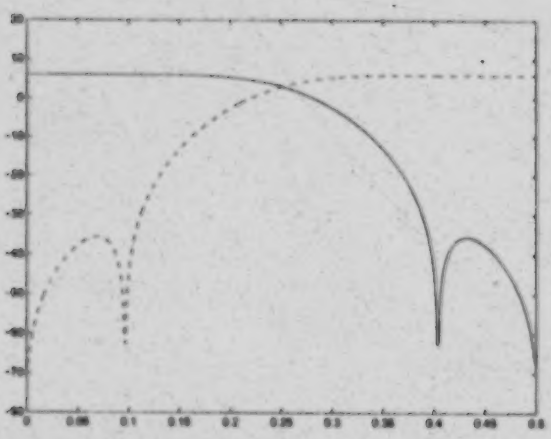

Figure 4.3: The magnitude Bode plots for the designed analysis filters (both of length 14) H_0 (solid) and H_1 (dotted): dB versus $\omega/2\pi$.

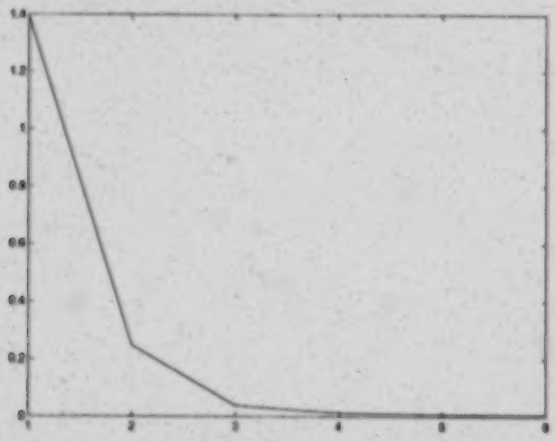

Figure 4.4: The composite distortion measure J_l versus l.

e.g., $l > 6$ in this example, will not further improve the reconstruction performance; 2) shorter filter length can be achieved at the expense of a bit worse reconstruction performance. The composite distortion measure $J_l = 0.0078$ when $l = 6$, which indicates that the designed transmultiplexer can achieve close-to perfect reconstruction: The crosstalk, magnitude, and phase distortions [54, 89] are all bounded by 0.0078.

Example 2: A three-channel uniform-band transmultiplexer. This three-

channel transmultiplexer is designed using the proposed two-phase algorithm. We initially choose the synthesis filters F_0, F_1, and F_2 (of length 15) as shown in Figure 4.5, and pre-set $\varepsilon = 0.002$ and time delays $d_0 = d_1 = d_2 = 8$.

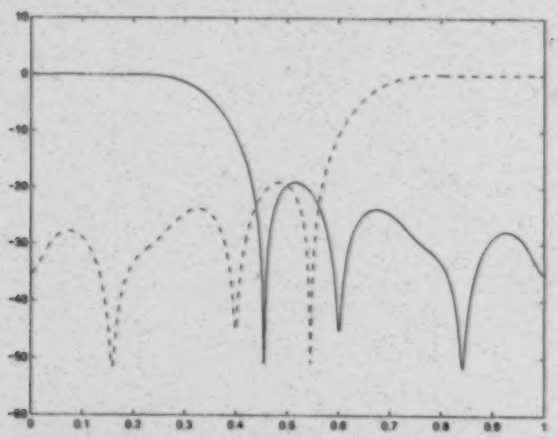

Figure 4.5: The magnitude Bode plots for the pre-designed synthesis filters F_0 (solid), F_1 (dotted), and F_2 (dash-dot): dB versus $\omega/2\pi$.

The two-phase algorithm stops at $l = 5$ and $m = 8$, and the lengths of analysis and synthesis filters are finally designed to be 18 and 27, respectively; the designed synthesis and analysis filters are shown in Figure 4.6 and Figure 4.7, respectively. The composite distortion measure J is finally $J = 0.0516$, indicating good reconstruction performance (Table 4.2). The results also show that the two-phase algorithm can design synthesis and analysis filters jointly, and improve the reconstruction performance.

In fact, there is a trade-off between the reconstruction performance and the filters' frequency selectivity characteristics [74]. As we are focusing on the reconstruction performance of the transmultiplexer, the designed filters do not have clear band-split characteristics in this example. In order to improve this, we need to further incorporate the frequency selectivity characteristics, such as stopband energy and passband magnitude constraints [74], into the design optimization.

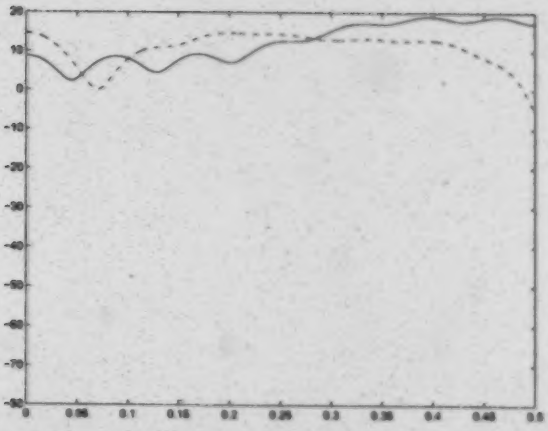

Figure 4.6: The magnitude Bode plots for the designed analysis filters (of length 18) H_0 (solid), H_1 (dotted), and H_2 (dash-dot): dB versus $\omega/2\pi$.

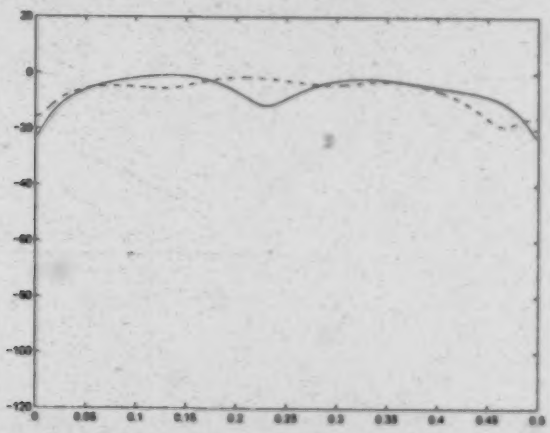

Figure 4.7: The magnitude Bode plots for the designed synthesis filters (of length 27) F_0 (solid), F_1 (dotted), and F_2 (dash-dot): dB versus $\omega/2\pi$.

4.5 Conclusion

Unlike most existing transmultiplexer design methods with filter length fixed, motivated by facts that shorter length filters offer considerable improvements in computation and hardware implementation, and that the transmultiplexer design with *designable* filter length brings more design flexibility, we proposed an efficient recur-

Table 4.2: Composite distortion measure J for recursively increasing l and m using the two-phase algorithm.

	Analysis Filters	Synthesis Filters	Composite Distortion Measure J
Phase 1: RAD-ANA	$l = 1$	$m = 6$	1.5522
	$l = 2$	$m = 6$	0.8386
	$l = 3$	$m = 6$	0.2004
	$l = 4$	$m = 6$	0.0570
	$l = 5$	$m = 6$	0.0568
Phase 2: RAD-SYN	$l = 5$	$m = 7$	0.0517
	$l = 5$	$m = 8$	0.0516

sive design method. It recursively computes the parameters of the filters involved and evaluates the related 2-norm based composite distortion measure for different filter length, and thus, it can not only achieve close-to-perfect reconstruction but also obtain the most appropriate filter length. We believe that our work is novel in the sense that, to the best of our knowledge, it is the first to address the issue of *designable* filter length in transmultiplexer design. The proposed method can be extended to the design of filter bank systems, nonuniform-band transmultiplexers and related applications.

Chapter 5

Multirate Crosstalk Identification in xDSL Systems

5.1 Introduction

Digital Subscriber Line (DSL) technology is a modem technology that uses existing twisted-pair telephone lines to transport high-bandwidth data, such as multimedia and video, to service subscribers [81]. The term xDSL covers a number of similar yet competing forms of DSL, including ADSL (Asymmetric DSL), SDSL (Single-pair, Symmetric DSL), HDSL (High-bit-rate DSL), and VDSL (Very-high-bit-rate DSL). xDSL services are dedicated, point-to-point, public network over twisted-pair copper wire on the local loop "last mile" between a network service provider's (NSP's) central office and the customer site, or on local loops created either intra-building or intra-campus. xDSL is drawing significant attention from practitioners and service providers because it promises to deliver high-bandwidth data rates to dispersed locations with relatively small changes to the existing telecommunication infrastructure [81].

However, because it was designed for voice-grade communications, the physical makeup of telephone cables gives rise to a series of impairment at broadband speeds. One of them, whose impact is minor at voice-band frequencies but potentially crippling at wider bandwidths, is the capacitive and inductive coupling between the signals transported in different subscriber loops known as crosstalk [81]. Crosstalk may be produced by a transmitter located at either the same (NEXT: Near End Crosstalk) or the opposite end (FEXT: Far End Crosstalk) of the cable relative to the position of the disturbed receiver. The major restriction on xDSL is crosstalk [35], which increases with both frequency and number of xDSL transmissions in a connecting cable bundle.

Successful crosstalk identification and cancellation will improve the reliability, reach, and capacity of xDSL systems [7, 36, 105, 80]. These advantages will translate into profits for the service providers. Recently, crosstalk identification in xDSL

systems has attracted a lot of attention due to the significant benefits of having an accurate description of all cable services that generate crosstalk into a given pair. Basically the current research can be divided into two categories:

- **Non-modem based method** [36]: Crosstalk sources are identified and determined in the frequency domain by finding the maximum correlation with a "basis set" of representative measured crosstalk functions [36].

- **Modem based method** [65, 105]: A real-time FEXT crosstalk identification is studied in [65] by exploiting the initialization procedure of a new activated modem. The crosstalk function is identified using a least squares estimator and the accuracy of the identification method is examined by simulation from several aspects. Zeng, *et al.* [105] proposed the idea of an impartial third party that identifies the crosstalk functions among the twisted pairs of a binder. The third-party site collects the transmitted and received signals from all modems in the binder during a given time span. Initially, a cross-correlation technique is applied to estimate the timing differences between the signals from different providers in the same bundle, and then a least squares method is used to jointly estimate the crosstalk functions and the finer scale of the timing-offset among different operators. The proposal of the impartial third-party site will play an important role in setting up crosstalk profiles.

However, to our best knowledge, the crosstalk identification for xDSL systems has not been fully investigated, especially for multirate system models when different services are transmitted in different symbol rates, which is the focus of this work. As many different services exist in the same bundle of the telephone lines and have different sampling rates, the discrete (sampled) crosstalk function will vary with time if the receiver and the crosstalk transmitter belong to different services and

have different symbol rates. Thus in [105], a resampling scheme is used to transform the multirate identification problem to a single-rate one by assuming the receiver low-pass filter to be ideal. However, in practice it is hard to implement ideal low-pass filters.

The contributions of this work are as follows:

1. Contrary to the single-rate identification [105], our work is developed along the line of multirate analysis to directly use all available input and output data, which captures the multirate characteristics of practical applications. Multirate models are obtained by using the blocking technique [89, 14]. With the multirate crosstalk models, we can directly make full use of the measured data information.

2. Instead of performing the off-line identification [105], the proposed algorithm can be used for online identification of the multirate crosstalk model. The dynamically updated crosstalk profiles are more useful for the telephone operators to maintain, diagnose, and expand the current systems.

3. The convergence rate and upper bound of parameter estimation errors for the multirate recursive identification algorithm are derived. With the help of the upper bound, we are able to answer the important question: How large a data set one needs to collect to guarantee that the parameter estimation error is less than a preset level?

The rest of the chapter is organized as follows. In Section 5.2 we discuss the problem formulation of the multirate crosstalk identification in xDSL systems. In Section 5.3 the multirate crosstalk model is then developed by using the blocking technique. In Section 5.4, based on this multirate crosstalk model, we propose the recursive least squares algorithm for identification, and analyze the performance of

the algorithm. In Section 5.5 we present an illustrative example to demonstrate the effectiveness of the proposed method. Finally, we offer some concluding remarks in Section 5.6.

5.2 Problem Formulation

In order to identify the crosstalk functions for the receiver, the impartial third-party site is proposed [105] to collect the transmitted and the received data from all modems during certain time span. However, an important and practical problem is still open: How to identify the crosstalk functions when many different services exist in the same bundle of the telephone lines and have different sampling rates? Figure 5.1 depicts the multirate scenario: The transmitted signals u_1, u_2, $\cdots$, u_K and the received signal y are practically of different sampling rates. In fact, the discrete crosstalk functions will vary with time if the receiver and transmitters belong to different services and have different symbol rates.

The focus of this chapter is on the identification of a multirate system – the *multi-input single-output* (MISO) system with additive noise – as depicted in Figure 5.1.

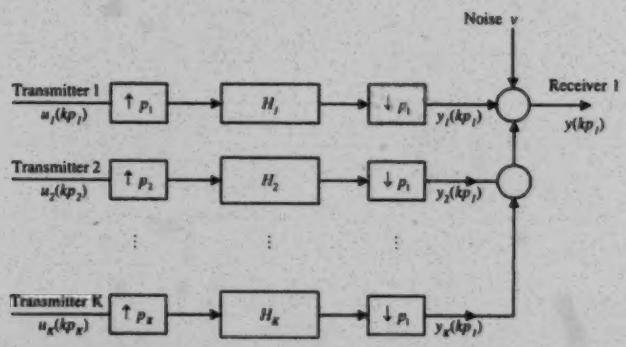

u_i: transmitted signals; H_i: discrete-time FIR (Finite Impulse Response) channel ($i = 1$) or FIR crosstalk functions ($i > 1$); v: noise; $K - 1$: number of crosstalkers; $\uparrow p_K$: upsampler by a factor of p_K; $\downarrow p_1$: downsampler by a factor of p_1.

Figure 5.1: Network model of multirate xDSL systems for one receiver.

Without loss of generality, we assume that the sampling period of the i-th transmitted signal is $T_i = p_i h$, p_1, p_2, $\cdots$, p_K being coprime integers, for otherwise, we can absorb any common factor into h, a positive real number called the *base period*. The sampling period of the received signal y is $T_1 = p_1 h$, same as that of the transmitted signal at the primary channel.

For such a multirate MISO sampled-data system, the input-output data are:

- $\{u_1(kp_1) : \ k = 0, 1, 2, \cdots\}$,
- $\{u_2(kp_2) : \ k = 0, 1, 2, \cdots\}$,

  $\vdots$

- $\{u_K(kp_K) : \ k = 0, 1, 2, \cdots\}$, and
- $\{y(kp_1) : \ k = 0, 1, 2, \cdots\}$.

In fact, based on the impartial third-party idea [105], these input-output data are available at the network maintenance center where the crosstalk identification is performed. As this work is focusing on the multirate crosstalk identification problem, we assume that the input-output date are already time-aligned by using certain time offset estimator, for example, the technique used in [105].

Although the discrete-time systems H_i $(i = 1, 2, \cdots, K)$ are linear time invariant (LTI) with sampling period h, the system from $u_i(kp_i)$ to $y(kp_1)$ in Figure 5.1 is linear periodically time-varying due to different sampling periods. For such a multirate MISO system, our objective is two-fold:

- First, by using the blocking technique, to establish the multirate model of the system from multiple inputs $u_i(kp_i)$ $(i = 1, 2, \cdots, K)$ to single output $y(kp_1)$; that is, to find the mapping relationship between all *available* input and output data.

- Second, to identify the crosstalk functions and study the accuracy of the obtained model.

5.3 Multirate Crosstalk Model

The blocking technique is widely used in multirate digital signal processing and communications [89], and systems and control [14]: It can transform a periodic time-varying system into a time-invariant one with a larger period (frame period). To develop an easy-to-use multirate model to capture the real scenario (multirate characteristics) and further to identify the FIR crosstalk functions (filters) by making full use of all available input and output data, the blocking technique is applied here to the multirate MISO network model in Figure 5.1. In addition, the state-space representation of an FIR filter is employed as a bridge to derive the mapping relationship between all available input and output data. It is assumed that the FIR crosstalk functions have the same known order.

5.3.1 State-space model for an FIR crosstalk function

An FIR filter of length $n+1$ with the transfer function

$$H_i(z) = a_{i0} + a_{i1}z^{-1} + a_{i2}z^{-2} + \cdots + a_{in}z^{-n}$$

can be represented by the following state-space model

$$\begin{cases} x_i(k+1) = A_i x_i(k) + B_i u_i(k), \\ y_i(k) = C_i x_i(k) + D_i u_i(k), \end{cases} \tag{5.1}$$

where $x_i(k) \in \mathbb{R}^{n\times 1}$ is the state vector, $u_i(k)$ is the i-th input signal, $y_i(k)$ is the i-th output signal, $A_i \in \mathbb{R}^{n\times n}$, $B_i \in \mathbb{R}^{n\times 1}$, $C_i \in \mathbb{R}^{1\times n}$, $D_i \in \mathbb{R}^{1\times 1}$ are the system matrices with the following forms:

$$A_i = \begin{bmatrix} 0 & 1 & 0 & \cdots & 0 \\ 0 & 0 & 1 & \cdots & 0 \\ \vdots & \vdots & \vdots & & \vdots \\ 0 & 0 & 0 & \cdots & 1 \\ 0 & 0 & 0 & \cdots & 0 \end{bmatrix}, \quad B_i = \begin{bmatrix} 0 \\ 0 \\ \vdots \\ 0 \\ 1 \end{bmatrix},$$

$$C_i = [\ a_{in} \quad a_{i,n-1} \quad \cdots \quad a_{i1}\ ], \quad D_i = a_{i0}.$$

Here, a_{i0}, a_{i1}, $\cdots$, a_{in}, are the model parameters.

5.3.2 The blocked state-space model

For the multirate MISO system shown in Figure 5.1, let σ be the least common multiple of $p_1, p_2, \cdots, p_K$

$$\sigma = \mathrm{LCM}[p_1, p_2, \cdots, p_K],$$

$T = \sigma h$ (frame period), $\nu_i = \frac{\sigma}{p_i}$, $i = 1, 2, \cdots, K$, $\mu = \nu_1 = \frac{\sigma}{p_1}$.

Replacing k in (5.1) with $k\sigma$, we have

$$\begin{cases} x_i(k\sigma + 1) = A_i x_i(k\sigma) + B_i u_i(k\sigma), \\ y_i(k\sigma) = C_i x_i(k\sigma) + D_i u_i(k\sigma). \end{cases} \tag{5.2}$$

From the state equation in (5.2), by recursion we can easily obtain

$$\begin{aligned} x_i(k\sigma + l) \;=\; & A_i^l x_i(k\sigma) + A_i^{l-1} B_i u_i(k\sigma) + A_i^{l-2} B_i u_i(k\sigma + 1) + \cdots + \\ & A_i B_i u_i(k\sigma + l - 2) + B_i u_i(k\sigma + l - 1), \quad l = 1, 2, \cdots \end{aligned} \tag{5.3}$$

Since the sampling rate of the i-th transmitted signal u_i is $p_i h$, we have

$$u_i(k\sigma + l) = 0, \quad \text{for } \ l \neq m p_i, \ m \in \mathcal{Z}, \tag{5.4}$$

where $\mathcal{Z}$ represents the field of integer numbers. Hence, replacing l in (5.3) with σ, and taking into account the 0 values of the inputs as (5.4), we can write the state equation with all the available input data as follows:

$$\begin{aligned} x_i(k\sigma + \sigma) \;=\; & A_i^\sigma x_i(k\sigma) + A_i^{\sigma-1} B_i u_i(k\sigma) + A_i^{\sigma - p_i - 1} B_i u_i(k\sigma + p_i) + \cdots \\ & + A_i^{\sigma - (\nu_i - 1)p_i - 1} B_i u_i(k\sigma + (\nu_i - 1)p_i) \\ =\; & A_i^\sigma x_i(k\sigma) + \end{aligned}$$

$$[A_i^{\sigma-1}B_i,\ A_i^{\sigma-p_i-1}B_i,\ \cdots,\ A_i^{\sigma-(\nu_i-1)p_i-1}B_i]\begin{bmatrix} u_i(k\sigma) \\ u_i(k\sigma+p_i) \\ \vdots \\ u_i(k\sigma+(\nu_i-1)p_i) \end{bmatrix} \tag{5.5}$$

Similarly, since the sampling period of the received signal y_i is $p_1 h$, we can also represent the output samples based on all the available input data from the output equation in (5.2) and (5.3)

$$\begin{aligned} y_i(k\sigma+lp_1) &= C_iA_i^{lp_1}x_i(k\sigma)+C_iA_i^{lp_1-1}B_iu_i(k\sigma)+C_iA_i^{lp_1-2}B_iu_i(k\sigma+1)+\cdots \\ &\quad +C_iA_iB_iu_i(k\sigma+lp_1-2)+C_iB_iu_i(k\sigma+lp_1-1)+D_iu_i(k\sigma+lp_1) \\ &= C_iA_i^{lp_1}x_i(k\sigma)+\sum_{q=0}^{\lceil lp_1/p_i\rceil} C_iA_i^{lp_1-qp_i-1}B_iu_i(k\sigma+qp_i)+D_iu_i(k\sigma+(\lceil lp_1/p_i\rceil+1)p_i), \end{aligned}$$

where $\lceil lp_1/p_i\rceil$ represents the largest integer number less than lp_1/p_i.

Then we obtain the i-th output at time instant $k\sigma+(\mu-1)p_1$ as

$$y_i(k\sigma+(\mu-1)p_1)=C_iA_i^{(\mu-1)p_1}x_i(k\sigma)$$

$$+[C_iA_i^{(\mu-1)p_1-1}B_i,\ C_iA_i^{(\mu-1)p_1-2}B_i,\ \cdots,\ C_iB_i,\ D_i]\begin{bmatrix} u_i(k\sigma) \\ \vdots \\ u_i(k\sigma+(\nu_i-1)p_i) \end{bmatrix}. \tag{5.6}$$

To this end, we denote the blocked input and output as $\underline{u}_i(k\sigma)$ and $\underline{y}_i(k\sigma)$, respectively

$$\underline{u}_i(k\sigma)=\begin{bmatrix} u_i(k\sigma) \\ u_i(k\sigma+p_i) \\ \vdots \\ u_i(k\sigma+(\nu_i-1)p_i) \end{bmatrix}\in\mathbb{R}^{\nu_i\times 1},\quad \underline{y}_i(k\sigma)=\begin{bmatrix} y_i(k\sigma) \\ y_i(k\sigma+p_1) \\ \vdots \\ y_i(k\sigma+(\mu-1)p_1) \end{bmatrix}\in\mathbb{R}^{\mu\times 1}.$$

Combining (5.5) with (5.6) leads directly to the blocked state-space model for each crosstalk function represented by

$$\begin{cases} x_i(k\sigma+\sigma)=A_i^{\sigma}x_i(k\sigma)+\Omega_i\underline{u}_i(k\sigma), \\ \underline{y}_i(k\sigma)=\Gamma_ix_i(k\sigma)+Q_i\underline{u}_i(k\sigma). \end{cases} \tag{5.7}$$

Here,

$$\Omega_i=[A_i^{\sigma-1}B_i,\ A_i^{\sigma-p_i-1}B_i,\ \cdots,\ A_i^{\sigma-(\nu_i-1)p_i-1}B_i]\in\mathbb{R}^{n\times\nu_i},$$

$$\Gamma_i = \begin{bmatrix} C_i \\ C_i A_i^{p_i} \\ \vdots \\ C_i A_i^{(\mu-1)p_i} \end{bmatrix} \in \mathbb{R}^{\mu \times n},$$

$$Q_i = \begin{bmatrix} D_i & 0 & 0 & \cdots & 0 & 0 \\ C_i A_i^{p_i} & D_i & 0 & \cdots & 0 & 0 \\ \vdots & \vdots & & & \vdots & \vdots \\ C_i A_i^{(\mu-1)p_i-2} B_i & C_i A_i^{(\mu-1)p_i-3} B_i & C_i A_i^{(\mu-1)p_i-4} B_i & \cdots & D_i & 0 \\ C_i A_i^{(\mu-1)p_i-1} B_i & C_i A_i^{(\mu-1)p_i-2} B_i & C_i A_i^{(\mu-1)p_i-3} B_i & \cdots & C_i B_i & D_i \end{bmatrix} \in \mathbb{R}^{\mu \times n}.$$

5.3.3 Mapping between available input and output data

Now we are in a position to derive the mapping relationship between input and output data. From the blocked state-space model in (5.7), we can easily write the transfer function from the blocked input $\underline{u}_i(k\sigma)$ to the blocked output $\underline{y}_i(k\sigma)$

$$\underline{y}_i(k\sigma) = \left[\Gamma_i (zI - A_i^\sigma)^{-1} \Omega_i + Q_i\right] \underline{u}_i(k\sigma),$$

where z^{-1} is the unit delay operator $[z^{-1}y(t) = y(t-1)]$.

Recalling $A_i \in \mathbb{R}^{n \times n}$ with the special structure has the property

$$A_i^p = 0, \quad \text{if } p \geq n,$$

and applying the identity $(1-x)^{-1} = 1 + x + x^2 + x^3 + \cdots \quad (|x| < 1)$, we have

$$\underline{y}_i(k\sigma) = Q_i \underline{u}_i(k\sigma) + \Gamma_i \Omega_i \underline{u}_i(k\sigma - \sigma) + \Gamma_i A_i^\sigma \Omega_i \underline{u}_i(k\sigma - 2\sigma) + \cdots + \Gamma_i A_i^{\sigma(m_i-1)} \Omega_i \underline{u}_i(k\sigma - m_i\sigma), \tag{5.8}$$

where $m_i = \lfloor \frac{n}{\sigma} \rfloor$ is the least integer larger than $\frac{n}{\sigma}$.

We can further rewrite the output equation (5.8) in a compact form

$$\underline{y}_i(k\sigma) = \theta_i^T \varphi_i(k\sigma), \tag{5.9}$$

where the superscript T denotes the matrix transpose, and θ_i is the parameter matrix and φ_i is the information vector of the i-th subsystem with the following form:

$$\theta_i^{\mathrm{T}} = \left[Q_i,\ \Gamma_i\Omega_i,\ \Gamma_i A_i^{\sigma}\Omega_i,\ \cdots,\ \Gamma_i A_i^{\sigma(m_i-1)}\Omega_i\right] \in \mathbb{R}^{n\times(m_i+1)\nu_i},$$

$$\varphi_i(k\sigma) = \begin{bmatrix} \underline{u}_i(k\sigma) \\ \underline{u}_i(k\sigma-\sigma) \\ \vdots \\ \underline{u}_i(k\sigma-m_i\sigma) \end{bmatrix} \in \mathbb{R}^{(m_i+1)\nu_i\times 1}.$$

As shown in Figure 5.1, summing up the received signals of each channel y_i and the background noise v, we obtain the blocked received signal of the primary channel

$$\underline{y}(k\sigma) = \sum_{i=1}^{K} \underline{y}_i(k\sigma) + \underline{v}(k\sigma) = \theta^{\mathrm{T}}\varphi(k\sigma) + \underline{v}(k\sigma), \tag{5.10}$$

where $\underline{v}(k\sigma)$ represents the blocked noise vector, and

$$\theta^{\mathrm{T}} = \left[\theta_1^{\mathrm{T}},\ \theta_2^{\mathrm{T}},\ \cdots,\ \theta_K^{\mathrm{T}}\right] \in \mathbb{R}^{n\times m},\quad \varphi(k\sigma) = \begin{bmatrix} \varphi_1(k\sigma) \\ \varphi_2(k\sigma) \\ \vdots \\ \varphi_K(k\sigma) \end{bmatrix} \in \mathbb{R}^{m\times 1}.$$

Here, $m = \sum_{i=1}^{K}(m_i+1)\nu_i$. As $k = 1,\ 2,\ \cdots$, the model in (5.10) express the mapping relationship of all available measurement data. In the next section, we propose the recursive least squares algorithm based on the model in (5.10), and establish the convergence properties.

Remark: The mapping relationship described by (5.10) has incorporated all available input and output data. Unlike the resampling scheme [105], identification directly based on this model provides an alternative way to identify crosstalk functions in multirate xDSL systems.

5.4 Multirate Recursive Identification Algorithm and Analysis

In this section, we first derive the recursive least squares algorithm based on the model in (5.10), and then analyze the convergence property of the algorithm.

5.4.1 Multirate recursive least squares algorithm

Based on the model (5.10), we can form the prediction error criterion

$$J(\theta) = \sum_{i=1}^{k} \|\underline{y}(i\sigma) - \theta^{\mathrm{T}}\varphi(i\sigma)\|^2. \tag{5.11}$$

Here, k is the data length. Define the extended matrix $Y(k\sigma)$ and augmented information matrix $\Phi(k\sigma)$ as

$$\begin{aligned} Y(k\sigma) &= [\ \underline{y}(\sigma),\ \underline{y}(2\sigma),\ \cdots,\ \underline{y}(k\sigma)\ ], \\ \Phi(k\sigma) &= [\ \varphi(\sigma),\ \varphi(2\sigma),\ \cdots,\ \varphi(k\sigma)\ ]. \end{aligned}$$

Letting the derivatives of $J(\theta)$ with respect to θ be zero gives the estimate $\hat{\theta}$ of θ as follows:

$$\hat{\theta}^{\mathrm{T}}(k\sigma)[\Phi(k\sigma)\Phi^{\mathrm{T}}(k\sigma)] = Y(k\sigma)\Phi^{\mathrm{T}}(k\sigma). \tag{5.12}$$

If the input and output measurement data are sufficiently rich, then the matrix $[\Phi^{\mathrm{T}}(k\sigma)\Phi(k\sigma)]$ is non-singular, which is generally quantified by the persistent excitation condition [8]. Hence, we have

$$\hat{\theta}(k\sigma) = [\Phi(k\sigma)\Phi^{\mathrm{T}}(k\sigma)]^{-1}\Phi(k\sigma)Y(k\sigma)^{\mathrm{T}}. \tag{5.13}$$

From the expression above, $\hat{\theta}(k\sigma)$ depend on the inversion of the matrix $[\Phi(k\sigma)\Phi^{\mathrm{T}}(k\sigma)]$. In order to avoid computing the inversion, we will derive the recursive algorithm of computing the estimate $\hat{\theta}(k\sigma)$. If we define $P^{-1}(k\sigma) = \Phi(k\sigma)\Phi^{\mathrm{T}}(k\sigma)$ and $P^{-1}(k\sigma) \in \mathbb{R}^{n_0 \times n_0}$, then we have

$$P^{-1}(k\sigma) = P^{-1}(k\sigma - \sigma) + \varphi(k\sigma)\varphi^{\mathrm{T}}(k\sigma). \tag{5.14}$$

From the definitions of $Y(k\sigma)$ and $\Phi(k\sigma)$, we have

$$\begin{aligned} \hat{\theta}(k\sigma) &= P(k\sigma)\Phi(k\sigma)Y(k\sigma)^{\mathrm{T}} \\ &= P(k\sigma)[\Phi(k\sigma - \sigma)Y(k\sigma - \sigma)^{\mathrm{T}} + \varphi(k\sigma)\underline{y}^{\mathrm{T}}(k\sigma)] \end{aligned}$$

$$
\begin{aligned}
&= P(k\sigma)[P^{-1}(k\sigma-\sigma)P(k\sigma-\sigma)\Phi(k\sigma-\sigma)Y(k\sigma-\sigma)^{\mathrm{T}}+\varphi(k\sigma)\underline{y}^{\mathrm{T}}(k\sigma)] \\
&= P(k\sigma)[P^{-1}(k\sigma)-\varphi(k\sigma)\varphi^{\mathrm{T}}(k\sigma)]\hat{\theta}(k\sigma-\sigma)+P(k\sigma)\varphi(k\sigma)\underline{y}^{\mathrm{T}}(k\sigma) \\
&= \hat{\theta}(k\sigma-\sigma)+P(k\sigma)\varphi(k\sigma)[\underline{y}^{\mathrm{T}}(k\sigma)-\varphi^{\mathrm{T}}(k\sigma)\hat{\theta}(k\sigma-\sigma)]. \\
&= \hat{\theta}(k\sigma-\sigma)+P(k\sigma)\varphi(k\sigma)[\underline{y}(k\sigma)-\hat{\theta}^{\mathrm{T}}(k\sigma-\sigma)\varphi(k\sigma)]^{\mathrm{T}}. \qquad (5.15)
\end{aligned}
$$

Applying the matrix inversion formula

$$(A+BC)^{-1}=A^{-1}-A^{-1}B(I+CA^{-1}B)^{-1}CA^{-1}$$

to (5.14) gives

$$P(k\sigma)=P(k\sigma-\sigma)-P(k\sigma-\sigma)\varphi(k\sigma)[1+\varphi^{\mathrm{T}}(k\sigma)P(k\sigma-\sigma)\varphi(k\sigma)]^{-1}\varphi^{\mathrm{T}}(k\sigma)P(k\sigma-\sigma). \qquad (5.16)$$

Define a gain matrix

$$L(k\sigma):=P(k\sigma)\varphi(k\sigma).$$

Post-multiplying (5.16) by $\varphi(k\sigma)$ yields

$$L(k\sigma)=P(k\sigma-\sigma)\varphi(k\sigma)[1+\varphi^{\mathrm{T}}(k\sigma)P(k\sigma-\sigma)\varphi(k\sigma)]^{-1}. \qquad (5.17)$$

Now, we are in a position to summarize the recursive least squares identification algorithm of estimating the parameter matrix θ as follows:

Step 1 To initialize the algorithm, we take $P(0)=p_0I$ with p_0 normally a large positive number (e.g., $p_0=10^6$), and $\hat{\theta}(0)=\hat{\theta}_0$, some small real matrix.

Step 2 Compute $\hat{\theta}(k\sigma)$ using (5.15)

Step 3 Update $L(k\sigma)$ (Equation (5.17)) and $P(k\sigma)$ (Equation (5.16)), respectively.

Step 4 Increment k by 1 and go to step 2; terminate the algorithm till appropriate k.

Comment on the computational complexity: To implement the proposed algorithm, for each iteration step, numbers of multiplications and additions are $2m^2 + 3m + 2nm$ and $2m^2 + 2nm + m$, respectively.

5.4.2 Convergence analysis

In practice, only limited length of data can be collected for identification purpose. Hence, we are more interested in the convergence rate and the parameter estimation error bound for finite data samples.

The convergence property and the upper bound of the parameter estimation error are summarized in the following theorem.

Theorem 4 *For the multirate system in (5.10) and the recursive least squares algorithm, assume that $\underline{v}(k\sigma)$ is an independent white noise vector sequence with zero mean and bounded variance, i.e.,*

$$(A1) \qquad E[\underline{v}(k\sigma)] = 0,\ E[\underline{v}(k\sigma)\underline{v}^{\mathrm{T}}(i\sigma)] = 0,\ k \neq i,$$

$$(A2) \qquad E[\|\underline{v}(k\sigma)\|^2] = \sigma_v^2(k\sigma) \leqslant \sigma_v^2 < \infty;$$

$\hat{\theta}(0)$ is independent of $\underline{v}(k\sigma)$ with $\|\hat{\theta}(0) - \theta\|^2 \leqslant \delta_0 < \infty$; and there exist positive constants c and k_0 such that for $k \geq k_0$, the following weak persistent excitation condition holds [53]:

$$(A3) \qquad \frac{1}{k}\sum_{i=1}^{k} \varphi(i\sigma)\varphi^{\mathrm{T}}(i\sigma) \geq c\,I,\ \text{a.s.}$$

Then the parameter estimate $\hat{\theta}(k\sigma)$ given by the multirate least squares algorithm converges to its true value θ at the rate of $\frac{1}{\sqrt{k}}$ for $k \geq k_0$:

$$E[\|\hat{\theta}(k\sigma) - \theta\|^2] \leqslant \frac{2\delta_0}{c^2 p_0^2 k^2} + \frac{2n_0\sigma_v^2}{ck} =: f_1(k\sigma),$$

where the norm of a matrix is the Frobenius one: $\|X\|^2 = \mathrm{tr}[XX^{\mathrm{T}}]$, $\mathrm{tr}[X]$ denoting the trace of the matrix X. Thus

$$\lim_{k\to\infty} \hat{\theta}(k\sigma) = \theta.$$

Proof Define

$$\tilde{\theta}(k\sigma) = \hat{\theta}(k\sigma) - \theta.$$

Substituting (5.15) into the above equation and using (5.10) yield

$$\begin{aligned}
\tilde{\theta}(k\sigma) &= \tilde{\theta}(k\sigma - \sigma) - \theta + P(k\sigma)\varphi(k\sigma)[\varphi^{\mathrm{T}}(k\sigma)\theta + \underline{y}^{\mathrm{T}}(k\sigma) - \varphi^{\mathrm{T}}(k\sigma)\hat{\theta}(k\sigma - \sigma)] \\
&= \tilde{\theta}(k\sigma - \sigma) + P(k\sigma)\varphi(k\sigma)[-\varphi^{\mathrm{T}}(k\sigma)\tilde{\theta}(k\sigma - \sigma) + \underline{y}^{\mathrm{T}}(k\sigma)] \\
&= [I - P(k\sigma)\varphi(k\sigma)\varphi^{\mathrm{T}}(k\sigma)]\tilde{\theta}(k\sigma - \sigma) + P(k\sigma)\varphi(k\sigma)\underline{y}^{T}(k\sigma).
\end{aligned}$$

Multiplying both sides of (5.14) by $P(k\sigma)$ gives

$$I - P(k\sigma)\varphi(k\sigma)\varphi^{\mathrm{T}}(k\sigma) = P(k\sigma)P^{-1}(k\sigma - \sigma).$$

Using the above equation, we have

$$\begin{aligned}
\tilde{\theta}(k\sigma) &= P(k\sigma)P^{-1}(k\sigma - \sigma)\tilde{\theta}(k\sigma - \sigma) + P(k\sigma)\varphi(k\sigma)\underline{y}^{\mathrm{T}}(k\sigma) \\
&= P(k\sigma)P^{-1}(k\sigma - 2\sigma)\tilde{\theta}(k\sigma - 2\sigma) + P(k\sigma)\varphi(k\sigma - \sigma)\underline{y}^{\mathrm{T}}(k\sigma - \sigma) + P(k\sigma)\varphi(k\sigma)\underline{y}^{\mathrm{T}}(k\sigma) \\
&= P(k\sigma)P^{-1}(0)\tilde{\theta}(0) + P(k\sigma)\sum_{i=1}^{k}\varphi(i\sigma)\underline{y}^{\mathrm{T}}(i\sigma) =: \gamma_1(k\sigma) + \gamma_2(k\sigma), \qquad (5.18)
\end{aligned}$$

where

$$\gamma_1(k\sigma) := P(k\sigma)P^{-1}(0)\tilde{\theta}(0), \quad \gamma_2(k\sigma) := P(k)\sum_{i=1}^{k}\varphi(i\sigma)\underline{y}^{\mathrm{T}}(i\sigma).$$

Let

$$U_k = \begin{bmatrix} \varphi^{\mathrm{T}}(\sigma) \\ \varphi^{\mathrm{T}}(2\sigma) \\ \vdots \\ \varphi^{\mathrm{T}}(k\sigma) \end{bmatrix}, \quad V_k = \begin{bmatrix} \underline{y}^{\mathrm{T}}(\sigma) \\ \underline{y}^{\mathrm{T}}(2\sigma) \\ \vdots \\ \underline{y}^{\mathrm{T}}(k\sigma) \end{bmatrix}. \qquad (5.19)$$

From (A3) and (5.14), we have, for $k \geq k_0$

$$\begin{aligned}
U_k^{\mathrm{T}}U_k &\geq ckI, \\
P^{-1}(k\sigma) &= U_k^{\mathrm{T}}U_k + P^{-1}(0) \geq ckI + P^{-1}(0) \geq ckI, \\
P(k\sigma) &\leqslant \frac{I}{ck}.
\end{aligned}$$

Let $\lambda_{\max}[X]$ represents the maximum eigenvalue of X. Hence

$$\begin{aligned} E[\|\gamma_1(k\sigma)\|^2] &= E[\tilde{\theta}^{\mathrm{T}}(0)P^{-1}(0)P^2(k\sigma)P^{-1}(0)\tilde{\theta}(0)] \\ &\leqslant \frac{\lambda^2_{\max}[P^{-1}(0)]}{c^2k^2}E[\|\tilde{\theta}(0)\|^2] \leqslant \frac{\lambda^2_{\max}[P^{-1}(0)]\delta_0}{c^2k^2}, \quad k \geq k_0, \quad (5.20) \\ E[\|\gamma_2(k\sigma)\|^2] &= E[\|P(k\sigma)\sum_{i=1}^{k}\psi(i\sigma)\underline{v}^{\mathrm{T}}(i\sigma)\|^2] = E[\|P(k\sigma)U_k^{\mathrm{T}}V_k\|^2] \\ &= E\{\mathrm{tr}[P(k\sigma)U_k^{\mathrm{T}}V_kV_k^{\mathrm{T}}U_kP(k\sigma)]\} \leqslant \mathrm{tr}\{E[U_kP^2(k\sigma)U_k^{\mathrm{T}}]\}\sigma_v^2 \\ &\leqslant \mathrm{tr}\{E[U_kP(k\sigma)U_k^{\mathrm{T}}]\}\frac{\sigma_v^2}{ck} \leqslant \frac{n_0\sigma_v^2}{ck}, \quad \text{for } k \geq k_0. \end{aligned}$$

The last inequality about $E[\|\gamma_2(k\sigma)\|^2]$ follows from: $I = P(k\sigma)U_k^{\mathrm{T}}U_k + P(k\sigma)P^{-1}(0) \geq P(k\sigma)U_k^{\mathrm{T}}U_k$ and $\mathrm{tr}(AB) = \mathrm{tr}(BA)$. From (5.18), we have

$$\begin{aligned} E[\|\tilde{\theta}(k\sigma)\|^2] &= E[\|\gamma_1(k\sigma) + \gamma_2(k\sigma)\|^2] \leqslant 2\{E[\|\gamma_1(k\sigma)\|^2] + E[\|\gamma_2(k\sigma)\|^2]\} \\ &\leqslant \frac{2\lambda^2_{\max}[P^{-1}(0)]\delta_0}{c^2k^2} + \frac{2n\sigma_v^2}{ck}, \quad \text{for } k \geq k_0. \end{aligned}$$

This proves Theorem 4. □

There are several interesting observations from Theorem 4 above:

- The assumptions in (A1) and (A2) imply that the noise vector $\underline{v}(k\sigma)$ is a white noise vector sequence with zero mean, time-varying but bounded variance. Assumption (A3) implies that the input is a persistently exciting signal such that the input-output data contain enough (rich) information from which the system parameters are identifiable.

- Theorem 4 shows that if the noise vector $\{\underline{v}(k\sigma)\}$ has a bounded variance, the parameter estimation error $\tilde{\theta}(k\sigma)$ converges to zero at the rate of $\frac{1}{\sqrt{k}}$.

- For identifying crosstalk functions in xDSL systems, we gather measurement input and output data. Therefore, according to (A3), we can compute c. Since p_0 is chosen to be a large number (e.g., $p_0 = 10^6$), taking $k = L$, the first term

of $f_1(k\sigma)$ in Theorem 4 is small and can be neglected; so we have

$$f_1(L\sigma) \approx \frac{2n_0\sigma_v^2}{cL}.$$

Note that n_0 is known, and σ_v^2 can be estimated by many existing methods.

- If the parameter estimation error is expected to be less than a preset small real number ε, that is

$$E[\|\tilde{\theta}(k\sigma)\|^2] \leqslant \varepsilon.$$

Then based on the above analysis, we can approximately determine how large the data length k we should choose:

$$k \geq \frac{2n_0\sigma_v^2}{c\varepsilon}.$$

- The error upper bound in Theorem 4 usually is not tight and hence is conservative. In fact, the true parameter estimation error is smaller than this upper bound $f_1(k\sigma)$.

5.5 Illustrative Examples

This section shows the simulation results of crosstalk identification in the upstream direction (from the subscriber to the central office). The receiver of interest is assumed to be an ADSL modem. The crosstalk environment is set up as (shown in Figure 5.2):

- One HDSL;
- One basic rate ISDN (BRI);
- One ADSL.

All twisted pairs are assumed to be 26-gauge (0.4 mm) [105]. In this example, we focus on the identification of NEXT as the dominant crosstalk signals are from

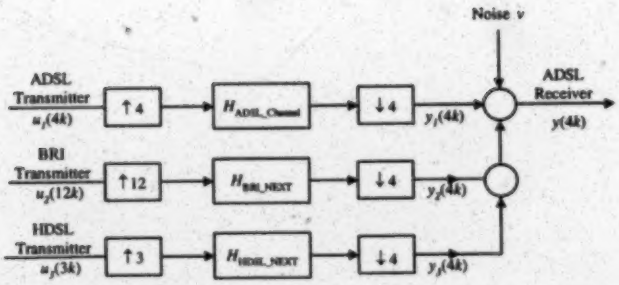

Figure 5.2: A simple network model of multirate xDSL system for one primary ADSL receiver with NEXTs.

NEXT by HDSL and BRI. It should be noted that the proposed algorithm can also be applied to identify smaller FEXTs after identifying and cancelling NEXTs from the received signal [105].

Several important characteristics of DSLs are taken from ITU-T Recommendation G.996.1 [46, 105] and summarized in Table 5.1. The model for NEXT of different

Table 5.1: xDSL Characteristics

xDSL	ADSL (up)	BRI	HDSL
Line code	DMT	2B1Q	2B1Q
Sampling rate (ks/sec)	276	80	392
Sampling period ($\times 10^{-6}$sec)$\approx$	4	12	3
Power (dBm)	12.5	13.6	13.6

types of xDSLs can also be found in [46]. The model for NEXT is commonly known as the 1% worst-case model [34, 35, 46, 105]

$$|T_{\mathrm{NEXT}}(f)|^2 \approx 10^{-14} f^{3/2},$$

and the interested NEXT function [46, 105] is

$$H_{\mathrm{NEXT}}(f) = P_{\mathrm{xDSL}}(f) T_{\mathrm{NEXT}}(f) H_{\mathrm{LPF}}(f),$$

where $H_{\mathrm{LPF}}(f)$ is the receiver low-pass filter and $P_{\mathrm{xDSL}}(f)$ is a generic term for the transmitter filter response of BRIs, HDSLs and ADSLs. Please note that it is assumed that all crosstalk functions are of linear phase [105], and their orders are fixed. The characteristics of the crosstalk functions can be found in the literature, e.g., [46, 105]. The 1% worst case model refers to the power-sum crosstalk loss, i.e., the sum of the power losses of all the other pairs in the binder into the pair of interest. Each pair-to-pair coupling exhibits a wide variation of coupling strength versus frequency, and it is the power summing that smoothes and averages these variations thus leading to the power sum NEXT model [34, 35]. It is worth to point out the limitation of using this kind of model: For crosstalk identification, what is actually of interest is not the power-sum loss but the individual pair-to-pair NEXT crosstalk coupling losses. However, in order to focus on showing the idea and the effectiveness (by comparison) of the proposed multirate crosstalk identification algorithm, we still use the 1% worst case model in the illustrative simulation example.

As the primary ADSL channel function is assumed to be known, the problem reduces to a multirate 2-input-1-output structure (shown in Figure 5.3). In fact, the

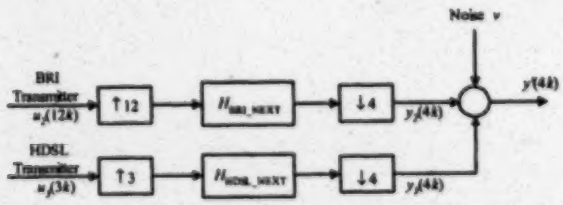

Figure 5.3: A simple network model of multirate xDSL system for identifying NEXTs.

loop make-up of the channel between the ADSL transmitter and receiver may not be known exactly, which could bring errors in the crosstalk identification. Therefore, in practice, we may need to perform loop make-up identification for ADSL channel before crosstalk identification.

Please note in Table 5.1, we approximately choose the sampling periods according to the sampling rates. In this case, $\sigma = 12$. We first generate the following input and output data:

- $\{u_2(12k)\}$, $\{u_3(3k)\}$ and
- $\{y'(4k)\}$.

Here $\{u_2(12k)\}$ and $\{u_3(3k)\}$ are taken as persistent excitation sequences with zero mean and unit variance, respectively, and $\{v\}$ as a white noise sequence with zero mean and scaled unit variance. In order to evaluate the estimation accuracy we use the absolute parameter estimation error $\delta_a = \|\hat{\theta}(k\sigma) - \theta\|$. We denote the parameter estimation error upper bound as $\delta_u = \sqrt{f_1(k\sigma)}$.

Using the first 3000 samples of data, we apply the recursive least squares algorithm to estimate the parameter matrix θ of the blocked system. From Figure 5.4,

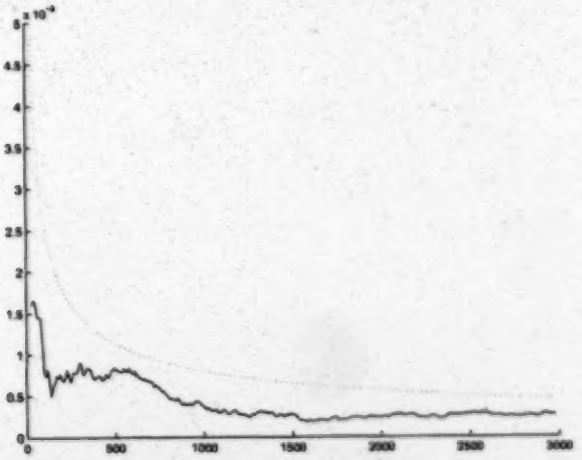

Solid line: δ_a vs. k; dotted line: δ_u vs. k.

Figure 5.4: The absolute estimation error and its upper bound.

it is clear that the absolute parameter estimation error δ_a is in general becoming

smaller as k increases. This indicates that more iterations lead to more accurate estimation results.

In order to compare our method with the resampling scheme used in [105], we apply the resampling method to our example:

1. Processing the data by using the resampling sinc function [105]. Then the problem is approximately simplified to that of single-rate identification.

2. Using the least squares method to identify the crosstalk functions using the single-rate data [105].

3. Using the identified crosstalk functions to predict the sub-channel's output: $\hat{y}_3(4k)$.

4. Comparing the predicted outputs with the last 1000 samples of the generated output y_3. Also we define the following relative prediction error to evaluate the prediction performance:

$$\rho = \sum_{k=3001}^{4000} \frac{[y_3(4k) - \hat{y}_3(4k)]^2}{[y_3(4k)]^2}.$$

The results are shown in Table 5.2. The comparison of the prediction performance

Table 5.2: Prediction performance.

	Multirate model based recursive identification	Resampling method [105]
Relative prediction error ρ	0.3026	0.5013

shows that recursive identification directly based on the multirate model outperforms the single-rate identification using the resampling scheme [105].

5.6 Conclusion

Crosstalk is a major impairment of xDSL systems, which significantly limits the data rate and the reach of the twisted pairs. It is invaluable to identify the crosstalk functions for each pair and, thus, offer better services for more users. In this chapter, we studied the *multirate* crosstalk identification for the practical case when different services are operating in different symbol rate. We showed that the following are the fundamental problems involved: a) How to model the *multirate* network model of xDSL systems? and b) How to estimate the parameter estimation upper bound, and further determine the relationship between the data length and a preset parameter estimation error level? We posed and solved these problems by reference to a general multirate MISO network model. We believe that our work is novel in the sense that, to the best of our knowledge, it is the first to address the modelling and identification of the *multirate* network model in xDSL systems.

The approach from the *multirate* perspective proposed here is a kind of exploratory work. Some future work are:

- It is worth to further develop new multirate identification algorithms with reduced computational complexity.
- In practice, the order of the crosstalk function of interest is unknown, how to simultaneously estimate the model order and parameters is an interesting topic.
- Important issues such as multirate crosstalk recognition, multirate crosstalk cancellation, and multirate dynamic spectrum management need further study.

Chapter 6

Crosstalk Identification in xDSL Systems with Unknown Model Order

6.1 Introduction

From the viewpoint of spectrum management for xDSL systems [80, 7], successful crosstalk identification and cancelation will improve the reliability, reach, and capacity of xDSL systems [7, 105, 80]. These advantages will translate into profits for the service providers. Recently, crosstalk identification in xDSL systems has attracted much attention due to the significant benefits of having an accurate description of all cable services [105, 80, 7]. A real-time FEXT crosstalk identification was studied in [65] by exploiting the initialization procedure of a newly activated modem. Zeng *et al.* [105] employed three techniques to identify FIR crosstalk functions among the twisted pairs of a binder: (1) the impartial third-party site idea was proposed to collect the transmitted and the received data from all modems during certain time span; (2) the cross-correlation method was used to estimate the timing differences between the crosstalk signals and the received signals; (3) a resampling scheme was employed to cope with the multirate services problem. However, we note that these crosstalk identification schemes all assumed prior knowledge of the model order for crosstalk functions. In many realistic situations, however, the model order is not known and must be estimated prior to solving the parameter estimation problem. In fact, the crosstalk model order determination plays an important role in dynamic spectrum management. In this chapter, we focus on the problem of identifying both the model order and the parameters of FIR crosstalk functions simultaneously.

Obviously, determining the model order is a key first step toward the goal of estimating the model parameters, and has attracted much attention, see [2, 3, 50, 1] and the references therein. Liang *et al.* [50] studied ARMA model order estimation based on the eigenvalues of the covariance matrix. Al-Smadi *et al.* extended the method in [50] to the case of colored Gaussian noise. However, these pieces of work including the FPE (Final Prediction Error) criterion [2] and AIC (Akaike's

Information Criterion) [3] approaches put more emphasis on the order determination problem, not on the parameter estimation. Moreover, they are not suitable for multi-channel cases. Based on the UDU^{T} factorization technique, Niu *et al.* studied the identification of model order and parameters for single-input-single-output (SISO) CARMA systems with the order descending. This requires choosing an initial maximum possible order, which results in either higher computational burden for higher initial order than the true one, or inaccurate identification results for lower one. Levison and Durbin [33, 39] proposed the recursive method to compute Yule-Walker equations; however, it is only suitable for AR models. To the authors' best knowledge, few publications have addressed identification algorithms of multi-channel crosstalk systems on estimating both model order and parameters, which is the focus of this work.

Briefly, this chapter is organized as follows. Section 6.2 describes the problem formulation of the crosstalk identification in xDSL systems. In Section 6.3, we extend Levison and Durbin's recursive idea to multi-channel crosstalk systems for simultaneously estimating the model order and parameters of FIR crosstalk functions. Section 6.4 presents an illustrative example to demonstrate the effectiveness of the proposed method. Finally, we offer some concluding remarks in Section 6.5.

6.2 Problem Formulation

The focus of this chapter is on the identification of the crosstalk functions in the xDSL network – a multi-channel crosstalk system with an additive noise, as depicted in Figure 6.1. u_0, u_1, u_2, $\cdots, u_r$ are signals to be transmitted, G_0 is the known transfer function of the primary channel, G_j $(j = 1, \cdots, r)$ the crosstalk functions, y_R the measured output at the primary receiver, v the white noise, and r the number of crosstalkers. We assume that the input data are resampled according to the clock

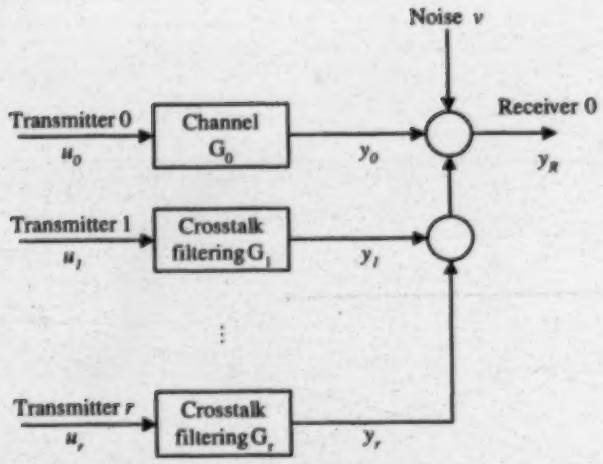

Figure 6.1: The network model of xDSL systems for one primary receiver.

rate of the primary receiver. Since the primary channel response is known *a priori*, and thus y_0 can be obtained , we are actually to identify the multi-channel crosstalk system involving $G_1, G_2, \cdots, G_r$ using the collected input data $u_1, u_2, \cdots, u_r$, and the computed output $y := y_R - y_0$.

Without loss of generality, the crosstalk functions can be expressed by

$$G_j(z) = g_{j0} + g_{j1}z^{-1} + g_{j2}z^{-2} + \cdots, \quad j = 1, 2, \cdots, r.$$

Then it is easy to represent the measured output as:

$$\begin{aligned} y(k) &= \sum_{j=1}^{r} G_j u_j(k) + v(k) \\ &= \sum_{j=1}^{r}\sum_{i=0}^{\infty} g_{ji} z^{-i} u_j(k) + v(k) \\ &= \sum_{j=1}^{r}\sum_{i=0}^{\infty} g_{ji} u_j(k-i) + v(k). \end{aligned}$$

In theory, the IIR model with infinite higher order is the best way to characterize the crosstalk scenario, whereas it is hard to determine infinite number of parameters because of computational complexity. Therefore, it is common to assume that the

number of parameters of each crosstalk is limited and given [105, 65]. If the number of parameters for each crosstalk is $N+1$, then it is equivalent to represent the output as:

$$y(k) = \sum_{j=1}^{r} \sum_{i=0}^{N} b_{ir+j} u_j(k-i) + v(k).$$

In practice, however, not only the parameters of the crosstalk functions, but also the model order are unknown. The drawback of assuming known order is obvious: On one hand, if the assumed order is lower than the true one, the identified crosstalk profiles will not characterize the true crosstalk scenario in the xDSL network; on the other hand, if higher, the computational complexity will inevitably increase. To this end, an important problem in crosstalk identification is still open: How to choose the appropriate model order?

In this work, by means of Levison and Durbin's idea [33, 39], we develop a recursive algorithm for identifying the multi-channel crosstalk system in xDSL network. Our objective is two-fold:

- First, simultaneously estimate the appropriate model order and the parameters of the FIR crosstalk functions by recursively increasing the number of parameters involved.
- Second, reduce the computational complexity of the identification algorithm, which motivate us to develop a recursive algorithm.

6.3 A Recursive Algorithm

In this section, we derive a recursive algorithm to identify the model order and parameters of the FIR crosstalk functions simultaneously, as the number of all parameters involved increases.

Let p be the data length ($p \gg N$), define (for some fixed l)

$$Y = \begin{bmatrix} y(l) \\ y(l+1) \\ \vdots \\ y(l+p-1) \end{bmatrix}, \quad V = \begin{bmatrix} v(l) \\ v(l+1) \\ \vdots \\ v(l+p-1) \end{bmatrix},$$

$$x_{ir+j} = \begin{bmatrix} u_j(l-i) \\ u_j(l-i+1) \\ \vdots \\ u_j(l-i+p-1) \end{bmatrix}, \; i = 0, 1, 2, 3, \cdots, \; j = 1, 2, \cdots, r,$$

and, further define the data matrix as:

$$\begin{aligned} H_{n+1} &= [x_1, \; x_2, \; \cdots, \; x_{n+1}] \in \mathbb{R}^{p \times (n+1)} \\ &= [H_n, \; x_{n+1}]. \end{aligned} \tag{6.1}$$

Here, note that $H_1 = x_1$. Group the parameters of all the crosstalk functions (FIR) in the following vector

$$\theta_n = [b_1, \; b_2, \; b_3, \; \cdots, \; b_n],$$

where n is the total number of all the parameters involved. Then the measured output can be further written as:

$$Y = H_n \theta_n + V. \tag{6.2}$$

In accordance with (6.2), define a quadratic cost function – the prediction error criterion

$$J(\hat{\theta}_n) = \|Y - H_n \hat{\theta}_n\|^2, \tag{6.3}$$

where $\|X\|^2 = \mathrm{tr}[XX^{\mathrm{T}}]$. Minimizing $J(\theta_n)$ leads to the following least squares solution [53]:

$$\hat{\theta}_n = (H_n^{\mathrm{T}} H_n)^{-1} H_n^{\mathrm{T}} Y. \tag{6.4}$$

Observing the least squares solution in (6.4), it is natural and common to suggest an iterative algorithm (as depicted in Figure 6.2) to search an appropriate model

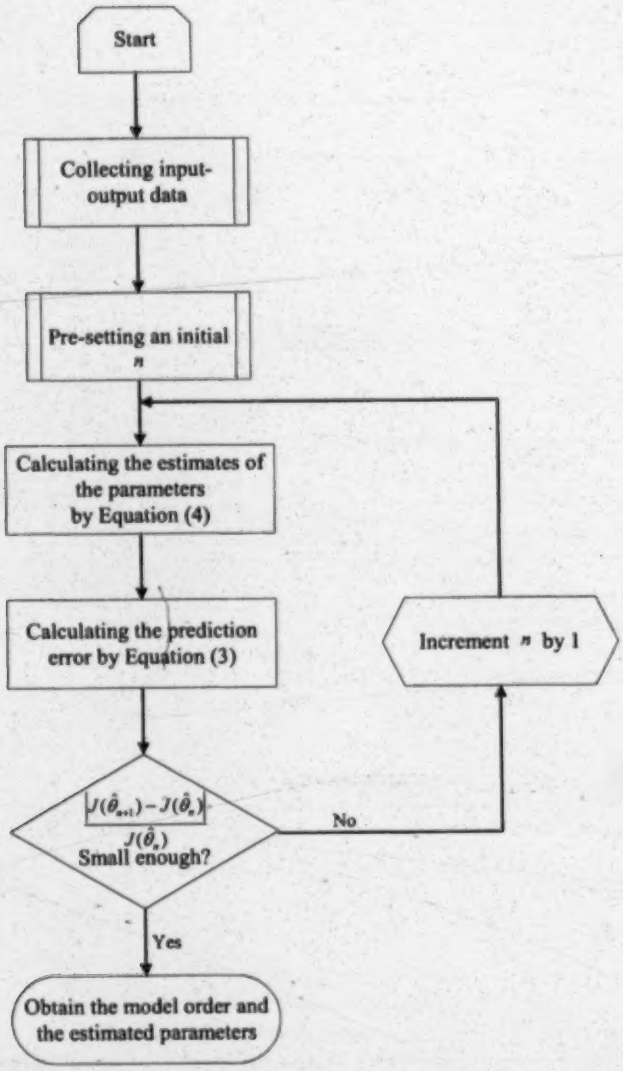
Start
Collecting input-output data
Pre-setting an initial n
Calculating the estimates of the parameters by Equation (4)
Calculating the prediction error by Equation (3)
Increment n by 1
$\frac{|J(\hat{\theta}_{n+1}) - J(\hat{\theta}_n)|}{J(\hat{\theta}_n)}$ Small enough?
No
Yes
Obtain the model order and the estimated parameters

Figure 6.2: An iterative algorithm with high computational burden.

order. However, it is obvious that the calculation of the inversion of a matrix is needed for different n in each iteration, which greatly increases the computational burden if n is large. Therefore, we are aiming to develop a recursive algorithm that can not only estimate model order and parameters simultaneously, but also have

less computational complexity.

In order to derive the recursive algorithm, we introduce the matrix inversion Lemma first.

Lemma 4 *[105] Let A be a square matrix partitioned as followed*

$$A := \begin{bmatrix} A_{11} & A_{12} \\ A_{21} & A_{22} \end{bmatrix},$$

where A_{11} and A_{22} are also square matrices. If A and A_{11} are nonsingular, then

$$\begin{bmatrix} A_{11} & A_{12} \\ A_{21} & A_{22} \end{bmatrix}^{-1} = \begin{bmatrix} A_{11}^{-1} + A_{11}^{-1}A_{12}T^{-1}A_{21}A_{11}^{-1} & -A_{11}^{-1}A_{12}T^{-1} \\ -T^{-1}A_{21}A_{11}^{-1} & T^{-1} \end{bmatrix},$$

where

$$T := A_{22} - A_{21}A_{11}^{-1}A_{12}.$$

Defining the data product moment matrix

$$S_n = H_n^{\mathrm{T}} H_n,$$

we have the following recursive relation:

$$S_{n+1} = [H_n, \ x_{n+1}]^{\mathrm{T}} [H_n, \ x_{n+1}] = \begin{bmatrix} S_n & H_n^{\mathrm{T}} x_{n+1} \\ x_{n+1}^{\mathrm{T}} H_n & \beta_{n+1} \end{bmatrix}, \tag{6.5}$$

where $\beta_{n+1} := x_{n+1}^{\mathrm{T}} x_{n+1}$ is a scalar. Directly applying Lemma 4, we can obtain the inversion

$$S_{n+1}^{-1} = \begin{bmatrix} S_n^{-1} + R_{n+1}x_{n+1}^{\mathrm{T}}H_{n+1}S_n^{-1} & -R_{n+1} \\ -R_{n+1}^{\mathrm{T}} & \alpha_{n+1}^{-1} \end{bmatrix}, \tag{6.6}$$

where $R_{n+1} := S_n^{-1}H_n^{\mathrm{T}}x_{n+1}\alpha_{n+1}^{-1}$, and $\alpha_{n+1} := \beta_{n+1} - x_{n+1}^{\mathrm{T}}H_{n+1}S_n^{-1}H_{n+1}^{\mathrm{T}}x_{n+1}$.

From (6.4) and (6.6), we can get the recursive formula for $\hat{\theta}_{n+1}$:

$$\begin{aligned} \hat{\theta}_{n+1} &= S_{n+1}^{-1}[H_n, \ x_{n+1}]^{\mathrm{T}}Y \\ &= \begin{bmatrix} S_n^{-1} + R_{n+1}x_{n+1}^{\mathrm{T}}H_{n+1}S_n^{-1} & -R_{n+1} \\ -R_{n+1}^{\mathrm{T}} & \alpha_{n+1}^{-1} \end{bmatrix} \begin{bmatrix} H_n^{\mathrm{T}} \\ x_{n+1}^{\mathrm{T}} \end{bmatrix} Y \\ &= \begin{bmatrix} S_n^{-1}H_nY - R_{n+1}x_{n+1}^{\mathrm{T}}(Y - H_{n+1}\hat{\theta}_n) \\ x_{n+1}^{\mathrm{T}}(Y - H_n\hat{\theta}_n)\alpha_{n+1}^{-1} \end{bmatrix} \\ &= \begin{bmatrix} \hat{\theta}_n - R_{n+1}x_{n+1}^{\mathrm{T}}(Y - H_{n+1}\hat{\theta}_n) \\ x_{n+1}^{\mathrm{T}}(Y - H_n\hat{\theta}_n)\alpha_{n+1}^{-1} \end{bmatrix}. \end{aligned} \tag{6.7}$$

With this recursive formula for $\hat{\theta}_{n+1}$, we are free from calculating the inversion of a matrix in each iteration, and thus, the computational complexity is greatly reduced. In order to determine the appropriate model order, we still need another recursive formula for evaluating the prediction error. Recall the prediction error criterion in (6.3) and rewrite it as:

$$\begin{aligned} J(\hat{\theta}_n) &= \|Y - H_n\hat{\theta}_n\|^2 \\ &= \|Y - H_n(H_n^{\mathrm{T}}H_n)^{-1}H_n^{\mathrm{T}}Y\|^2 \\ &= Y^{\mathrm{T}}[I - H_n(H_n^{\mathrm{T}}H_n)^{-1}H_n^{\mathrm{T}}]Y. \end{aligned} \tag{6.8}$$

Substituting (6.6) into (6.8) gives rise to the recursive formula for J_{n+1}:

$$\begin{aligned} J(\hat{\theta}_{n+1}) &= Y^{\mathrm{T}}[I - H_{n+1}(H_{n+1}^{\mathrm{T}}H_{n+1})^{-1}H_{n+1}^{\mathrm{T}}]Y \\ &= Y^{\mathrm{T}}\left\{I - [H_n,\ x_{n+1}]\begin{bmatrix} S_n^{-1} + R_{n+1}x_{n+1}^{\mathrm{T}}H_{n+1}S_n^{-1} & -R_{n+1} \\ -R_{n+1}^{\mathrm{T}} & \alpha_{n+1}^{-1} \end{bmatrix}\begin{bmatrix} H_n^{\mathrm{T}} \\ x_{n+1} \end{bmatrix}\right\}Y \\ &= J(\hat{\theta}_n) - Y^{\mathrm{T}}H_nS_n^{-1}H_n^{\mathrm{T}}x_{n+1}\alpha_{n+1}^{-1}x_{n+1}^{\mathrm{T}}H_nS_n^{-1}H_n^{\mathrm{T}}Y \\ &\quad -Y^{\mathrm{T}}H_nS_n^{-1}H_n^{\mathrm{T}}x_{n+1}\alpha_{n+1}^{-1}x_{n+1}^{\mathrm{T}}Y - Y^{\mathrm{T}}Q_{n+1}Y \\ &= J(\hat{\theta}_n) \\ &\quad -\hat{\theta}_n^{\mathrm{T}}H_n^{\mathrm{T}}x_{n+1}\alpha_{n+1}^{-1}x_{n+1}^{\mathrm{T}}H_n\hat{\theta}_n - \hat{\theta}_n^{\mathrm{T}}H_n^{\mathrm{T}}x_{n+1}\alpha_{n+1}^{-1}x_{n+1}^{\mathrm{T}}Y - Y^{\mathrm{T}}Q_{n+1}Y, \end{aligned} \tag{6.9}$$

where $Q_{n+1} := x_{n+1}R_{n+1}H_n^{\mathrm{T}} - x_{n+1}x_{n+1}^{\mathrm{T}}\alpha_{n+1}^{-1}$.

To summarize, we list the steps involved in recursively computing $\hat{\theta}_n$ and $J(\hat{\theta}_n)$ as n increases:

1 Select data length p and a fixed integer l, collect the input-output data $\{u(k),\ y(k)\}$.

2 To initialize, let the number of parameters of all FIR crosstalk functions be $n = 1$, and $\hat{\theta}_1 = (x_1^{\mathrm{T}}x_1)^{-1}x_1^{\mathrm{T}}Y$ and $J(\hat{\theta}_1) = \|Y - H_1\hat{\theta}_1\|^2 = Y^{\mathrm{T}}\left(I - x_1(x_1^{\mathrm{T}}x_1)^{-1}x_1^{\mathrm{T}}\right)Y$.

3 By using (6.7) and (6.9), compute $\hat{\theta}_{n+1}$ and $J(\hat{\theta}_{n+1})$.

4 Compare $J(\hat{\theta}_{n+1})$ with $J(\hat{\theta}_n)$: if they are sufficiently close, or for some pre-set small ε, if

$$\frac{|J(\hat{\theta}_{n+1}) - J(\hat{\theta}_n)|}{J(\hat{\theta}_n)} \leqslant \varepsilon,$$

terminate the procedure and obtain the appropriate total number of parameters n and the parameters' estimate $\hat{\theta}_n$; otherwise, increment n by 1 and go to step 3.

Remarks:

1. Equations (6.7) and (6.9) provide a simple means of estimating crosstalk function parameters of length $(n+1)$ given the estimated parameters of length n. Starting from $n = 1$, we can recursively compute the parameter estimates $\hat{\theta}_n$ and the prediction error $J(\hat{\theta}_n)$ by increasing n until the appropriate order is determined. This facility is one of the prime advantages of this recursive algorithm.

2. In the above recursive algorithm, in order to avoid calculating matrix inversion, the order of each crosstalk function is increased by 1 from the 1st channel to the rth channel within each iteration. When the iteration terminates, the model order of the crosstalk functions can be estimated as $\left(\lceil \frac{n}{r} \rceil + 1\right)$, where $\lceil \frac{n}{r} \rceil$ represents the largest integer number less than $\frac{n}{r}$.

6.4 Numerical Example

This section shows the simulation results of crosstalk identification in the upstream direction (from the subscriber to the central office). The receiver of interest is assumed to be an ADSL modem. We assume that the input data are already resampled according to the clock rate of the primary receiver. The crosstalk environment is set up as follows:

- One HDSL;
- One basic rate ISDN (BRI);
- One ADSL.

All twisted pairs are assumed to be 26-gauge (0.4 mm) and 9000-feet (2744 m) long [105]. In this example, we focus on the identification of NEXT as the dominant crosstalk signals are from NEXT by HDSL and BRI. Several important characteristics of DSLs are taken from ITU-T Recommendation G.996.1 [46, 105] and summarized in Table 6.4. The model for NEXT of different types of xDSLs can also

Table 6.1: xDSL Characteristics.

xDSL	ADSL (up)	BRL	HDSL
Line code	DMT	2B1Q	2B1Q
Sampling rate (ks/sec)	276	80	392
Power (dBm)	12.5	13.6	13.6

be found in [46].

As the primary ADSL channel function is assumed to be known, the problem is a two-channel crosstalk system. We first collect the following input and output data with data length $p = 1000$:

- $\{u_1(k)\}$, $\{u_2(k)\}$ and
- $\{y(k)\}$.

Here $\{u_1(k)\}$ and $\{u_2(k)\}$ are taken as persistent excitation sequences with zero mean and unit variance, respectively, and $\{v(k)\}$ as a zero mean white noise sequence. In order to evaluate the estimation accuracy we use the following metric (relative parameter estimation error):

$$\delta = \frac{\|\hat{\theta}_n - \theta\|}{\|\theta\|}.$$

$\delta_a = \|\hat{\theta}_n - \theta\|$ is the absolute parameter estimation error.

To initialize the recursive algorithm, we start with $n = 1$ and pre-set $\varepsilon = 10^{-3}$. Figure 6.3 depicts that $J(\hat{\theta}_n)$ is decreasing when n increases. The algorithm termi-

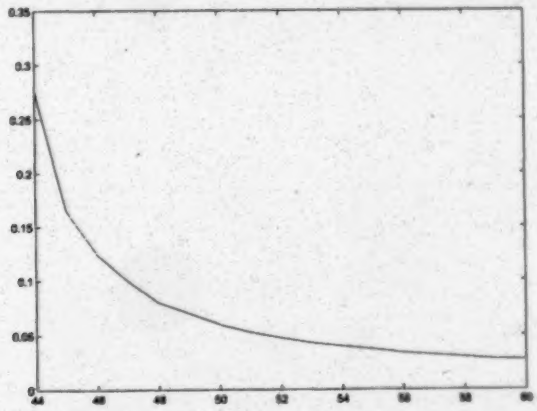

Figure 6.3: The cost function $J(\hat{\theta}_n)$ vs. the number of involved parameters n.

nates at $n = 60$. When $n = 60$, $\delta = 0.0136$. Therefore, the determined model order of crosstalk functions is $\lceil \frac{n}{r} \rceil + 1 = 31$.

6.5 Conclusion

Crosstalk is a major impairment of xDSL systems, which significantly limits the data rate and the reach of the twisted pairs. It is invaluable to identify the crosstalk functions for each pair and, thus, offer better services for more users. In this chapter, we developed a recursive algorithm to identify the model order and parameters of the crosstalk functions for multi-channel xDSL systems, simultaneously and effectively.

Chapter 7

Conclusions and Future Work

In this thesis, we have investigated design and estimation for multirate DSP and communication systems. This chapter summarizes the results reported in this thesis, and proposes some possible future research directions.

7.1 Conclusions

We have studied the problem of optimal design of filterbank-based transceivers. We proposed quantities to measure various distortions for this kind of multirate system. We also introduced a composite distortion that captures all distortions. Finally, by incorporating two important practical issues, the noise suppression and filter bandlimiting property, we developed an iterative design procedure. At each iteration, the least squares solution is found, thus the final transmitter and receiver filters can be obtained with relative ease.

Uniform and nonuniform transmultiplexer design problems have also been considered. The main contribution is the incorporation of stopband energy and passband magnitude constraints directly in the design optimization, thus making an important step forward in addressing practical issues about frequency selectivity. The design procedure proposed considers both signal reconstruction and filter characteristics.

Unlike most existing transmultiplexer design methods with fixed filter length, we have proposed an efficient recursive method to design parameters and length of involved filters simultaneously: It recursively computes the parameters of the filters involved and evaluates the related 2-norm based composite distortion measure for different filter length, and thus, it can not only achieve close-to-perfect reconstruction but also obtain the most appropriate filter length. By this method, we can obtain a good tradeoff between the reconstruction property and the implementation

cost of the designed transmulitplexer.

The other part of the thesis deals with the crosstalk identification for xDSL systems. We studied the *multirate* crosstalk identification for the practical case when different services are operating in different sampling rates. It is shown that the following are the fundamental problems involved: a) How to model the *multirate* network model of xDSL systems? and b) How to estimate the parameter estimation error upper bound, and further determine the relationship between the data length and a preset parameter estimation error level? We have posed and solved these problems by reference to a general multirate MISO network model. We believe that our work is novel in the sense that, to the best of our knowledge, it is the first to address the modeling and identification of the *multirate* network model in xDSL systems.

We have also studied the xDSL crosstalk identification with unknown model order. A recursive algorithm has been developed to identify the model order and parameters of the crosstalk functions for multi-channel xDSL systems, simultaneously and efficiently.

In the following section, we give some possible future research directions.

7.2 Future Work

Indeed, even though present design and estimation algorithms for multirate DSP and communication systems go a long way in facilitating reliable applications, in many aspects the research in this area is still at the beginning. We propose some future research topics.

- Most existing filterbank design methods are based on infinite precision arithmetic, and therefore lead to filters that cannot be readily implemented with

microprocessors. Such infinite precision filters have to be transformed into finite precision filters using techniques such as coefficient quantization and rounding before they can be implemented with hardware. This leads to two problems: (1) First, the likely sacrifice of filter performance because of the deviation from the infinite precision filter (which can be partially overcome by increasing the level of precision, although practical applications have a limit to the allowed wordlength); (2) second, the use of more bits tends to exacerbate the cost and complexity of hardware implementation. Hence, it is interesting to design filterbanks with FIR filters whose coefficients are restricted to a sum of signed powers of two (POT). This feature allows the filters to be implemented with simple adders and shifters only, eliminating the need to use any multipliers whose contribution to the cost and complexity is often great. This type of filterbanks is desirable in applications with high data rates as well as in portable computing and wireless communication applications. The design will be formulated as an integer programming problem under the framework of model matching.

- On another practical side, generalization of a DMT system can be obtained by using nonuniform filterbanks, and lower filter order and complexity are always required in many applications. It would be interesting to further study the design of nonuniform filterbanks with designable filter length, and apply it to the DMT system. In order to develop an efficient algorithm to simultaneously design both filter parameters and filter length, the structural constraint of nonuniform filterbanks would be a challenging issue.

- The performance of a transmultiplexer system is affected significantly by both the properties of the individual analysis and synthesis filters as well as by the structure and quality of the overall transmultiplexer system. In this thesis,

we have incorporated the frequency-domain properties of the analysis and synthesis filters into the transmultiplexer design. On the other hand, time-domain specifications are normally used to indicate certain requirements on the transient response, such as the pulse-shape requirement in digital data transmission systems, which is formulated in terms of envelope constraints. The envelope constraints on time-domain signals have significant applications in communication systems. It is, therefore, our interest to develop an algorithm that can simultaneously incorporate both frequency-domain and time-domain constraints into the design.

- To improve the xDSL service performance, methods are needed for the xDSL receiver to cancel or mitigate the impact of the crosstalk from other types of services. However, like xDSL crosstalk identification, most existing works were developed along the line of using approximate single-rate xDSL model for crosstalk cancellation. Hence, it would be interesting to develop multi-rate xDSL crosstalk cancellation methods that can directly characterize the multirate nature of xDSL systems.

Bibliography

[1] A. Al-Smadi and D. M. Wilkes, "Robust and accurate ARX and ARMA model order estimation of non-Gaussian processes," *IEEE Trans. Signal Processing*, vol. 50, no. 3, pp. 759-763, March 2002.

[2] H. Akaike, "Fitting autoregressive models for prediction," *Ann. Inst. of Stat. Math.*, vol. 21, pp. 243-347, 1969.

[3] H. Akaike, "A new look at the statistical model identification," *IEEE Trans. Automatic Control*, vol. 19, pp. 716-723, 1974.

[4] A. N. Akansu, M. V. Tazebay, and R. A. Haddad, "A new look at digital orthogonal transmultiplexers for CDMA communications," *IEEE Trans. Signal Processing*, vol. 45, no. 1, pp. 263-267, January 1997.

[5] A.N. Akansu, P. Duhamel, X. Lin, and M. de Courville, "Orthogonal transmultiplexers in communication: A review," *IEEE Trans. Signal Processing*, vol. 46, no. 4, pp. 979-995, April 1998.

[6] S. Akkarakaran and P. P. Vaidyanathan, "Filterbank optimization with convex objectives and the optimality of principal component forms," *IEEE Trans. Signal Processing*, vol. 49, no. 1, pp. 100-114, January 2001.

[7] ANSI, "Spectrum Management for Loop Transmission Systems," in *ANSI Standard T1.417*, January 2001.

[8] M. Bellanger, G. Bonnerot, and M. Coudreuse, "Digital filtering by polyphase network: application to sample rate alteration and filter banks," *IEEE Tran. Acoust. Speech and Signal Processing*, vol. ASSP-24, pp. 109-114, April 1976.

[9] L. Chai and L. Qiu, "Model validation of multirate systems from time-domain experimental data," *IEEE Trans. Automatic Control*, vol. 47, pp. 346-351, 2002.

[10] B.-S. Chen, C.-W. Lin, and Y.-L. Chen, "Optimal signal reconstruction in noisy filter bank systems: multirate kalman synthesis filtering approach," *IEEE Trans. Signal Processing*, vol. 43, no. 11, pp. 2693-2701, November 1995.

[11] Y. M. Cheng and B. S. Chen, "Nonuniform filter bank design with channel noises," *IEEE Trans. Signal Processing*, vol. 46, no. 9, pp. 2326-2344, September 1998.

[12] B.-S. Chen and L. Chen, "Optimal reconstruction in multirate transmultiplexer systems under channel noise: Wiener separation filtering approach," *Signal Processing*, vol. 80, pp. 637-657, 2000.

[13] B.-S. Chen, C.-L. Tsai, and Y.-F. Chen, "Mixed H_2/H_∞ design in multirate transmultiplexer systems: LMI approach," *IEEE Trans. Signal Processing*, vol. 49, no. 8, pp. 2693-2701, Aug. 2001.

[14] T. Chen and B. A. Francis, *Optimal Sampled-Data Control Systems*. Springer-Verlag, London, 1995.

[15] T. Chen and B. A. Francis, "Design of multirate filter banks by H_∞ optimization," *IEEE Trans. Signal Processing*, vol. 43, no. 12, pp. 2822-2830, December 1995.

[16] T. Chen, "Nonuniform multirate filter banks: Analysis and design with an H_∞ performance measure," *IEEE Trans. Signal Processing*, vol. 45, no. 3, pp. 572-582, March 1997.

[17] T. Chen and L. Qiu, "Linear periodically time-varying discrete-time systems: Aliasing and LTI approximations," *System and Control Letters*, vol. 30, no. 5, pp. 225-235, 1997.

[18] T. Chen, L. Qiu, and E. Bai, "General multirate building structures with application to nonuniform filter banks," *IEEE Trans. Circuits and Systems II*, vol. 45, pp. 948-958, Aug. 1998.

[19] E.W. Cheng, *Introduction to Approximation Theory*, 2nd Edition. Chelsea Publishing Company, New York, 1982.

[20] Y.M. Cheng, B.S. Chen, and L.M. Chen, "Minmax deconvolution design of multirate systems with channel noises: a unified approach," *IEEE Trans. Signal Processing*, vol. 47, pp. 3145-3149, no. 11, Novermber 1999.

[21] G. Cherubini, E. Eleftheriou, and S. O. Lcer, "Filter bank modulation techniques for very high-speed digital subscriber lines," *IEEE Communications Magazine*, vol. 38, no. 5, pp. 98-104, May 2000.

[22] A. Chevreuil, E. Serpedin, P. Loubaton, and G. B. Giannakis, "Blind channel identification and equalization using non-redundant periodic modulation precoders: performance anlaysis," *IEEE Trans. Signal Processing*, vol. 48, no. 6, pp. 1570-1586, June 2000.

[23] J. W. Cook, "The noise and crosstalk environment for ADSL and VDSL systems," *IEEE Communications Magazine*, vol. 37, pp. 73-78, May 1999.

[24] A. Croisier, D. Esteban, and C. Galand, "Perfect channel splitting by use of interpolation/decimation/tree decomposition techniques," in *Proc. ISICS*, Patras, Greece, 1976.

[25] R. Crochiere and L. R. Rabiner, *Multirate Digital Signal Processing*. Englewood Cliffs, NJ: Prentice-Hall, 1983.

[26] F. Ding and T. Chen, "Parameter estimation for dual-rate systems with finite measurement data," *Dynamics of Continuous, Discrete and Impulsive Systems, Series B: Applications & Algorithms*, vol. 11, no. 1-2, pp. 101-121, 2004.

[27] F. Ding and T. Chen, "Combined parameter and output estimation of dual-rate systems using an auxiliary model," *Automatica*, vol. 40, no. 10, pp. 1739-1748, October 2004.

[28] F. Ding and T. Chen, "Hierarchical least squares identification methods for multivariable systems," *IEEE Trans. Automatic Control*, vol. 50, no. 3, pp. 397-402, March 2005.

[29] F. Ding and T. Chen, "Parameter estimation of dual-rate stochastic systems by using an output error method," *IEEE Trans. Automatic Control*, vol. 50, no. 9, pp. 1436-1441, September 2005.

[30] F. Ding, Y. Shi, and T. Chen, "Gradient based identification algorithms for nonlinear Hammerstein ARMAX models," *Nonlinear Dynamics*, in press, 2005.

[31] F. Ding, Y. Shi, and T. Chen, "Performance analysis of estimation algorithms of non-stationary ARMA processes," *IEEE Trans. Signal Processing*, in press, 2005.

[32] F. Ding, Y. Shi, and T. Chen, "Auxiliary model based least-squares identification methods for Hammerstein output-error systems," Revised for *System & Control Letters*, September 2005.

[33] J. Franke, "A Levinson-Durbin recursion for autoregressive-moving average processes," *Biometrika*, vol. 72, no. 3, pp. 573-581, 1985.

[34] S. Galli and K. J. Kerpez, "The problem of summing crosstalk from mixed sources," *IEEE Trans. Communications Letters.*, vol. 4, no. 11, pp. 325-327, Novermber 2000.

[35] S. Galli and K. J. Kerpez, "Methods of summing crosstalk from mixed sources - part I: theoretical analysis," *IEEE Trans. Commun.*, vol. 50, no. 3, pp. 453-461, March 2002.

[36] S. Galli, C. Valenti, K. J. Kerpez, "A frequency-domain approach to crosstalk identification in xDSL systems," *IEEE Journal on Selected Areas in Communications*, vol. 19, no. 8, pp. 1497-1506, August 2001.

[37] G. B. Giannakis, "Filterbanks for blind channel identification and equalization," *IEEE Signal Processing Letters*, vol. 4, no. 6, pp. 184-187, June 1997.

[38] G. H. Golub and C. F. Van Loan, *Matrix Computations*. The Johns Hopkins University Press, 3rd Edition, 1996.

[39] G. C. Goodwin and K. S. Sin, *Adaptive Filtering, Prediction and Control*. Prentice-Hall: Englewood Cliffs, NJ, 1984.

[40] S. Govardhanagiri, T. Karp, P. Heller, and T. Nguyen, "Performance analysis of multicarrier modulations systems using cosine modulated filter banks," in *Proc. IEEE ICASSP*, vol. 3, pp. 1405-1408, March 1999.

[41] G. Gu and J. Huang, "Convergence results on the design of QMF banks," *IEEE Trans. Signal Processing*, vol. 46, no. 3, pp. 758-761, March 1998.

[42] G. Gu and E. F. Badran, "Optimal design for channel equalization via the filterbank approach," *IEEE Trans. Signal Processing*, vol. 52, no. 2, pp. 536-545, Feburary 2004.

[43] P.-Q. Hoang and P.P. Vaidyanathan, "Nonuniform multirate filter banks: Theory and design," in *Proc. IEEE ISCAS*, pp. 371-374, 1989.

[44] J. Huang and G. Gu, "A direct approach to the design of QMF banks via frequency domain optimization," *IEEE Trans. Signal Processing*, vol. 46, no. 8, pp. 2131-2138, August 1998.

[45] ITU, "Overview of digital subscriber line (DSL) recommendations," in *ITU-T Recommendation G.995.1*, June 1999.

[46] ITU, "Test procedure for digital subscribe line (DSL) transceivers," in *ITU-T Recommendation G.996.1*, June 1999.

[47] ITU, "Asymmetrical digital subscribe line (ADSL) transceivers," in *ITU-T Recommendation G.992.1*, July 1999.

[48] R.D. Koilpillai, T.Q. Nguyen, and P.P. Vaidyanathan, "Some results on the theory of crosstalk-free transmultiplexers," *IEEE Trans. Signal Processing*, vol. 39, no. 2, pp. 2174-2183, October 1991.

[49] G. M. Kranc, "Input-output analysis of multirate feedback systems," *IEEE Trans. Automatic Control*, vol. AC-3, pp. 21-28, November 1957.

[50] G. Liang, D. M. Wilkes, and J. Cadzow, "ARMA model order estimation based on the eigenvalues of the covariance matrix," *IEEE Trans. Signal Processing*, vol. 41, no. 10, pp. 3003-3009, October 1993.

[51] Y.-P. Lin and S.-M. Phoong, "Perfect discrete multitone modulation with optimal transceivers," *IEEE Trans. Signal Processing*, vol. 48, no. 6, pp. 1702-1711, June 2000.

[52] Y.-P. Lin and S.-M. Phoong, "ISI-free FIR filterbank transceivers for frequency-selective channels," *IEEE Trans. Signal Processing*, vol. 49, no. 11, pp. 2648-2658, November 2001.

[53] L. Ljung, *System Identification: Theory for the User*, 2nd Edition. Englewood Cliffs, NJ: Prentice Hall, 1999.

[54] T. Liu and T. Chen, "Optimal design of multi-channel transmultiplexers," *Signal Processing*, vol. 80, pp. 2141-2149, Oct. 2000.

[55] T. Liu and T. Chen, "Design of multi-channel nonuniform transmultiplexers using general building blocks," *IEEE Trans. Signal Processing*, vol. 49, pp. 91-99, Jan. 2001.

[56] A. S. Mehr and T. Chen, "Optimal design of nonuniform multirate filter banks," *Circuits, Systems, and Signal Processing*, vol. 18, no. 5, pp. 505-521, 1999.

[57] A. S. Mehr and T. Chen, "Design of nonuniform multirate filter banks by semidefinite programming," *IEEE Trans. Circuits and Systems II: Analog and Digital Signal Processing*, vol. 47, no. 11, pp. 1311-1314, Novermber 2000.

[58] S. Mirabbasi, B. A. Francis, and T. Chen, "Controlling distortions in maximally decimated filter banks," *IEEE Trans. Circuits and Systems II: Analog and Digital Signal Processing*, vol. 44, no. 7, pp. 597-600, July 1997.

[59] P. Moulin, M. Anitescu, and K. Ramchandran, "Theory of rate-distortion-optimal, constrained filterbanksCapplication to IIR and FIR biorthogonal designs," *IEEE Trans. Signal Processing*, vol. 48, no. 4, pp. 1120-1132, April 2000.

[60] K. Nayebi, T. Barnwell, and M. J. T. Smith, "A general time domain analysis and design framework for exactly reconstructing FIR analysis/synthesis filter banks," in *Proc. IEEE ISCAS*, pp. 2022-2025, May 1990.

[61] K. Nayebi, T. Barnwell, and M. J. T. Smith, "Time domain conditions for exact reconstruction in analysis/synthesis systems based on maximally decimated filter banks," in *Proc. 19th Southeastern Symposium on System Theory*, pp. 498-502, March 1987.

[62] S. Niu, D. Xiao, D. G. Fisher, "A recursive algorithm for simultaneous identification of model order and parameters," *IEEE Trans. Acoustics, Speech, and Signal Processing*, vol. 38, no. 5, pp. 884-890, May 1990.

[63] H. J. Nussbaumer, "Pseudo QMF filter bank," *IBM Tech. Disclosure Bulletin*, vol. 24, pp. 3081-3087, 1981.

[64] J. G. Proakis, *Digital Communications*. McGraw Hill, 1995.

[65] N. Papandreou, T. Antonakopoulos, "Real-time FEXT crosstalk identification in ADSL systems," *IEEE International Symposium on Intelligent Signal Processing*, pp. 61-66, September 2003.

[66] R.P. Ramachandran and P. Kabal, "Transmultiplexers: Perfect reconstruction and compensation of channel distortion," *Signal Processing*, vol. 21, pp. 261-274, 1990.

[67] A. D. Rizos, J. G. Proakis, and T. Q. Nguyen, "Comparison of DFT and cosine modulated filter banks in multicarrier modulation," in *Proc. IEEE Global Telecommunications Conference*, vol. 2, 1994, pp. 687-691.

[68] A. Scaglione, G. B. Giannakis, and S. Barbarossa, "Redundant filterank precoders and equalizers, Part 1: Unification and optimal designs," *IEEE Trans. Signal Processing*, vol. 47, no. 7, pp. 1983-2006, July 1999.

[69] R. G. Shenoy, D. Burnside, and T. W. Parks, "Linear periodic systems and multirate filter design," *IEEE Trans. Signal Processing*, vol. 42, pp. 2242-2256, 1994.

[70] R. G. Shenoy, "Analysis of multirate components and application to multirate filter design," in *Proc. IEEE ICASSP*, vol. 3, pp. 121-124, 1994.

[71] R. G. Shenoy, "Model-matching design of sample-rate changers: asymptotic analysis," in *Proc. IEEE ISCAS*, vol. 3, pp. 1904-1907, 1995.

[72] R. G. Shenoy, "Multirate specifications via alias-component matrices," *IEEE Trans. Circuits Syst. II*, vol. 45, no. 3, pp. 314-320, March 1998.

[73] Y. Shi and T. Chen, "Optimal design of multi-channel transmultiplexers with stopband energy constraints," in *Proc. IEEE Pacific Rim Conference on Communications, Computers and Signal Processing*, vol. 2, pp. 559-562, Victoria, Canada, Aug. 26-28, 2001.

[74] Y. Shi and T. Chen, "Optimal design of multi-channel transmultiplexers with stopband energy and passband magnitude constraints," *IEEE Trans. Circuits Syst. II*, vol. 50, no. 9, pp. 659-662, September 2003.

[75] Y. Shi and T. Chen, "An iterative method for designing filterbank-based transceivers," Submitted to *IEEE Trans. Circuits and Systems II: Analog and Digital Signal Processing*, May 2004.

[76] Y. Shi, F. Ding, and T. Chen, "Crosstalk identification in xDSL systems with unknown model order," Submitted to *Journal of Communications and Networks*, September 2004.

[77] Y. Shi, F. Ding, and T. Chen, "2-norm based recursive design of transmultiplexers with designable filter length," Revised for *Circuits, Systems, and Signal Processing*, May 2005.

[78] Y. Shi, F. Ding, and T. Chen, "Multirate crosstalk identification in xDSL systems," Revised for *IEEE Trans. Communications*, September 2005.

[79] H. Shu, T. Chen, and B. A. Francis, "Minimax design of hybrid multirate filter banks," *IEEE Trans. Circuits Syst. II*, vol. 44, no. 2, pp. 120-128, Feburary 1997.

[80] K. B. Song, S. T. Chung, G. Ginis, and J. M. Cioffi, "Dynamic spectrum management for next-generation DSL systems," *IEEE Communications Magazine*, vol. 40, no. 10, pp. 101-109, October 2002.

[81] T. Starr, J. M. Cioffi, and P. J. Silverman, *Understanding Digital Subscriber Line Technology*. Englewood Cliffs, NJ: Prentice-Hall, 1998.

[82] T. Starr, M. Sorbara, J. M. Cioffi, and P. J. Silverman, *DSL Advances*. Englewood Cliffs, NJ: Prentice-Hall, 2003.

[83] A. Takcenko and P. P. Vaidyanathan, "Iterative algorithm for the design of optimal FIR analysis/synthesis filters for overdecimated filter banks," in *Proc. IEEE ISCAS*, vol. 3, pp. 23-26, May 2004.

[84] L. Tong, G. Xu and T. Kailath, "Blind identification and equalization based on second-order statistics: A time domain approach," *IEEE Trans. Information Theory*, vol. 40, no. 3, pp. 340-349, March 1994.

[85] T.D. Tran, "M-channel linear phase perfect reconstruction filter bank with rational coefficients," *IEEE Trans. Circuits and Systems I*, vol. 49, no. 7, pp. 914-927, July 2002.

[86] M. K. Tsatsanis and G. B. Giannakis, "Principal component filter banks for optimal multiresolution analysis," *IEEE Trans. Signal Processing*, vol. 43, no. 8, pp. 1766-1777, August 1995.

[87] H. D. Tuan, T. T. Son, P. Apkarian, and T. Q. Nguyen "Low-order IIR filter bank design," *IEEE Trans. Circuits and Systems I*, vol. 52, no. 8, pp. 1673-1683, August 2004.

[88] P.P. Vaidyanathan, "Theory and design of M-channel maximally decimated quadrature mirror filters with arbitrary M, having the perfect-reconstruction property," *IEEE Trans. on Acoustics, Speech, and Signal Processing*, vol. 35, no. 4, pp. 476-492, 1987.

[89] P.P. Vaidyanathan, *Multirate Systems and Filter Banks*. Prentice-Hall, Englewood Cliffs, NJ, 1993.

[90] P. P. Vaidyanathan, "Theory of optimal orthonormal subband coders," *IEEE Trans. Signal Processing*, vol. 46, no. 6, pp. 1528-1543, June 1998.

[91] P. P. Vaidyanathan and A. Kyrac, "Results on optimal biorthogonal filter banks," *IEEE Trans. Circuits and System II*, vol. 45, no. 8, pp. 932-947, August 1998.

[92] P. P. Vaidyanathan, "Filter banks in digital communications," *IEEE Circuits and Systems Magazine*, vol. 1, no. 2, pp. 4-25, 2001.

[93] P. P. Vaidyanathan, Y.-P. Lin, S. Akkarakaran, and S.-M. Phoong, "Optimality of principal component filter banks for discrete multitone communication systems," *Proc. IEEE ISCAS*, Geneva, May 2000.

[94] P. P. Vaidyanathan and B. Vrcelj, "Transmultiplexers as precoders in modern digital communication: a tutorial review," in *Proc. IEEE ISCAS*, vol. 5, pp. 405-412, May 2004.

[95] M. Vetterli, "Perfect transmultiplexers," in *Proc. IEEE ICASSP*, pp. 2567-2570, April 1986.

[96] G.W. Wornell, "Emerging applications of multirate signal processing and wavelets in digital communications," *Proc. of the IEEE*, vol. 84, no. 4, pp. 586-603, April 1996.

[97] X.-G. Xia, "New precoding for intersymbol interference cancelation using nonmaximally decimated multirate filterbanks with ideal FIR equalizers," *IEEE Trans. Signal Processing*, vol. 45, no. 10, pp. 2431-2440, October 1997.

[98] Y. Xiao, Y.-Y. Cao, and Z. Lin, "Robust filtering for discrete-time systems with saturation and its application to transmultiplexers," *IEEE Trans. Signal Processing*, vol. 52, no. 5, pp. 1266-1277, May 2004.

[99] L. Xie, H. Zhou, and C. Zhang, "Optimal deconvolution of periodic systems with application to multirate filter bank design," in *Proc. 3rd Int. Conf. on Information, Communications and Signal Processing*, Oct. 2001.

[100] H. Xu, W. Lu, and A. Antoniou, "Improved iterative methods for the design of quadrature mirror-image filter banks," *IEEE Trans. Circuits Syst. II*, vol. 43, no. 5, pp. 363-371, May 1996.

[101] B. Xuan and R. I. Bamberger, "FIR principal component filter banks," *IEEE Tran. Signal Processing*, vol. 46, no. 4, pp. 930-940, April 1998.

[102] Y. Yamamoto and P. P. Khargonekar, "From sampled-data control to signal processing," in *Learning, Control and Hybrid Systems*, Y. Yamamoto and S. Hara, Eds. New York: Springer-Verlag, pp. 108-126, 1998

[103] S.-J. Yang, J.-H. Lee and B.-C. Chieu, "Perfect-reconstruction filter banks having linear-phase FIR filters with equiripple response." *IEEE Trans. Signal Processing*, vol. 46, pp. 3246-3255, December 1998.

[104] C. Zeng, "Crosstalk Identification and cancellation in DSL systems," PhD Dissertation, Stanford Universtiy, July 2001.

[105] C. Zeng, C. Aldana, A. A. Salvekar, and J. M. Cioffi, "Crosstalk Identification in xDSL Systems," *IEEE Journal on Selected Areas in Communications*, vol. 19, no. 8, pp. 1488-1496, August 2001.

[106] C. Zhang, S. Wang, and L. Xie, "Sequentially operated FIR multirate filter banks," in *Proc. Int. Conf. Signal Processing (ICSP2000)*, Beijing, August 2000.

[107] L. Zhang, Y. Shi, T. Chen, and B. Huang, "A new method for stabilization of networked control systems with random delays," *IEEE Trans. Automatic Control*, vol. 50, no. 8, pp. 1177-1181, August 2005.

[108] H. Zhou, L. Xie, and C. Zhang, "A direct approach to H_2 optimal deconvolution of periodic digital channels," *IEEE Trans. Signal Processing*, vol. 50, no. 7, pp. 1685-1698, July 2002.

[109] H. Zhou, L. Xie, and C. Zhang, "Optimal bit-rate allocation and synthesis filter bank design for multirate subband coding systems," in *Proc. IEEE ICASSP*, vol. 5, pp. 105-108, June 2003.

[110] H. Zhou, *H_2 and H_∞ optimal design of multirate filter bank systsms*, PhD Dissertation, Nanyang Technological University, 2003.

[111] K. Zhou, J. C. Doyle and K. Glover, *Robust and Optimal Control*. Prentice Hall, 1996.

[112] M. Zimand, *Computational complexity : a quantitative perspective*. Elsevier, 2004.